

Enabling Fast Charging:

A Technology Gap Assessment

October 2017

(This page intentionally left blank)

Authors

DOE Authors:

David Howell, Steven Boyd, Brian Cunningham, Samm Gillard, Lee Slezak

National Laboratory Authors:

Argonne National Laboratory (ANL): Shabbir Ahmed, Ira Bloom, Andrew Burnham, Keith Hardy, Andrew N. Jansen, Paul A. Nelson, David C. Robertson, Thomas Stephens, Ram Vijayagopal

Idaho National Laboratory (INL): Richard B. Carlson, Fernando Dias, Eric J. Dufek, Christopher J. Michelbacher, Manish Mohanpurkar, Don Scoffield, Matthew Shirk, Tanvir Tanim

National Renewable Energy Laboratory (NREL): Matthew Keyser, Cory Kreuzer, Oibo Li, Anthony Markel, Andrew Meintz, Ahmad Pesaran, Shriram Santhanagopalan, Kandler Smith, Eric Wood, Jiucan Zhang

Acknowledgments

This work was performed under the auspices of the U.S. Department of Energy, under Contract Nos. DE-AC02-06CH11357 (Argonne National Laboratory), DE-AC07-99ID13727 (Idaho National Laboratory), and DE-AC36-08GO28308 (National Renewable Energy Laboratory). Funding for the work was provided by the DOE Office of Energy Efficiency and Renewable Energy, Vehicle Technologies Office. Specific thanks to Michael Berube, Tien Duong, and Peter Faguy for their guidance and technical support. Additional thanks to Joseph Harmon (ANL), LauraLee Gourley (INL), Judy Fairchild (INL) Christina Komeslian (NREL), and Stephanie Price (NREL) for providing timely and thorough reviews.

Special thanks to those who contributed reviews during various phases of the work, including:

- Kevin Bennion (National Renewable Energy Laboratory)
- Andrew Colclasure (National Renewable Energy Laboratory)
- Jack Deppe (Deppe Consulting)
- Chris Gearhart (National Renewable Energy Laboratory)
- Boryann Liaw (Idaho National Laboratory)
- John Farrell (National Renewable Energy Laboratory)
- Sreekant Narumanchi (National Renewable Energy Laboratory)
- Aron Saxon (National Renewable Energy Laboratory)
- John Smart (Idaho National Laboratory)
- Kevin Walkowicz (National Renewable Energy Laboratory)

The U.S. Government retains for itself, and others acting on its behalf, a paid-up nonexclusive, irrevocable worldwide license in said article to reproduce, prepare derivative works, distribute copies to the public, and perform publicly and display publicly, by or on behalf of the Government.

This report is being disseminated by the Department of Energy. As such, the document was prepared in compliance with Section 515 of the Treasury and General Government Appropriations Act for Fiscal Year 2001 (Public Law 106-554) and information quality guidelines issued by the Department of Energy. Though this report does not constitute “influential” information, as that term is defined in DOE’s information quality guidelines or the Office of Management and Budget’s Information Quality Bulletin for Peer Review (Bulletin), as detailed in Acknowledgements, the report was reviewed both internally and externally prior to publication.

List of Acronyms

ADA	Americans with Disabilities Act
AHJ	authority having jurisdiction
AWG	American Wire Gauge
BatPaC	battery performance and cost
BEV	battery electric vehicle
BLAST	Battery Lifetime Analysis and Simulation Tool
BTMS	Battery Thermal Management System
CCS	combined charging system
DC	direct current
DCFC	direct current fast charge
DOE	U.S. Department of Energy
DOT	U.S. Department of Transportation
DSM	demand side management
EV	electric vehicle
EVSE	electric vehicle service equipment
Gr	graphite
ICEV	internal combustion engine vehicle
IGBT	insulated-gate bipolar transistor
LFP	lithium iron phosphate
MACD	maximum allowable current density
MOSFET	metal-oxide-semiconductor field-effect transistor
NMC	lithium nickel manganese cobalt oxide
NMC622	$\text{LiNi}_{0.6}\text{Mn}_{0.2}\text{Co}_{0.2}\text{O}_2$
LMO	lithium manganese oxide, LiMn_2O_4
LTO	lithium titanate, $\text{Li}_4\text{Ti}_5\text{O}_{12}$
NEC	National Electric Code
NFPA	National Fire Protection Association
OEM	original equipment manufacturer
OSHA	Occupational Safety and Health Administration
PEV	plug-in electric vehicle (includes both EVs and plug-in hybrid EVs)
PUC	public utility commission
SAE	Society of Automotive Engineers
SEI	solid electrolyte interphase
SOC	state of charge
TCO	total cost of ownership
USABC	U.S. Advanced Battery Consortium
VTTs	value-of-travel-time-savings
XFC	extreme fast charging

Executive Summary

Decreasing energy consumption across the U. S. transportation sector, especially in commercial light-duty vehicles, is essential for the United States to gain energy independence. Recently, powertrain electrification with plug-in electric vehicles (PEVs) have gained traction as an alternative due to their inherent efficiency advantages compared to the traditional internal combustion engine vehicle (ICEV). Even though there are many different classes of PEVs, the intent of this study is to focus on non-hybrid powertrains, or battery electric vehicles (BEVs).

Despite rapid drops in cost within the BEV powertrain of over four times in the last 10 years and significant improvements in drivability and performance, the BEV market still only accounts for approximately 1% of new light-duty vehicle sales annually. BEV powertrain costs are not quite at parity with the ICEV; however, another identified gap to wider adoption of BEVs is the ability to refuel quickly or to fast charge. The majority of BEV recharging is done at home, but having access to public direct current (DC) fast chargers can have a big impact on BEV utility from a consumer perspective (see Figure 1). Studies have shown that in areas where drivers have access to 50-kW or 120-kW fast charge stations, annual electric vehicle (EV) miles traveled (i.e., eVMT) increased by over 25%, even in cases where fast charging was used for 1% to 5% of total charging events (Figure 1) [1, 2]. Having access to these fast charge stations can help alleviate the “range anxiety” commonly cited as a reason for consumer’s hesitation to buy a BEV.

To be truly competitive to the ICEV refueling experience, even higher power stations are necessary. To address the fast charge barrier, charging at 400-kW, or extreme fast charging (XFC), has been proposed and will serve as the basis for discussion in this report.

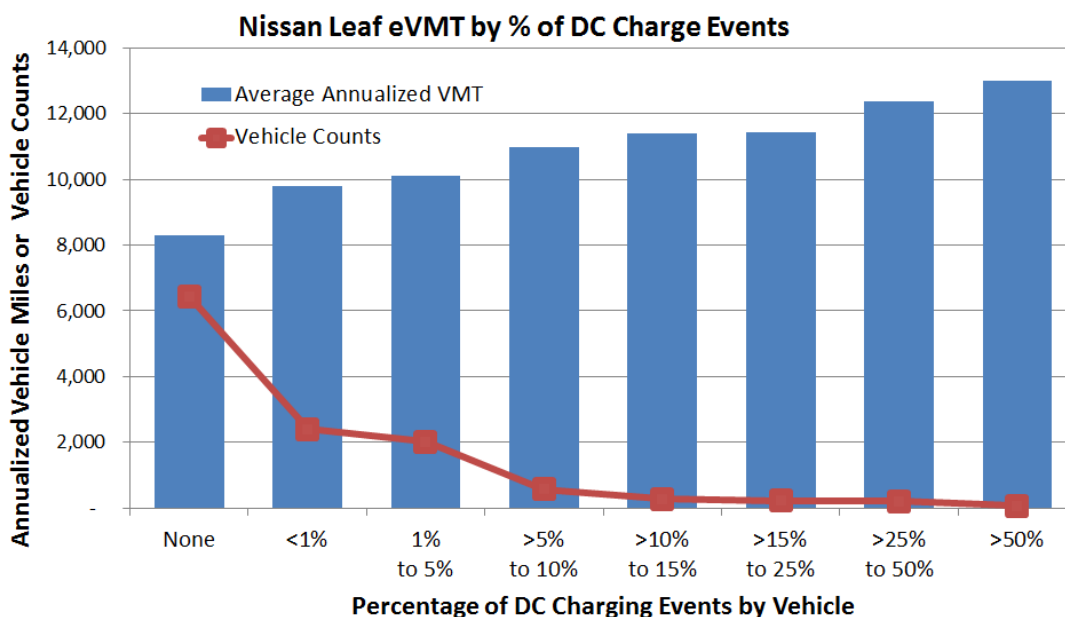


Figure 1. Analysis by the California Air Resource Board (CARB) shows increased yearly vehicle miles traveled when using 50-kW fast charging. When compared with a vehicle that never fast charged, nearly a 25% increase in annual miles traveled was realized when 1 to 5% of total charging events were fast charges [1, 2].

These XFC stations should be able to recharge a BEV in less than 10 minutes and provide approximately 200 additional miles of driving. However, this introduces a host of new challenges that need to be addressed. As a result, it is expected that packs designed to meet XFC will initially be significantly more expensive than BEVs optimized for current charging technology.

Table 1. Description of currently available charging infrastructure compared with XFC. It is assumed that while driving, the vehicle energy consumption will be 285 Wh per mile and this does not account for charge efficiency [Appendix C].

	Level 1 (110V, 1.4 kW)	Level 2 (220V, 7.2 kW)	DC Fast Charger (480V, 50 kW)	Tesla SuperCharger (480V, 140 kW)	XFC (800+V, 400 kW)
Range Per Minute of Charge (miles)	0.082	0.42	2.92	8.17	23.3
Time to Charge for 200 Miles (minutes)	2,143	417	60	21,	7.5

From the battery cell to the power grid these 400-kW chargers are connected to, this study will discuss issues that need to be addressed at each level in order to implement a 400-kW charging network. Although this report is U.S.-focused, the findings should be applicable to other countries with mature automotive infrastructures. The technical gaps are highlighted and discussed below, each with an attached appendix that provides further technical detail.

Barriers to XFC

Battery

The U.S. Department of Energy (DOE) has a goal of reducing the production cost of a BEV battery to ultimately \$80/kWh, increase the range of EVs to 300 miles, and decrease charge time to 15 minutes or less. In order to achieve this goal, a major effort within the battery research community has focused on increasing the energy density of the cell, which refers to the amount of energy stored in a specified weight or volume. Increasing electrode thickness is an effective way of improving the energy density of a cell.

However, thicker electrodes present several barriers to fast charging. As electrode thickness increases, charge times must also increase in order to avoid lithium plating. Lithium plating occurs when the charge rate exceeds the rate the lithium ions can intercalate into the crystal structure of the anode, which causes metallic lithium to form on the surface. Lithium plating can negatively affect performance of the electrode and lead to accelerated degradation of the battery, as well as impact cell safety. Therefore, it is thought that thinner electrodes are better suited for XFC applications, but this occurs with a tradeoff in increased battery cost. The analysis conducted in this report indicates that fast charge nearly doubles cell cost from \$103/kWh to \$196/kWh. The increase in cell cost is largely based on decreasing the anode thickness. Using thinner electrodes requires more cells to achieve the same energy density. Managing the heat generated in the battery during a charging event is also a potential barrier to XFC because temperatures in excess of 45°C will rapidly degrade battery lifetime. Higher temperatures can also introduce safety concerns as materials contained within the battery can begin to chemically and mechanically degrade.

Vehicles

Similarly as with the battery, the vehicle is constrained by cost, weight, and volume. For XFC-capable vehicles, these parameters are greatly influenced by the current delivered to the vehicle during a 400-kW charge, where all parameters rise with increased current. By increasing the BEV battery pack voltage from the current industry standard of 400 V to more than 800 V, the current needed for XFC drops by at least half. However, increasing the pack voltage impacts components such as the electric drive motor and the power

electronics onboard the vehicle, including the power inverters. Higher voltages also bring new challenges associated with interoperability because legacy and XFC-enabled vehicles interface with charging infrastructure. Developing an XFC-capable vehicle may introduce challenges with the high-voltage system architecture, power electronics and electric machines, the charging system, thermal management, cyber and physical security, and BEV/EVSE interoperability. The trade-off between driving range and recharge time has historically been a barrier to BEV adoption. XFC seeks to balance these parameters, along with vehicle cost.

Infrastructure

Successful installation of nationwide, 400-kW capable, public infrastructure requires many barriers to be addressed. A key challenge is to coordinate across the many stakeholders such as vehicle manufacturers, utility suppliers, XFC charger manufacturers and network operators, battery developers, codes and standards bodies, and policy makers. Specific topics such as power requirements for XFC charger installations, utility rate structures, and the connector type for vehicle-to-charger connections can impact the effectiveness of XFC and should be considered by stakeholders as a group. XFC infrastructure should be able to accommodate all vehicle types, even if the vehicle is not XFC capable. Optimization of XFC charging station location is needed within cities and across highway corridors to account for user convenience and availability of power from the utility. Co-located distributed energy resources may be needed to minimize station operation costs, limit grid impacts, and accommodate ideal XFC station placement.

R&D Needs

Battery

Materials R&D is needed in order to minimize or mitigate localized heating and lithium plating with thicker electrodes. Research in electrode design can help with implementation of advances made through materials' innovations. A study of the impact of XFC on the existing current-state-of-the-art can inform material, electrode, and cell design research. These studies may also reveal differences in the safety of cells subjected to XFC protocols, which is an area also in need of more research to fully understand the impacts and to develop mitigations. Research toward development of new charging protocols that may extend battery life should also be considered.

Development of new technologies for XFC battery pack thermal management is needed in order to preserve battery life. More complex battery management systems may be needed to cope with higher pack voltages, more complex thermal management systems, and cell balancing during charging. Higher voltage packs also bring additional electrical safety concerns that need to be understood.

Vehicle

BEV owners require consistent charging experiences. Interoperability of XFC charging systems with vehicles of different models and charging capabilities could be studied. Cybersecurity research of the vehicle and charger communications is needed to ensure BEVs provide reliable transportation. Furthermore, standardization to ensure interoperability between new and legacy vehicles accessing XFC and existing networks is needed. Testing and evaluation of existing vehicles to XFC charger connectors to determine safe, reliable, and robust operating limits could be considered. Researching the impact higher pack voltage has on the overall volume, weight, and cost for power electronics may be needed for XFC-enabled vehicles. Increased system bus voltages will require reevaluation of semiconductor materials used in vehicle power electronics, in addition to improved insulation materials needed to maintain electrical safety and durability.

Infrastructure

Researching advanced materials to reduce and manage thermal loads within the charger and the cable connecting the vehicle-to-charger is needed for XFC applications. Automation for XFC should be considered;

however, this may increase overall system cost. Stakeholder engagement to harmonize XFC station permitting and siting requirements, along with codes and standards related to liquid-cooled cables and vehicle-to-charger connector design, should be a focus. Best conducted by industry, understanding where XFC stations need to be sited to serve demand, both commercial and private, and where appropriate grid resources exist to initially serve the greatest number of consumers should be investigated. The tradeoffs and operational benefits realized by using co-located distributed energy resources integrated with utility generation could be considered and studied.

Report Structure and Overview

This report has been broken into three sections: (1) an executive summary, (2) a summary report, and (3) appendices complete with four technical manuscripts. The executive summary is intended to introduce XFC and convey the high-level technical challenges/gaps and introduce potential R&D solutions with minimal technical discussion. In the summary report, these gaps and R&D solutions are addressed with more technical detail. The reader should be able to understand the bulk issues and linking technicalities associated with XFC by reading the summary report; however, the reader does not need to be an expert in the field. The manuscripts contained in the appendices are intended for persons with technical backgrounds or those looking to learn more about XFC technologies through a technical lens. The appendices were written with the intent to be published in technical peer-reviewed journals.

References

- [1] Lutsey, N., S. Searle, S. Chambliss, and A. Bandivadekar, 2015, "Assessment of Leading Electric Vehicle Promotion activities in United States Cities," *International Council for Clean Transportation*, July 2015.
- [2] McCarthy, Michael, 2017, "California ZEV Policy Update," *SAE 2017 Government/Industry Meeting*, Society of Automotive Engineers, January 25, 2017, Walter E. Washington Convention Center, Washington, DC, conference presentation.

Table of Contents

Executive Summary	4
1 Introduction	11
2 Battery	12
2.1 Introduction	12
2.2 Battery Cost.....	12
2.3 Cell Level 13	
Lithium Plating	13
Anode Materials.....	14
Cathode Materials	15
Electrode Design.....	15
Other Cell Materials.....	15
2.4 Pack Level Design.....	15
2.5 Battery Thermal Management	16
Thermal System Design.....	16
2.6 Summary of Battery R&D Needs	16
Appendices A and B contain detailed technical discussions and reference material concerning battery R&D needs.....	16
Material and Cell Level Needs	16
Pack Level Needs.....	16
3 Vehicle	17
3.1 Introduction	17
3.2 Range and Battery Capacity for XFC Capable Vehicles	17
3.3 Electrical Architectures	18
Appendix C contains detailed technical discussions and reference material concerning vehicle electrical architectures.....	18
High-Voltage System Architecture.....	18
XFC Voltage Impacts on Power Electronics and Electric Machines.....	19
XFC Impacts on Battery Electric Vehicle Charging System Design.....	20
3.4 Vehicle Thermal Management	21
3.5 XFC Vehicle Cybersecurity.....	21
3.6 Summary of Vehicle R&D Needs	22
Appendix C contains detailed technical discussions and reference material concerning vehicle R&D needs.	22
Electrical Architecture	22
Power Electronics and Electric Machines.....	22
Cybersecurity and Interoperability	22
4 Infrastructure	23
4.1 Introduction	23
4.2 XFC Infrastructure Technical and Cost Considerations	23

Appendix D contains detailed technical discussions and reference material concerning XFC infrastructure technical and cost considerations..... 23

Infrastructure Costs..... 23

Charging Stations..... 23

Electric Vehicle Supply Equipment – Technical Issues (Cables, Voltage, and Connector) 24

Electric Vehicle Supply Equipment Installation and Equipment Costs 25

XFC Station Siting..... 25

4.3 XFC Utility Impacts and Demand Charges 25

 Distributed Energy Resources – Generation and Storage..... 26

4.4 XFC Infrastructure Cyber and Physical Security 26

4.5 Summary of Infrastructure R&D Needs 27

 Appendix D contains detailed technical discussions and reference material concerning infrastructure R&D needs..... 27

 EVSE R&D Needs..... 27

 Industry Focused R&D 27

5 Conclusion..... 27

Appendices..... 29

Appendix A 30

Enabling Fast Charging – A Battery Technology Gap Assessment 31

Appendix B 44

Enabling Fast Charging – A Battery Thermal Technology Gap Assessment 45

Appendix C..... 54

Enabling Fast Charging — Vehicle Considerations 55

Appendix D..... 67

Enabling Fast Charging — Infrastructure and Economic Considerations 68

List of Figures

Figure 1. Analysis by the California Air Resource Board (CARB) shows increased yearly vehicle miles traveled when using 50-kW fast charging. When compared with a vehicle that never fast charged, nearly a 25% increase in annual miles traveled was realized when 1 to 5% of total charging events were fast charges [1, 2].4

Figure 2. Current EVs with DCFC capabilities and the number of driving range miles replenished per minute of charge. Based on 285 Wh per mile energy consumed or 3.5 miles per kWh of charge [Appendix A]..... 11

Figure 3. At high charge rates, a much larger number of lithium ions move to intercalate into graphite as represented by the red dots. However, there is not enough time or space for intercalations; therefore, lithium ions may start plating as metal onto the surface of the graphite electrode (shown as the thick red line) [Goodenough, J.; Kim, Y. Chem. Mater. 2010,

22, pp. 587-603]..... 14

Figure 4. Images of graphite electrode after aging in NMC622/Gr pouch cells. Lithium plating appears as metallic deposits on the surface of the electrode and increases with higher loading (mAh/cm²) as shown from left to right [Appendix A]..... 14

Figure 5. Charge current with respect to charge power for different battery pack voltages. The 400-V configuration shown in red is representative of a typical EV battery pack today. 15

Figure 6. Intercity travel from Salt Lake City to Denver – ICEV versus BEV [Appendix C]. 18

Figure 7. Options of 1,000-V BEV architectures [Appendix C]. 19

Figure 8. Charging connector voltage and current range for new and existing vehicles [Appendix C].21

Figure 9. Comparison of uncooled cabling for EVSE operating at 400 or 800 V. Calculations use different copper cables that meet NEC ampacity ratings and use the current weight of a CHAdeMO connector [Appendix D]..... 24

List of Tables

Table 1. Description of currently available charging infrastructure compared with XFC. It is assumed while driving; the vehicle energy consumption is 285 Wh per mile and does not account for charge efficiency.5

Table 2. BatPaC simulation comparing the effects of charging time on the required anode thickness, the heat generation in the pack and the resulting temperature rise, the pack cost, and the incremental cost of charging faster than 1-C (60 minutes) rate. Cell Chemistry: NMC 622-Graphite; Pack Energy: 85 kWh; Rated Power (10 sec burst): 300 kW; MACD (Maximum Allowable Current Density): 4 mA/cm²; Number of cells per pack: 240..... 13

1 Introduction

Current commercially available passenger BEVs are not capable of charging at rates that allow for a refueling time similar to ICEVs. Tesla vehicles offer the fastest recharge rates at 120 kW from their Supercharger stations (these chargers can support up to 145-kW charging). Porsche has demonstrated the Mission E BEV concept vehicle, which can support up to 400 kW charging at the DC voltage of 800 V and has plans to go into production with the vehicle in 2020 [Appendix C]. Other BEVs in today’s market (such as the Chevy Bolt, Nissan Leaf, and BMW i3) have been designed around the prevailing 50-kW DC fast charge (DCFC) infrastructure. In order to provide a comparable refueling time to ICEVs, it is expected that charging power will need to increase from 120 to 400 kW. For the purposes of this document, the next level of charging (i.e., 400-kW XFC) is defined as recharging up to 200 miles of driving range in 10 minutes or less.

Miles added per minute is another way of defining DCFC. Assuming 285 Wh of energy consumption per mile of, Figure 2 shows DCFC charging speed in terms of miles per minute for some available DCFC-capable EVs and an estimate of charging speed using a 400 kW charger. While the charging speed of most of the EVs remained below 3 miles per minute, Tesla can achieve up to 5.6 miles per minute with their state-of-the-art 120-kW DCFC. XFC could enable up to or even exceed 20 miles of driving distance added per minute of charge for a compatible battery.

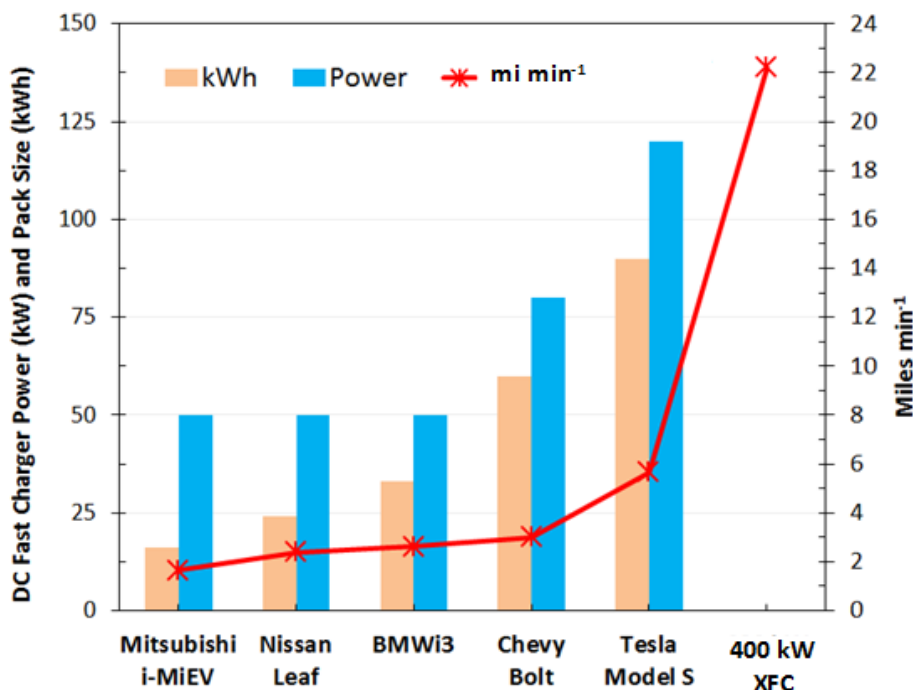


Figure 2. Current EVs with DCFC capabilities and the number of driving range miles replenished per minute of charge. Based on 285 Wh per mile energy consumed or 3.5 miles per kWh of charge [Appendix A].

The following sections contained within this summary report are meant to capture and distill the technical discussions and findings of those identified in the supporting journal manuscripts found at the end of this document in Appendices A through D. The summary report sections will be divided into three main topics: (1) battery, (2) vehicle, and (3) infrastructure. Topics covered include vehicle high-voltage battery materials and fast charge degradation mechanisms; the vehicle as a system, including power electronics and thermal management; EV charging infrastructure to include electric vehicle supply equipment (EVSE) and utility considerations; and economic considerations such as total cost of ownership and customer usage. Generally, Appendices A through D should be consulted for in-depth technical discussion, data, and referenced resources.

2 Battery

2.1 Introduction

Lithium-ion batteries are used in applications that need high energy or power densities. These density characteristics make them ideal for vehicle electrification. Typically, recharging these batteries takes much longer than refueling the average liquid-fueled ICEV. However, as EVs gain market share, the consumer may expect an electric refueling experience to be similar in duration to that of an ICEV (i.e., less than 10 minutes). The current suite of technology allows for batteries to charge at these high rates; however, the cell cost is nearly double that of a non-XFC capable design.

Looking specifically at battery technology, perhaps the primary differentiator between a power and energy cell is the thickness of the anode and cathode electrodes. Thicker active material coatings generally result in higher energy density or the amount of energy that can be stored in a specific weight or volume. Having an energy dense cell is ideal for a BEV from a pack cost and driving range perspective. With these properties in mind, battery R&D over the last decade or more has focused on increasing the energy density of the cell, primarily via higher capacity materials and thicker electrodes. However, this attribute has one rather large drawback as it relates to XFC; it is difficult for these thicker electrode systems to perform at higher charge rates. Degradation of thicker electrodes can occur more rapidly if charged too quickly when compared to thinner-coated electrodes.

Slower charge rates are needed in order to allow the lithium-ions to reach all storage sites of the active material on the electrode. In general, the more storage sites per unit area a material has, the more time is required for those sites to accept lithium ions. Charging at too high of a rate runs the risk of exposing those materials to lithium ions at a rate they are unable to accept. This results in lithium plating on the surface of the anode, increased battery temperature, and other detrimental side chemical reactions that decrease life and performance characteristics.

The discussion that follows will be limited to what is in the battery pack, meaning, cells, interconnects, and the battery management system. Everything outside the pack was considered part of the vehicle, charging station, or infrastructure and will be discussed in later sections. Reference Appendices A and B for more in-depth discussions and reference materials for batteries as they relate to XFC.

2.2 Battery Cost

Appendix A contains detailed technical discussions and reference material concerning battery cost analysis.

For EV batteries, thicker anodes are ideal because they allow for greater energy density and specific energy or the amount of energy per weight and volume represented as Wh/L and Wh/kg, respectively. However, for fast charge, thinner electrodes are more suitable in order to mitigate lithium plating. Lithium plating and other technical barriers and explanations related to the role that electrode thickness plays in the fast charging of batteries is discussed in later sections.

To investigate the incremental cost associated with XFC, a battery performance and cost (BatPaC) simulation was performed. Design for the battery pack assumes production volumes of 100,000 units per year. Table 2 shows the change in cost of an 85-kWh pack when charging time is decreased. This analysis assumes a change in state-of-charge (SOC) of 60% (51 kWh) and 80% (68 kWh) added to the pack, which, when assuming 3.5 miles added per kWh charged, translates to 178.5 miles and 238 miles, respectively. From Table 2, it is shown that cost increases from \$103/kWh to \$196/kWh at the cell level when charge time is reduced from 61 minutes to 10 minutes, respectively. The cost increase is inversely proportional to the thickness of the anode.

Summary Report

Table 2. BatPaC simulation comparing the effects of charging time on the required anode thickness, heat generation in the pack, and the resulting temperature rise, pack cost, and incremental cost of charging faster than 1-C (60 minutes) rate. Cell Chemistry: NMC 622-Graphite; Pack Energy: 85 kWh; Rated Power (10-second burst): 300 kW; maximum allowable current density: 4 mA/cm²; number of cells per pack: 240 [Appendix A].

Charging Time, ΔSOC=80%, minute	8	10	23	47	53	61
Charging Time, ΔSOC=60%, minute	5	7	15	30	34	39
Charger Power Needed, kW	601	461	199	100	88	77
Anode Thickness, μm	14	19	43	87	98	103
Heat Generated during Charge, kWh per pack	2.35	2.20	1.89	1.77	1.75	1.45
Post-Charge Cell Temperature (ΔSOC=80%), degrees C	22.4	24.4	25.9	26.4	26.4	19.5
Cell Mass, kg	2.75	2.40	1.74	1.49	1.46	1.45
Cell Cost to Original Equipment Manufacturer, \$ per kWh	\$229	\$196	\$132	\$107	\$104	\$103
Cost Difference, \$ per kWh	\$126	\$93	\$30	\$4	\$1	\$0

2.3 Cell Level

Appendix A contains detailed technical discussions and reference material concerning batteries at the cell level.

Lithium Plating

During charging, lithium ions move from the cathode electrode and intercalate, or get inserted, into the graphite anode electrode. As the charge rate increases, more lithium ions move from the cathode into the anode. At high charging rates, the lithium ions cannot move into the graphite because the carbon sites are filled or nearly filled and intercalation slows down, typically seen at high states of charge. As a result, lithium ions deposit, or plate, as lithium metal on the surface of the anode as seen in Figure 3. Lithium plating can lead to capacity loss, increases in resistance, and potentially a short circuit.

The quantity of lithium deposited on the surface can depend on the areal density (i.e., loading, electrode thickness, expressed in mAh/cm²) of the electrode (Figure 4). The desired areal density from a performance and cost perspective is 4.4 mAh/cm², but, as shown in Figure 4, when fast charged, the higher loading plates more lithium metal on the surface of the graphite anode. Under the best circumstances, the deposited lithium can be removed using a very slow discharge cycle. However, this is not necessarily feasible with an EV because the discharge cycle is dictated by the user and surrounding traffic patterns. Impacts to performance and life will be realized if the plating is non-reversible.

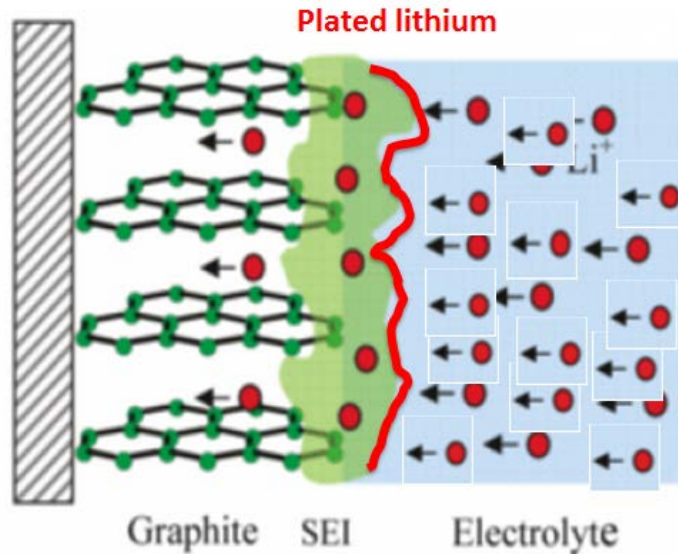


Figure 3. At high charge rates, a much larger number of lithium ions move to intercalate into graphite as represented by the red dots. However, there is not enough time or space for intercalations; therefore, lithium ions may start plating as metal onto the surface of the graphite electrode (shown as the thick red line) [Goodenough, J.; Kim, Y. *Chem. Mater.* 2010, 22, pp. 587-603].

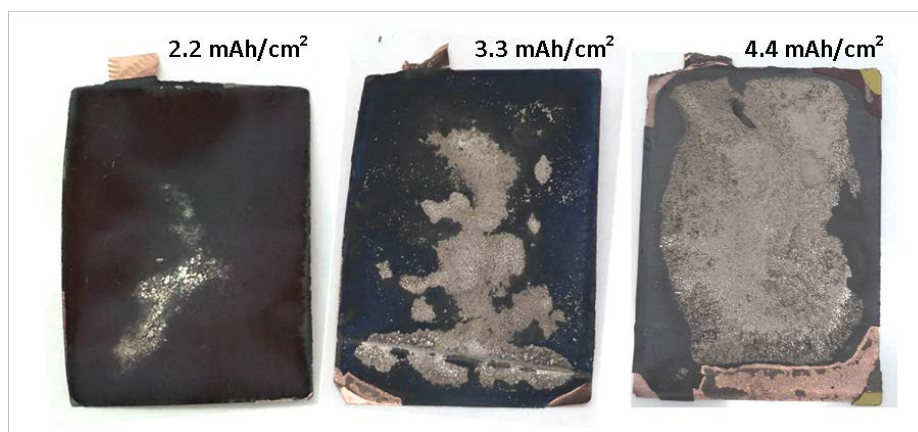


Figure 4. Images of graphite electrode after aging in NMC622/Gr pouch cells. Lithium plating appears as metallic deposits on the surface of the electrode and increases with higher loading (mAh/cm²) as shown from left to right [Appendix A].

Anode Materials

There are many anode chemistries with varying degrees of technology maturity. Carbon-based anodes such as graphite are some of the most prolific materials in the lithium-ion battery industry (automotive included). However, when graphite is lithiated during recharge, the electrochemical potential of the electrode can become very low. Therefore, lithium plating can more easily occur, especially as the battery approaches the fully charged state. Lithium titanate (LTO) possesses a much higher potential, albeit with lower density, when fully lithiated compared to graphite, which suggests plating lithium may be more difficult. LTO has much data supporting the suitability of the material to repeatedly and reliably charge at rates as high as 10-C. Silicon offers advantages for fast charge in the form of reduced anode thickness due to very high areal capacity when compared with a graphite anode. However, electrodes containing silicon for fast charge applications have not been described in the literature and their status as a viable XFC candidate is not currently known despite the technology's rapid maturation. Lithium metal technology needs to mature; therefore, it may not be a suitable candidate for XFC applications in its current state.

Cathode Materials

A review of the literature shows that the impact of high-rate charging on cathode electrodes has not been discussed. However, some reports investigate the impacts of stress-induced voids, cracks, and fragmentation of the cathode brought on by volume changes and concentration gradients as the cells are repeatedly charged and discharged. It is thought that XFC applications could exacerbate these effects.

Electrode Design

Increasing the areal capacity, often referred to as electrode thickness or loading, in lithium-ion batteries is one possible means of increasing pack level energy density while simultaneously lowering cost. Most currently produced automotive lithium-ion cells utilize modest loadings in order to optimize life throughout vehicle battery operation. This trend can be attributed to poorly understood physics that limit the use of high areal capacity as a function of battery power to energy ratio. In general, increases in areal capacity yield larger performance and life degradation as charge rate increases.

Other Cell Materials

A review of the literature does not yield anything regarding the effect of XFC on binder, electrolyte, and separator, but these battery materials can degrade when subjected to higher temperatures.

2.4 Pack Level Design

Appendix A contains detailed technical discussions and reference material concerning batteries at the pack level.

An adequately designed pack in terms of voltage and current is crucially important to enabling XFC. Today, most of the existing EV battery packs are rated at or below 400 V with a maximum current rating up to 300 A during charging. Figure 5 shows charge current with respect to charge power for different battery pack voltages. Higher currents would generate more heat, which would increase thermal load on the pack cooling system. More robust bus bars, tabs, current collector foils, fuses, disconnect switches, and insulation would also be needed to accommodate the higher currents, thus increasing pack weight and cost. The EVSE would have to accommodate the higher current.

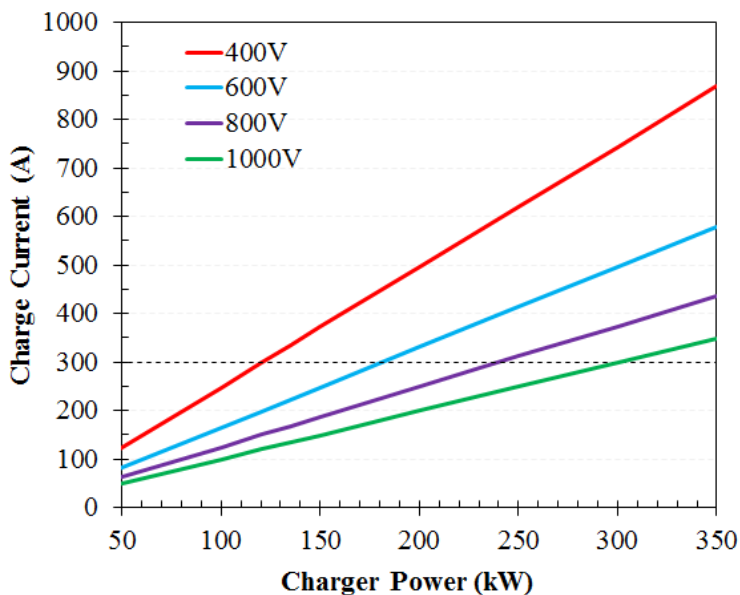


Figure 5. Charge current with respect to charge power for different battery pack voltages. The 400-V configuration shown in red is representative of a typical EV battery pack today.

Issues associated with high currents during XFC could be eliminated by increasing the pack voltage (Figure 5). An increase in charging voltages to 600 V, 800 V, and 1,000 V would reduce the charging current by 33, 50, and 60%, respectively, compared to the existing 400-V packs. This could lead to significant reductions in pack weight and cost. Increased voltage would also decrease the pack capacity by approximately the same factor, thus the effective charging C-rate (or charging time) remains the same.

Cell balancing during XFC poses another potential issue in pack design. Over time, it is possible for the cells to age at slightly different rates, leading some cells to have higher capacities than others. Advanced battery management systems and algorithms will be needed to minimize the impact of cell imbalance on pack life and performance.

2.5 Battery Thermal Management

Appendix B contains detailed technical discussions and reference materials concerning battery thermal management as they relate to battery XFC.

Thermal System Design

Thermal management as it relates to XFC will be a challenging barrier to overcome. Currently, many of the thermal issues, such as those identified in the cell level sections, can be addressed by using low energy density or power cells in combination with an oversized thermal management system. However, this system will not meet DOE cost, mass, and volume targets for a BEV and the cost alone could pose a barrier for mass market penetration. In order to meet these targets, we will need to investigate new thermal management strategies for cell and pack cooling and will need to greatly improve thermal efficiency of many advanced cathodes and anodes presently under development. The cell thermal design for these advanced chemistries will also need to be optimized in order to limit the lifecycle effects on the battery pack associated with XFC. Thermal modeling and simulations of these XFC capable systems will help develop, advance, and verify the technology. Based on a simulation outlined in Appendix B, the temperature rise for a XFC pack during a 10-minute fast charge can be more than 270°C.

2.6 Summary of Battery R&D Needs

Appendices A and B contain detailed technical discussions and reference material concerning battery R&D needs.

Material and Cell Level Needs

- Anode materials R&D in order to prevent or mitigate lithium plating and minimize cell heat generation. Focus should be placed on fast reaction kinetics to enable high-energy content and low potential in the lithiated anode material.
- Electrode designs that accommodate the need for fast diffusion in and out of a reaction site need to be developed.
- Study of the impact XFC has on existing current state-of-the-art materials and cell chemistries.
- Understand/detect/prevent lithium plating in operation to remedy safety and performance issues.
- Abuse response of battery (i.e., mechanical, thermal, and electrical) due to XFC.

Pack Level Needs

- Thermal management improvement for better heat transfer from the cell and finding the most suitable method of heat rejection outside the pack.
- Electrical safety and insulators for voltages up to 1,000 V.

- Charging protocol optimization to minimize degradation of the pack, such as multi-stage constant current/power charging.
- Robust battery control and management algorithms to control a pack with a greater number of cells in series.

3 Vehicle

3.1 Introduction

For the BEV market to be successful, it is anticipated that significant improvements in battery performance and range will be needed, along with a dramatic reduction in charge time. XFC looks to accomplish these tasks, which will help significantly mitigate the shortcomings of BEVs for long-distance travel. Furthermore, XFC can provide alternative charging in densely populated areas, servicing those who live in multiple occupancy dwellings and users without access to overnight home charging or charging at their workplace. The potential to reduce range anxiety for travel within a city when charging may be unplanned could also be realized with XFC. Lastly, XFC-capable BEVs should continue to support home and workplace charging with AC onboard chargers that provide the easiest and most convenient means for vehicle charging.

BEVs that support XFC may bring other benefits to their users. Higher discharge and charge power capability may offer quicker acceleration and more effective regenerative braking. XFC charge powers can charge a larger battery in a shorter time, which could enable more travel and may allow the owner to take advantage of lower electrical fuel costs.

The discussion that follows will be limited to what is in the vehicle. Meaning, power electronics, system interconnects, and battery pack as a system are considered. Everything outside the vehicle is discussed in the battery or infrastructure sections. Appendix C contains more in-depth discussions and reference materials for vehicles as they relate to XFC.

3.2 Range and Battery Capacity for XFC Capable Vehicles

Appendix C contains detailed technical discussions and reference material concerning range and battery capacity for XFC capable vehicles.

To expose the potential differences in travel time for long distance motoring in a BEV and ICEV, a hypothetical drive from Denver, Colorado to Salt Lake City, Utah covering 525 miles was analyzed. Figure 6 shows the results breakdown for four different vehicle types. Interestingly enough, there is only an 8-minute difference in travel time between ICEV and the XFC-enabled BEV with a 300-mile range battery.

Summary Report

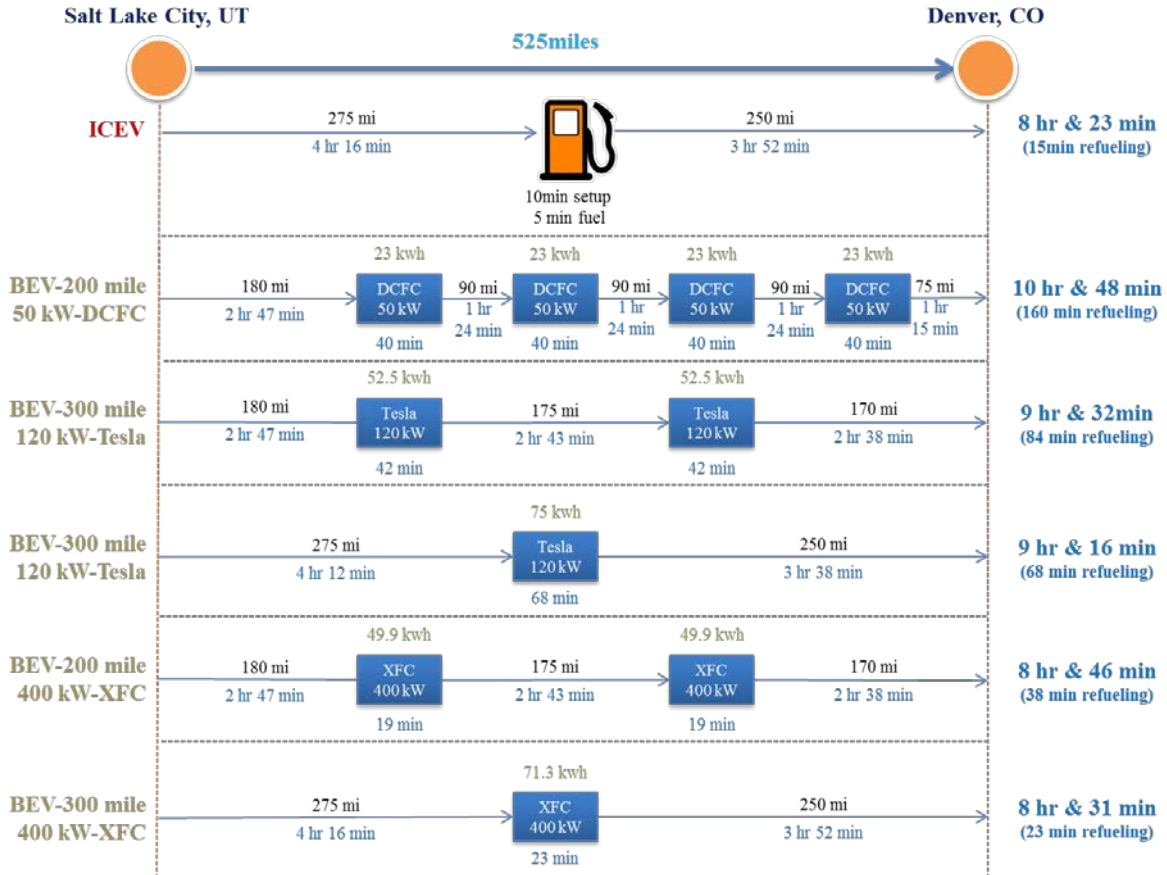


Figure 6. Intercity travel from Salt Lake City to Denver – ICEV versus BEV [Appendix C].

3.3 Electrical Architectures

Appendix C contains detailed technical discussions and reference material concerning vehicle electrical architectures.

High-Voltage System Architecture

A higher charging voltage will reduce the cable size between the charger and the vehicle. However, this requires an innovative power electronics architecture and component changes inside the XFC-capable BEV. Figure 7 presents four possible options for XFC voltage-capable BEV architectures.

The first option (Figure 7(a)) adopts the existing BEV architecture, but upgrades each component to support 1,000-V and 400-kW charging. A discussion about impact to the power electronic component design for this voltage change is included in the following section.

The second option (Figure 7(b)) is to design a configurable battery that can connect in series to provide 1,000 V for charging and connect in parallel to provide a 500-V DC bus for driving. This architecture requires complex battery management and electronics to convert the battery connection from series to parallel or vice versa. Implementing this connection can be challenging because the two battery strings may have different impedance and temperature conditions that could lead to state-of-charge imbalances.

Summary Report

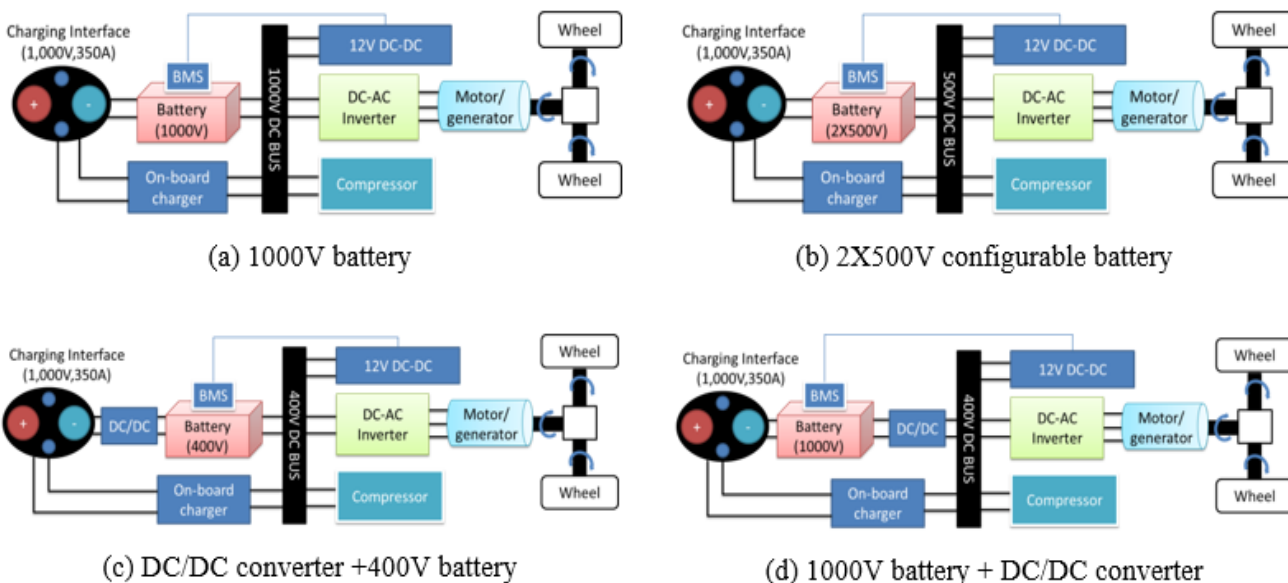


Figure 7. Options of 1,000-V BEV architectures [Appendix C].

The third design (Figure 7(c)) is to add an additional DC/DC converter between the charge interface and the battery to allow for existing 400-V power electronic components. The converter between the charge port and battery would need to be capable of 400 kW to maximize the benefit of XFC infrastructure. Implementing this design would burden the vehicle with additional volume, mass, and cost constraints of a converter, which only provides benefit for use with XFC infrastructure.

The final design (Figure 7(d)) adds an additional DC/DC converter between a 1,000-V battery and the 400-V DC bus to allow the power electronic components to remain at their existing rating. This variant could allow for continued use of common auxiliary components across a manufacturer's hybrid electric vehicle, plug-in hybrid electric vehicle, and BEV vehicle models.

There are several challenges for designing new BEV architecture and components.

- Existing power electronics at the 1,000-V level have proven industry-standard components and technologies; however, there is limited exposure to automotive applications in this work.
- Increased voltage will require increased insulation and creepage requirements that may add volume and mass to the vehicles' electrical components, connectors, and cabling.
- Fusing in the vehicle from the main pack line to the sensing lines will require better clearing ratings. This may require new materials and fuse designs to meet the low -resistance requirements for high-accuracy measurements.

Analysis work is needed to understand how electrical architecture and corresponding component design will provide the most effective design that enhances the value of XFC charging and driving efficiency given use of the vehicle.

XFC Voltage Impacts on Power Electronics and Electric Machines

A higher XFC voltage rating will impact design of the internal electronics for inverters, which support the traction motor and alternating current compressor, and for the converters, which support the 14-V electrical onboard charger and battery management systems. Because automotive power electronics do not currently operate at these elevated voltages, R&D for components, subcomponents, and system designs would be

Summary Report

needed. Switches for these devices could be replaced by 1,700-V insulated-gate bipolar transistors (IGBTs) or 1,700-V silicon carbide metal-oxide-semiconductor field-effect transistors (MOSFETs) (both are available). However, the maturity of the MOSFETs is not as far along as the IGBTs. Film capacitors for the DC bus also exist in the 1,400 to 1,700-V range and could be substituted for existing components. However, design of gate drivers and other sensing and control components would need to be modified to account for the higher isolation requirements.

Similarly, design of electric machines in the vehicle would need to change as a result of higher operating voltages. This would impact the traction motor design and refrigerant compressor motors depending on the auxiliary component design for the BEV. These motor designs would need new insulation, winding, and magnetics designs to account for the higher system voltage. The higher voltage should improve the motor's power density and allow for higher base speed operation in the design. However, changes to insulation material or thickness could impact thermal performance of the motor, which may lead to lower power density to achieve adequate cooling performance.

Higher voltage is expected to allow for better use of wide bandgap semiconductor devices (i.e., silicon-carbide or gallium nitride), which have superior performance characteristics compared to current state-of-the-art silicon devices. R&D efforts are needed in applying these devices to automotive systems. Specifically, package stack thermal resistance may increase, leading to reduced heat transfer and increased need for research in thermal management and thermal reliability.

XFC Impacts on Battery Electric Vehicle Charging System Design

Several factors should be considered to ensure appropriate cables are selected to support 1,000-V and 400-A XFC is needed. The connector shapes and interfaces should be standardized to assure interoperability with new and existing BEVs. Existing connectors that manufacturers are offering at the maximum current rating of 250-A and with convective cooling cannot support 400-A XFC. One option is to integrate a liquid cooling circuit into the cables and connectors. With the new liquid-cooled cable and connector system, a constant charging current of 350 A and short-term events up to 400-A DC maximum are possible while still providing a flexible, small-diameter and low-weight cable solution. A summary of the existing and proposed connectors with voltage and current ranges are shown in Figure 8.

Summary Report

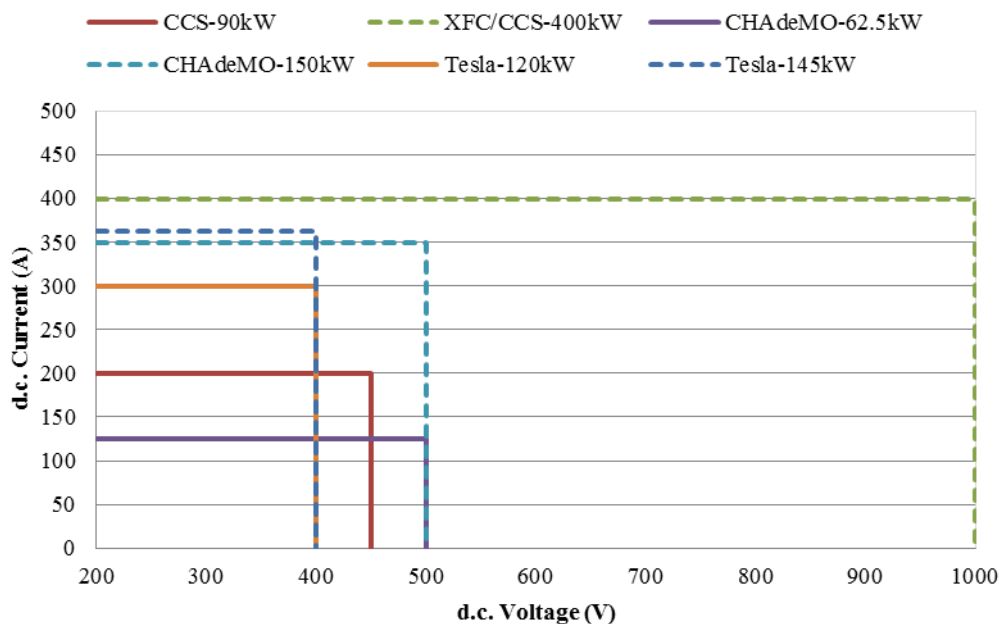


Figure 8. Charging connector voltage and current range for new and existing vehicles [Appendix C].

Pack configuration, size, rated voltage, and battery chemistry can potentially differ between BEV manufacturers, which may lead to a different or unique charging protocol. Even if the model of BEV is the same, different battery SOC, states of health, and battery temperatures at charge time may require different charging rates and charging voltages. Interoperability across all existing and new charging architecture must be a requirement.

3.4 Vehicle Thermal Management

Appendix C contains detailed technical discussions and reference material concerning vehicle thermal management.

Implementation of XFC is expected to have a significant impact on the vehicle's thermal system design. Existing EV thermal systems must meet many design criteria, including requirements for thermal management of the traction battery, power electronics, electric motor, and vehicle cabin thermal management. These conditions must be met while undergoing dramatically varying environmental conditions. Thermal system architectures vary in their complexity, from numerous independent thermal subsystems to a fully integrated combined system. Existing design capacities for these systems are based on peak and continuous heat rejection requirements for power electronics, electric motor, and battery system demands.

At 70% to 90% charging efficiency for the XFC event, depending on the cell type selected, thermal losses and subsequent battery cooling demands are expected to far exceed existing design capacities. Thus, in order to meet the cooling demands of the XFC event, either the onboard thermal system capacity will need to increase significantly or an independent cooling system associated with the XFC charging infrastructure will be necessary.

3.5 XFC Vehicle Cybersecurity

Appendix C contains detailed technical discussions and reference material concerning vehicle cybersecurity.

XFC and existing DC charging require critical communication between a BEV and the charging infrastructure to coordinate charging voltage and current. Unlike alternating current charging, this creates a vulnerability

Summary Report

because the onboard charge controller must communicate important battery constraints to the off-board battery charger. Enabling BEVs to support 1,000-V and 400-kW XFC charging could give hackers an enticing vulnerability to exploit. The higher power level could be used more easily to impact the grid than with other components. Furthermore, if XFC allows for a larger portion of the transportation fleet to become electrified, then a larger disruption to the transportation system could be effected by attacking this infrastructure.

The nature of XFC and existing DCFCs where vehicles may move from one charger to the next creates an interesting cybersecurity situation. It may be possible for a vehicle infected with malicious code to infect a charger, which then proceeds to infect other vehicles. The drivers of these newly infected vehicles could then unknowingly spread the malicious code to other chargers and infect the DC charging network. Therefore, a critical need exists for consistent security for BEVs to ensure safe, secure, and resilient DC charging. The point where the vulnerabilities could be used to gain access and exploit infrastructure beyond that of the BEVs to XFC should be identified. Cybersecurity must be built into the design criteria of BEV architecture, battery management systems, and XFC infrastructure.

3.6 Summary of Vehicle R&D Needs

Appendix C contains detailed technical discussions and reference material concerning vehicle R&D needs.

Electrical Architecture

- Assess how higher battery pack voltages (beyond current 400-V systems) will impact the overall volume, weight, and cost for power electronics in XFC-enabled BEVs.
- Analysis is needed to understand how best to design a vehicle electrical architecture for XFC that includes the vehicle duty cycles.
- Insulation requirements should be investigated to understand if extension of current practices to higher voltages is acceptable.
- Simulation and modelling efforts are needed to understand the tradeoff between a vehicle XFC-recharge range and the total recharge time.

Power Electronics and Electric Machines

- Development of automotive power electronic components and subcomponents that can handle elevated voltages, specifically including connectors and semiconductor devices.
- Motor designs for higher voltages with considerations for new insulation, winding, and magnetic designs to account for the higher system voltages.
- Research into a combined thermal loop for electric drive motor, power electronics, and the battery.

Cybersecurity and Interoperability

- Cybersecurity research of vehicle and EVSE communications is needed to ensure XFC and legacy vehicles can provide reliable transportation. Meaning, cybersecurity events will not disrupt the ability of the vehicle to serve as a primary mode of transportation.
- Evaluations and testing of existing combined charging system (CCS) connectors for XFC applications are needed to determine safe, reliable, and robust operating limits.
- Standardization efforts are needed to ensure interoperability so new and legacy vehicles are able to access XFC and existing DCFC networks.
- Interoperability of XFC charging systems and capabilities of different vehicle models and charging infrastructure.

4 Infrastructure

4.1 Introduction

The push to reduce charging time needed for BEVs creates a suite of intertwined R&D challenges. In addition to the R&D challenges for vehicles and battery technologies that have been described elsewhere, there is a distinct need to understand how fast charging up to 400 kW will impact the electrical grid, the design of EVSE, impacts brought by demand charges, and XFC-related infrastructure costs.

Public fast charging could increase BEV market penetration by allowing consumers who do not have access to either residential or workplace charging to use it as their primary means of charging. The use of BEVs in commercial applications (such as taxi, ride-share, or car-share services) where vehicles are heavily utilized could be enabled due to the added convenience of fast charging.

Early evaluations of the impact of DCFC up to 50 kW highlights the added flexibility that faster charging gives to BEV users. Presently, most BEV users charge at home followed by the workplace. With the emergence of DCFC (up to 50-kW) capability for Nissan Leafs, it has been observed that longer range trips using BEVs have occurred in the northwestern portion of the United States. The ability to use DCFC for longer trips, combined with automotive manufacturers producing a greater number of BEVs with range above 100 miles, closes the ‘range anxiety’ gap that exists between ICEVs and BEVs.

The discussion that follows will be limited to XFC-related equipment and grid infrastructure. Items specific to the battery and vehicle are discussed in prior sections. Appendix D contains more in-depth discussions and reference materials for infrastructure as it relates to XFC.

4.2 XFC Infrastructure Technical and Cost Considerations

Appendix D contains detailed technical discussions and reference material concerning XFC infrastructure technical and cost considerations.

Infrastructure Costs

Because of the complex nature of the infrastructure needed for XFC, three different areas were defined for analysis: (1) grid and utility needs, (2) charging station needs, and (3) EVSE needs. Across these areas, a successful development of codes and standards is needed on the part of multiple organizations that include industry and codes and standards bodies such as the National Fire Protection Association (NFPA). To address the safety of XFC, coordination between industry, local authorities, various authorities having jurisdiction (AHJs), and public utility commissions (PUCs) will become important. Stakeholder education and engagement will need to take place early and often in parallel with planning.

Charging Stations

Design of these charging stations needs to take into account a host of different issues such as power electronics and their thermal management, co-located energy storage or generation, and communications and interoperability. The stations also need to be part of corridor planning, which takes into account the human psychological perspective to allow consumers to feel unburdened by the distance between XFC charging stations. Satisfying this condition may require some overbuilding of infrastructure or more robust education and distribution of pertinent information (e.g., range) to consumers.

Regional variation and corridor optimization may also be key considerations during the planning process. Advanced understanding of BEV use patterns and how they are expected to change as BEV adoption rates increase and range increases also will be needed. Corridor planning efforts must be cognizant of grid issues such as anticipated changes in generation mix, aging substations, and distribution and transmission lines.

Summary Report

The general layout of an XFC station would entail multiple charging ports that would be situated to optimize flow of vehicles. Facilitation of XFC station throughput could be aided by standardization of the location of vehicle charge ports across manufacturers or the development of longer cables.

Electric Vehicle Supply Equipment – Technical Issues (Cables, Voltage, and Connector)

Among the most significant challenges are those associated with the type of charger and its compatibility with existing BEVs. Of particular impact is unification of codes and standards put out by the Society of Automotive Engineers (SAE) and National Electric Code (NEC) put out by NFPA, while still meeting the needs of the Occupational Safety and Health Administration (OSHA).

XFC-capable systems operating without a significantly higher voltage than what is currently used for DCFC require nearly 900 A of current. This requires wire gauge sizing that weighs over 10 lb/ft. Higher battery voltage significantly decreases cable wire gauge size. Figure 9 shows how, with increasing power levels, there is a distinct increase in cabling weight.

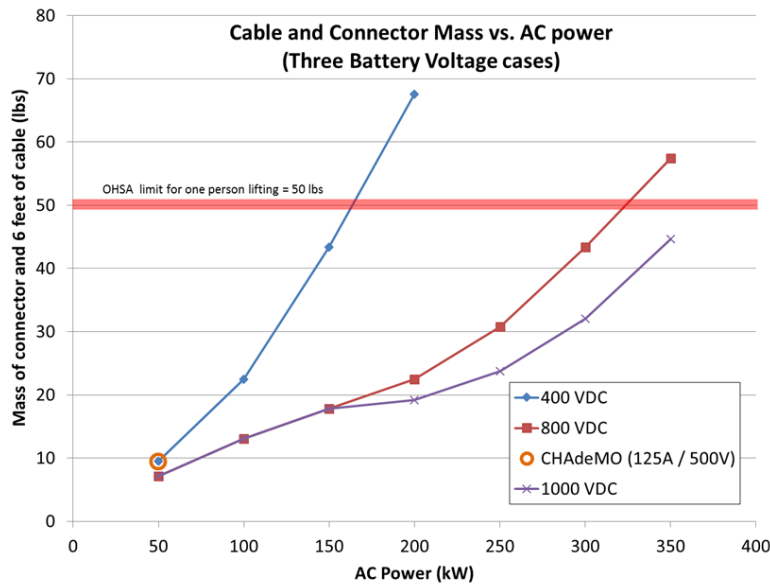


Figure 9. Comparison of uncooled cabling for EVSE operating at 400 or 800 V. Calculations use different copper cables that meet NEC ampacity ratings and use the current weight of a CHAdeMO connector [Appendix D].

Use of liquid cooling could significantly reduce overall cable mass and allow the average consumer the ability to charge using an XFC EVSE. However, currently there is no set agreement on how to accommodate liquid-cooled cables within NEC. Another option would be use of robotic or automated charging stations. A third option for not having heavy cables for conductive XFC is use of high-power wireless charging. To date, high-power wireless charging has been demonstrated at 50 kW, with plans for expansion to 200 kW and beyond for buses.

However, wireless power transfer of 400 kW in a light-duty vehicle application poses additional challenges. It is expected that the electromagnetic field generated by a wireless charger would have a larger radius and exceed allowable exposure limits outlined by the International Commission on Non-Ionizing Radiation Protection. To combat these limits, it is thought possible to shape the electromagnetic field in order to confine it to the undercarriage of the vehicle while focusing the field strength to the vehicle side charge receiving coil. Much research is needed in this area before commercialization can be realized.

Summary Report

Efforts to unite on a single connector for XFC purposes is something that will require direct codes and standards involvement on the part of industry (both vehicle and EVSE manufacturers) and independent specialists such as those located within the DOE national laboratory system.

Electric Vehicle Supply Equipment Installation and Equipment Costs

The cost of XFC installation and equipment is an important factor in understanding the business case of this technology. Current DCFC installation costs vary significantly and often depend on how close the EVSE is to existing power infrastructure. Analysis from the Recovery Act EV Project found that 111 DCFC installations ranged from \$8,500 to over \$50,000, with a median of \$22,600 [Appendix D]. Adding of new electrical service was the largest cost driver. The least costly installations were at retail shopping centers that had existing electric service to support DCFC EVSE.

Understanding the installation and interconnection cost of XFC at an “optimal” versus “non-optimal” site is necessary for planning XFC locations. A rough-order-of-magnitude analysis of a charging complex costs with six EVSE compared 50-kW DCFC and XFC EVSE at rural and urban corridor locations. The installation cost estimate per XFC EVSE ranged from \$40,300 to \$42,000. Estimated equipment costs for XFC EVSE are \$245,000 compared to the \$30,000 DCFC EVSE [Appendix D].

A distinct difference between lower-power DCFC and XFC equipment is cabling that is necessary for higher power. As charge power increases the current, the conductor size and weight increases. The addition of liquid cooling increases the complexity of an EVSE due to the need for pumps and a reservoir of coolant.

XFC Station Siting

Multiple charging stations will increase the overall power demand and hardware will create grid instabilities, along with an increased potential for power quality issues, or harmonics. Enhanced aging of transformers associated with high BEV adoption may also be possible. Siting and the appropriate power feed to an XFC location also need to be addressed. Direct interaction with multiple public utilities and coordination with multiple public utility commissions (PUCs) and other AHJs, which impact siting and requirements needed for permitting and registration of charging infrastructure, will need to be addressed. Broad variability in siting requirements across the country currently stands as a possible impediment to widespread implementation of XFC infrastructure.

4.3 XFC Utility Impacts and Demand Charges

Appendix D contains detailed technical discussions and reference material concerning XFC utility impacts and demand charges.

The cost of providing electricity for an EVSE at high power will be a crucial factor in the success of XFC. Electricity delivery cost is broadly inclusive of electricity generation, transmission, and distribution. Utilities often use demand charges, which are based on peak power usage, as a tool for accommodating the delivery of electricity to customers during high-demand periods. As such, demand charges are typically used for large electricity users that have high variability to provide compensation for the additional hardware and capacity needed to provide periodic high rates of power to the customer.

XFC is expected to be intermittent during its initial implementation and even after initial implementation some rural stations that are part of corridors may see low utilization. Often, when utilities install a new service (such as an XFC charging station), a connection fee is charged that covers a portion of the cost of the upgrade. The remainder of the cost is recovered through an energy charge (per kWh delivered) and/or a demand charge (per peak kW delivered). Demand charges can range from \$2/kW in Seattle to \$8/kW in New York and more than \$30/kW in Hawaii [Appendix D].

Summary Report

The impact of demand charges for fast charging is highly dependent on station utilization. When utilization is low, the energy provided is low and the demand charge per kWh delivered is high. With higher utilization, an EVSE's profitability becomes less dependent on demand charges.

Key technological possibilities to reduce the impact of demand charges are in incorporation of either onsite renewable generation that minimizes the total load needed from a utility or incorporation of stationary energy storage that could be used to supplement grid demand and, as a result, smooth use of energy and reduce total demand charges.

Distributed Energy Resources – Generation and Storage

Use of distributed energy resources to effectively minimize or remove demand charges requires that the storage be capable of operating during the high-power portions of charging events and also be able to remain in operation for extended periods of time. During high use times, multiple XFC events may occur either simultaneously at a single location or back-to-back at the same location. An effective energy storage solution would need to be able to buffer both the power and energy demands of such a station. The other key consideration for stationary energy storage is that it would need to charge at a sufficiently fast rate or be sufficiently oversized for a specific location to facilitate many events in a short timeframe (e.g., during a rush hour period). The inability to meet the demands of all XFC events would lead to increased demand charges and partially negate the benefits of stationary energy storage.

The side benefit of stationary energy storage is that during low use times, it may be possible to use the storage to provide ancillary services for grid operation or frequency regulation. However, there are challenges in providing ancillary grid services, particularly market size and market risk. Market size is limited; therefore, the market can saturate quickly. Market risk is also important, because prices for ancillary services are volatile.

For current installations, the highest use rates were closely aligned with the evening commute between the hours of 5 p.m. and 7 p.m. with very little use between midnight and 6 a.m. [Appendix D]. This suggests that it is probable that the enhanced implementation of other fast charging options such as XFC would have high use rates during the same time period.

Demand side management (DSM) has been used to mitigate impacts of peaky loads through control, including curtailment, of power demanded during times when the grid is operating near peak capacity. A key feature of DSM is that high-power loads are typically impacted at lower rates than lower power loads. An XFC station is likely to have instantaneous power demands, which are on the order or greater than what is seen for many mid-sized buildings in the United States. This level of power would suggest that XFC may not be an optimal choice for DSM and is counter to many discussions suggesting that BEVs could be a prime use case for DSM. Curtailing power to XFC stations, even briefly may decrease utilization of XFC stations by BEV drivers.

Total equipment and installation cost of the charging complex with photovoltaics (PV) and energy storage system (ESS) ranged from \$1.4 to \$1.7 million due primarily to the assumed higher cost of EVSEs [Appendix D].

4.4 XFC Infrastructure Cyber and Physical Security

Appendix D contains detailed technical discussions and reference material concerning XFC infrastructure cyber and physical security.

One area that crosses all three levels of infrastructure needs for XFC is combination of physical and cyber security. Because of the high rate of energy transfer needed for XFC, there has to be private and secure communication between the vehicle and EVSE. Communication between the grid and the charging station also is expected. This tiered communication presents the possibility that significant cyber security issues could arise with an expansive XFC network.

It is important to continuously assess the resiliency of a physical system such as an XFC charging station by using scientifically sound techniques. The impact of malicious operation of XFC on the power systems needs to be assessed and control actions to counter impact should be designed in advance.

4.5 Summary of Infrastructure R&D Needs

Appendix D contains detailed technical discussions and reference material concerning infrastructure R&D needs.

EVSE R&D Needs

- Research technological improvements for advanced materials with better thermal and electrical properties to reduce and manage thermal loads in EVSE, in particular, the cable, but more materials research and equipment design engineering are needed.
- Investigate automated EVSE for XFC applications.
- Research wireless power transfer technology electromagnetic field shaping and shielding for 400-kW light-duty vehicle applications

Industry Focused R&D

- Coordinate and harmonize permitting, siting, and regulatory requirements to simplify XFC planning and deployment.
- Unify and harmonize codes and standards including items such as applicability of liquid-cooled cables, connector design, and cabling limitations.
- Ensure industry and AHJ engagement in standardization organizations such as SAE, NFPA, and others.
- Research to support effective coordination of corridor planning. Understanding where XFC charging stations need to be sited to serve demand by BEV drivers and where the appropriate grid resources exist to initially serve the greatest number of consumers.

5 Conclusion

Many technical gaps and challenges for XFC have been identified in this report which impact several key technology sectors such as automotive OEMs, battery manufacturers, codes and standards bodies, EVSE manufacturers and network operators, and utility suppliers. For XFC to be successfully implemented, these technology sectors need to foster new levels of collaboration and communication regarding technology intersections and overlaps.

A large barrier to BEV adoption is the cost of batteries. XFC could increase the cost of a cell by more than 90% (\$103/kWh to \$196/kWh) with anode thickness the primary cost driver. Within battery cells, a bulk of the research needed centers around the anode and mitigating the onset of lithium plating and minimizing heat generation, which can lead to dramatic cell degradation and pose safety concerns. Heat generation in general is a known mechanism for electrochemical and mechanical battery material degradation. As such, thermal management of batteries when subjected to XFC protocols require R&D. Thermal management research coupled with robust battery management controls and charging protocols R&D will help achieve XFC while prolonging life.

For vehicles, higher voltage battery packs, up to 1000V from conventional BEV's 400V packs, can drive much research in the electrical architecture of the vehicle and the power electronics which support the electric drive system. With higher voltage comes the need for more robust insulators along electrical pathways that comply with ampacity requirements and meet strict vehicle weight, volume, and cost metrics. Specific to automotive applications, power electronic components and subcomponents as well as electric motors may need research to

Summary Report

cope with XFC duty cycles and high voltage vehicle electrical architectures. Cybersecurity and interoperability of vehicle and EVSE communications is needed to ensure XFC capable vehicles, and legacy vehicles alike, can provide reliable transportation and not be disrupted by cybersecurity events or differences in charging equipment.

EVSEs and the method in which power is delivered from the electric grid to the BEVs need investigating. For conductive charging, research into thermal management of the EVSE power electronics and charge cable are the largest areas of interest. In wireless power transfer, electromagnetic field shaping and field shielding require the most R&D investment. Infrastructure sees the introduction of the largest and most broad base of stakeholders ranging from EVSE manufacturers and network operators to utility suppliers and regulators. Coordination and cooperation within this group of stakeholders is recommended in order for XFC to make it to market. This relates to permitting, station siting, codes and standards harmonization through organization such as SAE and NFPA, and XFC network planning on transportation corridors.

This report and the gaps identified within could serve as a useful guide for research programs spanning varying degrees of technology maturity across a broad industry landscape. Identification and dissemination of XFC technical issues will help the stakeholder community focus and advance each technology area at a quicker pace than may otherwise be possible if each organization were to undertake a similar effort on its own.

Appendices

Appendix A



Enabling fast charging – A battery technology gap assessment



Shabbir Ahmed^a, Ira Bloom^{a,*}, Andrew N. Jansen^a, Tanvir Tanim^b, Eric J. Dufek^b, Ahmad Pesaran^c, Andrew Burnham^a, Richard B. Carlson^b, Fernando Dias^b, Keith Hardy^a, Matthew Keyser^c, Cory Kreuzer^c, Anthony Markel^c, Andrew Meintz^c, Christopher Michelbacher^b, Manish Mohanpurkar^b, Paul A. Nelson^a, David C. Robertson^a, Don Scofield^b, Matthew Shirk^b, Thomas Stephens^a, Ram Vijayagopal^a, Jiucai Zhang^c

^a Argonne National Laboratory, 9700 South Cass Avenue, Argonne, IL 60439, USA

^b Idaho National Laboratory, 2525 N. Fremont, Idaho Falls, ID 83415, USA

^c National Renewable Energy Laboratory, 15013 Denver West Parkway, Golden, CO 80401, USA

HIGHLIGHTS

- Key gaps in lithium-based battery technology are presented viz. extremely fast charging.
- At cell level, lithium plating on anode remains an issue.
- At cell level, stress-induced cracking of cathode material may be an issue.
- Safety at pack level must be explored.

ARTICLE INFO

Article history:

Received 22 April 2017

Accepted 18 June 2017

Keywords:

Lithium-ion battery
Extreme fast charging
Developmental needs

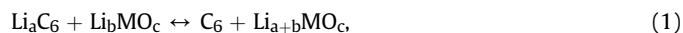
ABSTRACT

The battery technology literature is reviewed, with an emphasis on key elements that limit extreme fast charging. Key gaps in existing elements of the technology are presented as well as developmental needs. Among these needs are advanced models and methods to detect and prevent lithium plating; new positive-electrode materials which are less prone to stress-induced failure; better electrode designs to accommodate very rapid diffusion in and out of the electrode; measure temperature distributions during fast charge to enable/validate models; and develop thermal management and pack designs to accommodate the higher operating voltage.

© 2017 Elsevier B.V. All rights reserved.

1. Introduction

A lithium-ion cell usually consists of a metal oxide, such as LiCoO₂, as positive electrode; a mixture of organic carbonates containing a lithium-bearing salt as the electrolyte; and graphite as the negative electrode. During charging, lithium ions move from the positive electrode through the electrolyte and intercalate into the negative electrode; and, during discharge, they move in the reverse direction. The overall cell reaction is shown in Eq. (1) [1,2], with the charge reaction proceeding to the left and discharge, to the right:



where $a \approx 1$, and M is a metal such as Mn, Co, Ni, etc.

During cell operation, the electrode particles become coated with products from the reaction between the electrode and the electrolyte. This coating is called the “solid-electrolyte interphase” (SEI). At the positive electrode, the SEI layer consists of electrolyte oxidation products, and, at the negative, electrolyte reduction products. Thus, the SEI layers are compositionally different, but both serve to passivate the electrode surface. At the positive electrode, the surface film can consist of Li₂CO₃ (from handling in air) and lithiated carboxylates, such as ROCO₂Li and alkylated metal oxides [1]. At the negative electrode, the number of possible components in the SEI increases. Lithiated alkoxides and carboxylates are formed by a free-radical reaction of the electrolyte

* Corresponding author.

E-mail address: ira.bloom@anl.gov (I. Bloom).

solvent with the negative electrode. In addition, LiF and lithiated oxyfluorophosphates are formed by the reduction and reaction of LiPF_6 , a common salt used in the battery electrolyte [1,3,4].

Lithium-ion batteries are used in applications that need high energy or power densities. Thus, they are ideal for electric vehicles. Other battery technologies, such as Li/S and Li/O₂, in theory, can be used for the automotive application. But, as of this writing, these technologies are still immature and require much further development.

Typically, recharging lithium-ion batteries takes considerably longer than refueling of the internal-combustion-engine (ICE) car. Consumer acceptance of electric vehicles (EVs) will be facilitated by a recharge (“refueling”) experience similar to that of an ICE-powered car, roughly 8–10 min. Additionally, recharging does not have to be from a completely discharged battery (empty) to a completely charged one (full). As with an ICE car, partial recharging is possible and should not adversely affect the battery.

The increased rate necessary for fast charging can adversely affect the performance, safety, and life of the battery, such as increased probability of lithium plating, increased rate(s) of side reaction(s), and increased battery temperature. This paper will focus on just the issues in battery technology. The heat rejection/management aspects will be discussed in a separate manuscript.

Available direct current fast chargers on the market are capable of charging light-duty EV battery packs at rates up to 120 kW, which is not sufficient to offer nearly the same refueling experience as gasoline consumers. For the purpose of this document, the next level of charging, extreme fast charging (XFC), is defined as recharging up to 80% of the battery capacity in 10 min or less. This definition has two caveats. It does not define the starting point of charging, which is consumer behavior driven and an unknown at this point; and it does not consider pack size, i.e., for a given available charging power, a smaller pack would charge faster than a bigger pack but not necessarily provide more driving range, assuming there is no current limitation.

Fig. 1(a) shows a theoretical plot of recharge time up to 70% capacity [state of charge (SOC) increased from 10% to 80%] and the corresponding charging rate as a function of charging power for three battery pack sizes with existing 400-V maximum charging voltage. The lower SOC limit, 10%, was assumed to avoid consumer range anxiety, and the higher one, 80%, was assumed to mitigate accelerated aging and safety concerns during XFC. It is obvious that the charging rate increases (or charging time decreases) with charging power regardless of the size of the pack. At a specific charging rate, increased pack size requires more time to charge due

to reduced effective C-rate. This indicates that chargers should be scaled based on the pack size to achieve the desired 70% recharge in 10 min. If pack size is large, e.g., 90 kWh, charging at the 400 kW rate is not sufficient to meet the recharge goal in 10 min. Bigger packs, however, will add much more driving range than the smaller packs for the same SOC increment.

Miles added per minute (mi min^{-1}) is another way of defining XFC. The U.S. Department of Energy (DOE) has set a fast charge goal (average) of 20 mi min^{-1} [5] or more. Fig. 1(b) shows XFC charging speed in terms of mi min^{-1} for EVs available in the market with XFC capability [6–10]. Also shown is an estimate of charging speed using a 400 kW XFC charger, assuming 300 Wh mi^{-1} energy consumption. While the charging speed of most of the EVs remains below 3 mi min^{-1} , Tesla can achieve up to 5.6 mi min^{-1} with its state-of-the-art 120 kW direct-current fast charger, which is the highest rate among all the EVs available in the market today.

The discussion that follows will be limited to what is in the battery pack, that is, cells, interconnects, and the battery management system. Everything outside the pack was considered part of the vehicle, charging station, or infrastructure. These items will be discussed in separate papers. The remaining sections of this paper are organized according to aspects of the technology.

2. Cell level

2.1. Lithium plating

Lithium ions (Li^+) are transported from the positive to the negative electrode during charge. These ions then reach the interface between the electrolyte and the negative electrode. Under normal operating conditions, lithium (Li^+ plus an electron from the external circuit) intercalates, as in the case of graphite, into the negative electrode material in stages, filling the space between the graphite layers (galleries) in a step-wise fashion [11–14]. However, intercalation is a diffusion-limited process, only a certain amount of lithium can enter the galleries per unit time at a given temperature. As the galleries fill, the rate at which more lithium can enter decreases. If lithium transport to the surface of the negative electrode is faster than it can intercalate, lithium metal can plate on the surface of the negative electrode.

Lithium plating can occur when the local potential at the negative electrode is below 0 V (vs. Li/Li^+) [15–17]. This can happen when the net cell voltage is about 4 V or greater in a capacity-balanced cell system (negative-to-positive ratio near 1.1). Lithium plating was reported to increase with increasing current density

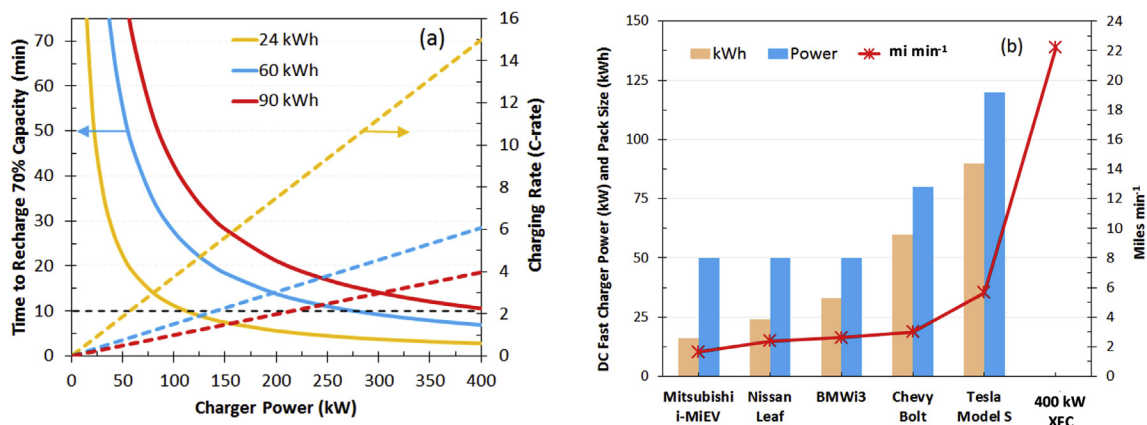


Fig. 1. (a) Time of charging and corresponding C-rate for different battery packs as a function of charger power. (b) Charging profiles for EVs with direct-current fast charging capabilities in the market [6–10].

and with decreasing temperatures [16–19]. Plating can occur at charge rates as low as about C/6 at $\sim 20^\circ\text{C}$ [17]. Additionally, there is a report that defects can cause lithium plating. Defects, “such as pore closure [in the separator], create local, high currents and overpotentials. If the overpotential exceeds the equilibrium potential in the negative electrode, plating can occur [20].”

As lithium deposits on the surface of the negative electrode, its quantity tends to depend on capacity loading in the electrode, as shown in Fig. 2. In the best case, the deposited lithium will be removed during the following discharge subcycle. However, in the work of Gallagher et al. [21], even slow discharges before cell disassembly failed to remove the lithium deposits to any noticeable extent. This finding suggests that the lithium deposits are not electronically connected to the graphite electrode. Under other circumstances, it can affect the performance and life of the cell.

Non-destructive (*in-situ*) methods to detect lithium plating have appeared in the literature [16,22–25]. The methods include high-precision coulometry during charge to detect changes in cell efficiency, volumetric measurement of small changes in cell volume, calorimetry to measure changes in cell heat flow, and voltage monitoring to detect a high-voltage plateau that corresponds to stripping lithium metal from the graphite surface.

With constant-current charging, lithium is delivered to the negative electrode at a constant rate. If the delivery rate is less than or equal to the rate at which lithium intercalates, then lithium will probably not be deposited on the electrode surface. Of course, other factors can change this so that lithium does *indeed* plate, such as an increase in local chemical potential.

The influence of capacity loading and charge rate on lithium plating was investigated by Gallagher et al. [21]. These results are summarized in Figs. 2 and 3 for cells with capacity loadings of 2.2–6.6 mAh cm⁻². These results were obtained with capacity-matched cells using graphite negative electrodes and LiNi_{0.6}Mn_{0.2}Co_{0.2}O₂ (NMC622) positive electrodes that were charged for 285 cycles at a C/3 rate, after which the charge rate was increased to C/1 followed by trickle charging to 4.2 V up to 549 cycles. The discharge rate was held at C/3 rate in all cases to remove that rate as a variable. The 2.2 mAh cm⁻² cell group shows no significant change in capacity fade, and the 3.3 mAh cm⁻² cell group displayed a relatively modest capacity fade. This suggests that the 3.3 mAh cm⁻² loading is near the maximum capacity loading for these materials and electrode design for operation at the C/1 rate. Further increasing the charge rate to 1.5-C at cycle 549 had a significant impact on the fade rate for the 3.3 mAh cm⁻² cells, and some modest effect on the 2.2 mAh cm⁻² cells, suggesting that the latter cells are near their maximum rate of 1.5-C. Increasing the charge rate from C/3 to C/1 had a severely negative effect on the performance of electrodes with loadings over 3.3 mAh cm⁻², as can be seen by large capacity loss in Fig. 3 and the extra lithium deposits

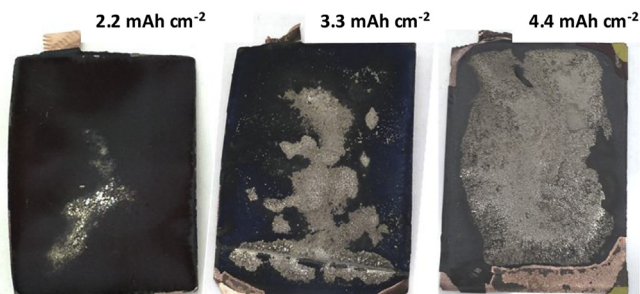


Fig. 2. Evidence of increasing lithium deposition (metallic gray) on graphite electrodes as a function of capacity loading. From Ref. [21].

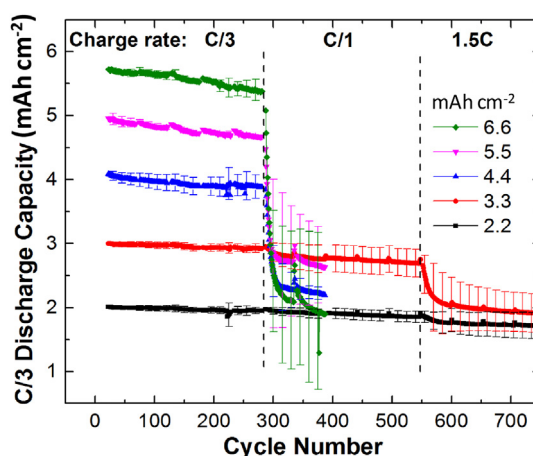


Fig. 3. Capacity fade for a series of graphite/NMC622 pouch cells of increasing areal capacity as a function of charge rate. Discharge rate was held constant at the C/3 rate. Figure reproduced from Ref. [21].

in Fig. 2. It is anticipated that modifying the charging current profile (e.g., fast charge at low SOC or slow charge at high SOC) could help prevent the formation of lithium deposits.

Evidence of lithium plating as a function of capacity loading and charge rate was further demonstrated by Gallagher [21] and is summarized in Fig. 2. These cells were disassembled in a dry room after a 24-h voltage hold at 3.75 V and then washed with dimethyl carbonate. As expected, cells with the largest capacity fade exhibited the most lithium deposits. Surprisingly, fully discharging one of the 4.4 mAh cm⁻² cells at a low rate before disassembly did not remove the lithium deposits from the negative electrode surface, which suggests that the lithium deposits became electrically isolated from the graphite electrode. This finding further suggests that occasional reconditioning of the battery pack (e.g., slow discharging) will not restore the lithium deposits to the positive electrode.

With fast charging, the rate of the above process would increase, limiting the life of the cell. The rate of the performance degradation (how fast) depends on the temperature at which the cell is operated; the nature of the active material and the design of the negative electrode; and, probably, the method by which the XFC is performed. Each of these topics will be discussed below.

2.2. Other negative electrode materials

The potential of completely lithiated graphite (LiC₆) can be as low as about 0.01 V vs. Li/Li⁺ [15–17]. The local chemical (and electrochemical) potential of the surface of the negative electrode plays an important role in the plating phenomenon. Thus, plating can easily occur on the graphite electrode, especially as it approaches full charge.

Other materials have been evaluated for use as the negative electrode in lithium-ion cells, such as Li₄Ti₅O₁₂ (LTO) and Si [26]. The potentials of these fully lithiated materials are 1.5 V (Li₇Ti₅O₁₂) and 0.05 V (Li_{4,4}Si) vs. Li/Li⁺ [27,28]. The consequence of the higher potentials at the negative electrode is that the energy content of the cell will be lower than those for graphite, but the higher potentials suggest that the conditions needed for lithium plating may be harder to obtain. There is also strong interest in using metallic lithium as the negative electrode, but the problems of lithium dendrite formation must be addressed to achieve long cycle life and acceptable safety.

2.2.1. $\text{Li}_4\text{Ti}_5\text{O}_{12}$

LTO seems to have the needed electrode kinetics to charge quickly. Several reports in the open literature mention that nanoparticles of this material can be charged at rates as high as 10-C repeatedly, with and without graphene coating or graphite additives [29–31]. The initial reversible capacity of graphene-coated LTO was reported to be about 121 mA h/g (uncoated: 75.4 mA h g^{-1}) at 10-C charge/discharge rates in half-cells. Further, the graphene-coated LTO possessed a capacity density of 104.8 mA h g^{-1} after one thousand cycles at the 10-C charge/10-C discharge rate, as compared to only 44.8 mA h g^{-1} for the uncoated material, again, in half-cells [29].

Doping LTO enhanced the electrochemical performance of the material. Bai et al. cycled $\text{La}_{0.06}\text{Li}_{3.94}\text{Ti}_5\text{O}_{12}$ at the 10-C rate for 1000 cycles. They observed a stable capacity of ~ 140 mA h g^{-1} [32]. Zhang et al. substituted Sc for Ti on the B-site on the spinel to improve the rate performance of LTO. They observed stable capacity for 50 cycles at the 20- and 40-C rates. The capacities at these high rates were ~ 110 and ~ 75 mA h g^{-1} , respectively, which was better than either pristine or coated LTO [33]. Xu et al. doped LTO with both Al^{3+} and F^- by coating pristine LTO particles with AlF_3 . After heat treatment at 400 °C, they found that Al^{3+} and F^- had entered the spinel structure and formed a composite material consisting of anatase and the doubly substituted spinel. The composite material displayed a stable capacity of ~ 171 mA h g^{-1} for 1000 cycles at the 1-C rate at room temperature [34].

There are reports that the sodium-bearing phases, $\text{Na}_2\text{Li}_{1.9}\text{Ti}_{5.9}\text{M}_{0.1}\text{O}_{14}$ ($M = \text{Al}, \text{Zr}, \text{V}$), have superior rate performance and cyclability to LTO. Indeed, Wang et al. reported that doping with the aliovalent cations increased the electronic conductivity and ionic diffusivity of the phase. They observed a charge capacity of 180.7 mA h g^{-1} from the Al-containing material while cycling at 1000 mA g^{-1} in coin half-cells [35]. Wang et al. continued their investigation on the effect of doping on the electrochemical performance of sodium lithium titanate. Phases containing metal dopants on the lithium site, $\text{Na}_2\text{Li}_{1.9}\text{M}_{0.1}\text{Ti}_6\text{O}_{14}$ ($M = \text{Na}^+, \text{Mg}^{2+}, \text{Cr}^{3+}, \text{Ti}^{4+}, \text{or } \text{V}^{5+}$), were prepared by solid-state reactions. These phases crystallize in the orthorhombic *Fmmm* space group. The Cr-bearing phase, $\text{Na}_2\text{Li}_{1.9}\text{Cr}_{0.1}\text{Ti}_6\text{O}_{14}$, was shown to have a capacity of 233.3 mA h g^{-1} at a charge rate of 700 mA g^{-1} in coin half-cells [36].

The electrochemical properties of sodium lithium titanate can also be changed by doping with non-metals. Ni et al. compared LTO phases that were doped with halides on the oxygen site, $\text{Li}_4\text{Ti}_5\text{X}_a\text{O}_{12-a}$ ($X = \text{Cl}, \text{Br}$), prepared by solid-state reactions. They reported that doping with halides was also a very effective means to change the electrochemical performance of these phases. They prepared and characterized the Br-substituted phases, $\text{Li}_4\text{Ti}_5\text{Br}_a\text{O}_{12-a}$ ($a = 0, 0.1, 0.2, 0.3$ and 0.4), from lithium acetate, LiBr, and tetrabutyl titanate by a liquid mix technique. They observed stable capacity of about 150 mA h g^{-1} over the course of 100 cycles at the 5-C rate (charge/discharge) in the $a = 0.2$ material. They attributed the improved performance to better electronic conductivity due to the presence of Ti^{3+} and to better particle dispersion [37].

Particle size and shape play an important role in the electrochemical performance of LTO-based phases. For example, P. Zhang et al. synthesized the doped LTO phase, $\text{Li}_{3.85}\text{Ti}_{4.70}\text{Cr}_{0.46}\text{O}_{12}$, as hierarchical mesoporous spheres using a single-pot co-precipitation method. They state that porous, homogeneous, spherical, nanometer-sized particles are important for high electrochemical activity [38] and cite work by Z. W. Zhang et al. using the Zn-substituted phase, $\text{Li}_{3.95}\text{Zn}_{0.05}\text{Ti}_5\text{O}_{12}$, as a point of reference. The Zn-substituted phase displayed a stable capacity of ~ 122 mA h g^{-1} during cycling at the 10-C rate [39]. The Cr-substituted, hierarchical material displayed ~ 153 mA h g^{-1} after 200 cycles at the 10-C rate.

Suitably-prepared LTO has been used as the negative electrode

material in commercial, high-charge-rate batteries, as evidenced by the following excerpts from the internet:

The [super charge ion] battery [SCiB] uses Toshiba's proprietary lithium titanate oxide to make a long-life cell that can go through 6000 charging cycles – about 2.5 times more than regular lithium ion batteries. The battery pack can do a rapid 80% recharge in just 15 minutes, and is capable of operating in temperatures as low as minus 30° Celcius [sic] The ability to recharge quickly is also an important selling point for potential EV customers. A quick charge with a dedicated recharging unit will restore a quarter of the battery capacity in 5 minutes. 10 minutes brings it up to 50% charge, and 80% is reached in just 15 minutes. Not quite as quick as refilling your tank, but then again with the abundance of electrical outlets and the future provision of charging points in parking lots, the idea of actually having to go to a particular place simply to get more energy for your car will seem rather quaint 10 years from now. The battery also emits much lower levels of heat when recharging and also requires less energy for cooling when in use [40].

The SCiB charges in about half the time of a typical Li-ion battery, Toshiba says. An SCiB 20Ah cell charged with an 80-A current will reach 80% of capacity in 15 minutes and 95% in an additional 3 minutes. The SCiB generates little heat even during this fast recharging, eliminating the need for power to cool the battery module. Moreover, the full charge-discharge cycle for SCiB is 4000 times, more than 2.5 times that of other Li-ion batteries. This long life could also contribute to the reuse of the battery [41].

Li-Titanate batteries are faster to charge than other lithium-ion batteries. Data shows that these batteries can be safely charged at rates higher than 10C [42].

Also, a graph displaying SOC versus time shows that the Toshiba SCiB cell can be fast charged at the 8-C rate [43].

2.2.2. Silicon

The response of the Si-containing electrode to fast charge conditions has not been described in the literature. Given the degradation propensity of the silicon electrode, both in terms of cycling performance and physically [26,44], it is not currently known if Si-containing electrodes would be viable candidates in this application, though there are claims that certain Si alloys and nanostructures are dimensionally stable [45–47].

2.2.3. Lithium metal

In their review, Aurbach et al. [48] stated that lithium metal cannot be used in applications requiring high power. Lithium was very reactive towards all electrolyte components and formed a complex SEI layer on the electrode surface. Moreover, the SEI did not prevent lithium dendrite formation, which formed during the charge process. Dendrites can grow and, eventually, breach the separator and short the cell.

López et al. [49,50] reported that the surface morphology of the lithium electrode was sensitive to cycling and the current density used to plate it. In the former experiment, the surface of lithium metal changed from smooth to rugged containing some dendrites. In the latter, there was a transition from smooth to dendritic, depending on current density.

Thus, the XFC operating conditions may exacerbate dendrite formation. Lithium metal thus may not be a suitable candidate for this application.

2.3. Positive electrode

The impact of high-rate charging on the positive electrode has not been discussed in the open literature. There are, however, reports that some positive electrode materials (lithiated metal oxides) are not dimensionally stable with cycling [51, 52, and references therein]. The diffusion of ions into and out of the host lattice can induce stress because of the associated volume change and concentration gradients [53]. A known cause of accelerated performance fade of lithium-ion batteries is voiding, cracking, and ultimate fragmentation of positive electrode active material particles due to diffusion-induced stress caused by high and repeated lithium intercalation/de-intercalation to and from the positive electrode matrix [54]. The fragmented primary particles disconnect from the positive electrode matrix and expose the active material to the electrolyte.

For example, Song et al. reported that the lithium-rich, layered material, $\text{Li}_{1.2}\text{Mn}_{0.54}\text{Ni}_{0.13}\text{Co}_{0.13}\text{O}_2$, underwent void formation, cracking, and fragmentation with cycling at even the C/4 rate. Starting with roughly spherical particles, a marked deterioration of the primary particle morphology occurred after about 50 cycles. Song et al. found that the average particle size decreased with cycling; the small particles were scattered throughout the electrode matrix [51].

Most research has investigated the failure mechanism caused by diffusion-induced stress when high-rate (up to 2-C) intercalation occurs into the positive electrode matrix for different positive electrode active materials, including LCO, LMO, LFP, NCM,¹ etc. [51,54–60]. The de-intercalation of Li ions from the positive electrode matrix during XFC could aggravate the diffusion-induced stress-related degradation mechanism at high rates and, especially, for non-uniform temperature scenarios.

2.4. Electrode design

The effect of increasing the areal capacity (loading) was studied by Gallagher et al. [21] for graphite (Gr)/NMC622 ($\text{LiNi}_{0.6}\text{Mn}_{0.2}\text{Co}_{0.2}\text{O}_2$) with the goal of demonstrating improved pack energy density and lower cost (i.e., less weight devoted to current collectors and separator). A thorough review was also discussed in this work, and focused on relating experimental results with modeling. These results are summarized in Fig. 4. Gallagher et al. [21] showed that electrolyte transport limits the utilization of the positive electrode (NMC622) at critical C-rates during discharge for each electrode loading level. Furthermore, as discussed before, a combination of electrolyte transport and polarization can lead to lithium plating on the graphite electrode during fast charging. Gallagher et al. proposed that conventional graphite cells should avoid charge current densities near or above 4 mA cm^{-2} unless additional precautions have been made. We have seen evidence from a teardown of a Ford Cmax battery, which indicates that current densities greater than 4 mA cm^{-2} may be tolerable. For EVs designed for fast charge, the electrodes need to be thinner than the typical 40–60 μm seen today.

2.5. Temperature/electrode kinetics

Lithium-ion battery power/resistance is highly dependent on temperature. As can be seen in Fig. 5, the total cell impedance follows an Arrhenius behavior over a wide temperature range [62,63]. Thus, the resistance during fast charge will increase the

temperature of the battery through i^2R heating, and will result in a lowering of the battery resistance due to faster kinetics. However, the electronic resistance of the electrode current collectors and terminals will increase as the temperature increases, and thereby offset some of the power gains from the faster kinetics.

The upper temperature limit of the cell/battery must be avoided during the fast charge for two main reasons. Firstly, if the temperature of a lithium-ion cell at full charge exceeds a pre-determined set point, the possibility of a thermal runaway is a serious concern. This temperature can be as low as 80 °C for some systems. Secondly, if the temperature of the electrolyte in the cell exceeds 60 °C, the LiPF_6 salt will start to decompose, and thus shorten the life of the battery.

2.6. Binders

These materials are used to adhere particles of active materials and conductive additives to each other and to the current collector foil. In most lithium-ion applications, the binder of choice is poly(vinylidene difluoride) [64]. Other materials, such as carboxymethylcellulose, have been used for this purpose [64–66]. There are many reports on the effect that the binder can have on cell performance and life [65,66] and reasons that certain binders work well for certain electrodes but not for others [65,66]. There is nothing in the open literature, however, regarding the effect that XFC can have on the binder or vice versa.

From the functional point of view, the presence of a binder between particles of active material would introduce an impedance to current flow. The impedance would produce local heating (i^2R), which, in turn, may degrade the properties of the binder.

Prezas et al. illustrated the effects of charging at successively higher rates on the physical integrity of the negative electrode in NMC/graphite cells. They found that, at rates less than about 4-C, the change in this electrode was minor. As the charge rate increased, the damage became more obvious, as shown in Fig. 6. There was evidence of delamination at 6-C. The possible causes of the delamination were stated as a metallic lithium reacting with the binder, destroying its adhesive properties, and/or local heating [67].

2.7. Electrolyte degradation

The electrolyte can impact the behavior of the electrode and cell. For example, it can cause structural changes in the graphite electrode. In particular, Aurbach et al. [68] reported a large, irreversible capacity loss and exfoliation of graphitic negative electrodes in cells containing propylene carbonate (PC)-based electrolytes. They hypothesized that the reduction products do not coat the graphite surface well; as a result, propylene gas, formed from the reduction of intercalated PC, was trapped in the crevices on the electrode surface. The resulting pressure buildup caused exfoliation. On the other hand, electrolytes containing linear carbonates, such as ethylmethyl carbonate, did not display this behavior because the resulting film was more cohesive and adhesive [68].

At present, no information is readily available on the effect of XFC on electrolyte degradation. It is possible that the heat generated and possible lithium plating degrade the conductivity and other properties of the electrolyte. Further research is thus needed on the impact of XFC on electrolyte performance.

2.8. Charging protocol

Many reports have been published on the effects that the charge protocol/method has on the performance and life of lithium-ion cells [15,67,69–74]. Accelerated performance degradation was

¹ LCO = lithium cobalt oxide; LMO = lithium manganese oxide; LFP = lithium iron phosphate; NCM = lithium nickel cobalt manganese oxide.

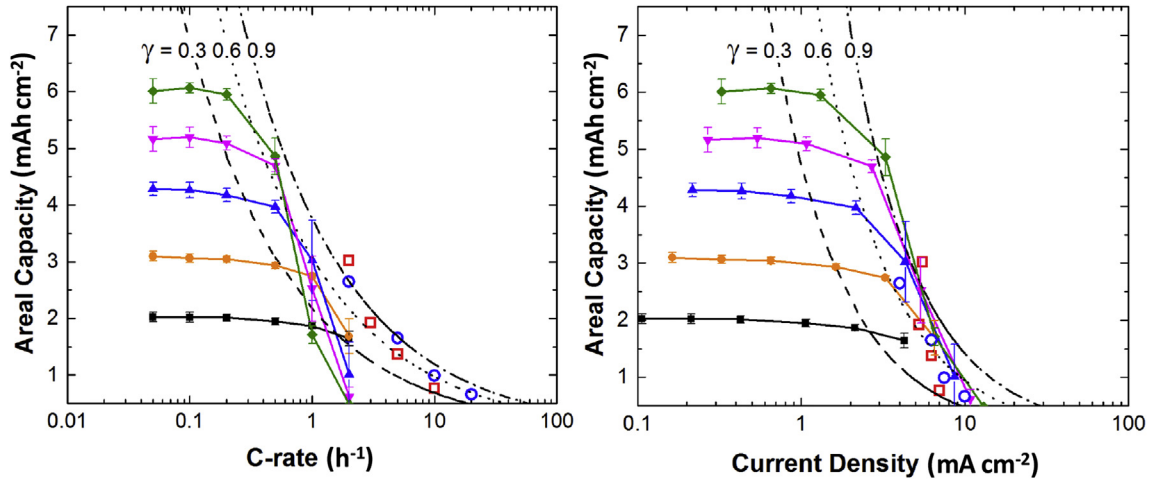


Fig. 4. Rate capability for a series of graphite/NMC622 pouch cells with increasing areal capacities shown versus C-rate (left) and current density (right). Dashed lines represent differing values of γ , which is the ratio of electrode thickness to electrode penetration depth. Open symbols of blue (LFP/Gr) and red (NMC333/Gr) were transformed from Zheng et al. [61]. Reproduced from Ref. [21]. (For interpretation of the references to colour in this figure legend, the reader is referred to the web version of this article.)

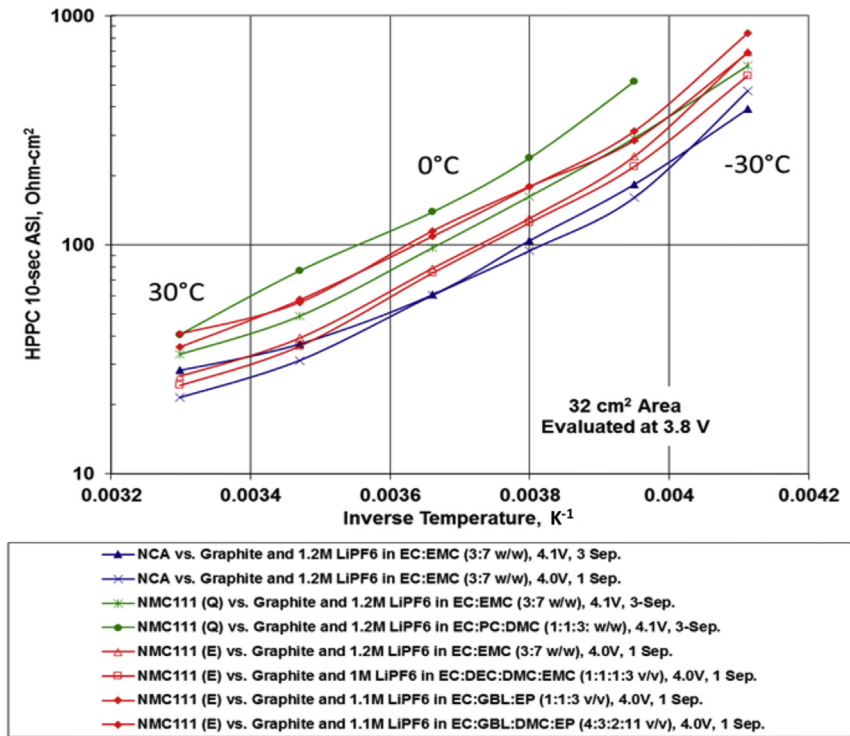


Fig. 5. Area specific impedance (ASI) vs. inverse temperature for a typical lithium-ion battery [62,63].

seen in four of these studies [15,67,69,71]. In one study, constant current, constant power, and multiple currents were used to charge small lithium-ion cells [15]. The charge rates used in the multiple-current experiment were 0.5-C (100 cycles) and 1-C (next 200 cycles). The rate of capacity fade using a 0.5-C rate discharge followed the order: constant power>multiple currents>constant current. Using a 1-C discharge rate, the capacity fade followed a different order: multiple currents>constant current>constant power. Zhang also observed high capacity loss rates at higher charge rates [15].

In another study using 18650-sized cells, Prezas et al. [67] found that constant-current charging at high C-rates and the charging method exacerbated capacity fade and resistance increase. The

effects of the charging protocol were seen when constant-current charging and the U.S. Advanced Battery Consortium’s fast-charge test were applied. The latter charging method used a profile in which the battery was charged at the C/3 rate, discharged to 40% SOC at the C/3 rate, and fast-charged to 80% SOC. The final discharge to 0% SOC was at the C/3 rate [75]. The fast charge rates in the 40–80% segment were 0.7-, 2-, 4-, and 6-C. As expected, the cells charged at the higher rates displayed higher rates of performance decline. There was an effect of the protocol also: those cells tested by the fast-charge protocol also displayed higher decline for the same charge rate [67].

Based on post-mortem results, performance degradation in the

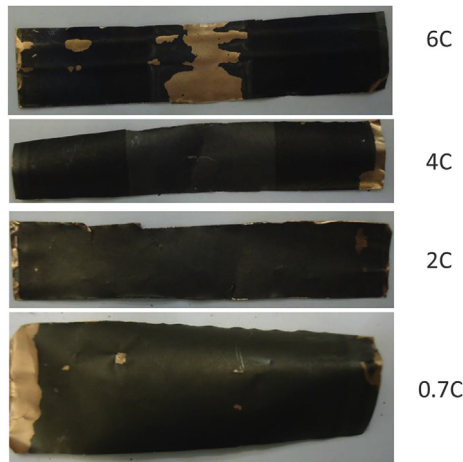


Fig. 6. Optical photographs of the negative electrodes from cells charged at the constant rate given to the right. The extent of change in both visible surface film and delamination of the negative electrode was proportional to the charge rate [67]. Reprinted with permission SAE 2016-01-1194 Copyright © 2017 SAE International. Further distribution of this material is not permitted without prior permission from SAE.

cells from the above work, which were charged at rates between 0.7- and 4-C (constant current), was primarily due to increases in SEI film thickness with increasing rate, with no discernable changes in film composition. At the 6-C charge rate, a significant change in film composition indicated that this was the primary cause for a resistance increase. The impact of high-rate charging was not uniform across the width of the electrode; the bulk of the change was located in a band at the middle of its width [69].

Constant-current, constant-voltage (CCCV) charging protocol is the widely adopted battery charging protocol within the battery and EV industries due to its simplicity and low cost of implementation. CCCV charging is entirely a voltage-based protocol, where the CC charging rate depends on battery type and charging temperature, and it could vary from 0.5-C to 3.2-C [76].

Some automakers have indicated [77] that XFC using the CCCV protocol degrades the performance, life, and safety of cells in the EV battery pack, primarily due to lithium plating in the negative electrode. With constant-current charging, lithium is delivered to the negative electrode at a constant rate. If the delivery rate is less than or equal to the rate at which lithium intercalates, then lithium will probably not be deposited on the electrode surface. The Li delivery rate at the negative electrode depends on several factors, including the negative electrode material, cell and electrode design, and charging condition. Previous research [16,17,21,78–80] suggested that several factors are favorable in suppressing lithium plating during CCCV charging even at higher C-rates: slightly oversized negative electrode; thinner, less porous, and less tortuous electrode; electrolyte additives; smaller round active material particles in the negative electrode; and increased charging temperature. Enabling XFC would require careful optimization of these design parameters and charging conditions without sacrificing specific energy and energy density.

In reality, with the popular CCCV charging protocol, battery pack voltage would rise to a maximum rather quickly during fast charging, leading to a condition where current must then be tapered so as not to exceed the maximum voltage. The tapered charging step is extremely inefficient and offers a diminishing return in terms of mi min^{-1} or time and, thus, should be avoided during high-rate DCFC.

Alternative charging protocols should be utilized during high-rate XFC to avoid accelerated performance decay and safety

concerns. Step-wise charging was found to be better. Using the concepts described above provides a reason for this. On the other hand, stepwise charging [81–84], where the charge rate decreases with time or state of charge, decreases the rate at which lithium is deposited on the electrode surface. The decreased charge rate, in principle, compensates for the lower rate of lithium intercalation with increased degree of charge (increased lithium occupancy in the galleries). This relaxes high polarization toward the end of charging along with lower overall battery temperature. Implementation of the step-wise charging protocol could, however, be costlier than the CCCV charging protocol [85].

In principle, another method that can decrease the probability of lithium deposition is pulse charging [86–90]. Here, time is allowed between pulses so that the system can reach an equilibrium or near-equilibrium state. That is, time is allowed for lithium to intercalate into the graphite structure. Yet another method would be to combine the above strategies, compensating for the degree of lithium occupancy and allowing time for lithium to intercalate into the structure. Pulse charging is more complex and expensive to implement and has only been tested in laboratories. Field implementation would require development of complex control algorithm and compatible hardware [81,82].

3. Pack level

3.1. Pack design

An adequately designed pack in terms of voltage and current is crucially important to enable XFC. Today, most existing EV battery packs are rated at or below 400 V, with maximum current rating up to 300 A during charging (e.g., the Tesla charger rating is 120 kW/300 A, and that for CHAdeMO and combined charging system (CCS) chargers is 50 kW/125 A [91–94]). A conventional 400-V battery pack going above 120 kW power rating would require the pack to accommodate significantly higher current than 300 A. The higher current would generate more i^2R heating within the pack circuitry and battery, which would increase the thermal load on the cooling system. Higher current would also significantly impact pack hardware and circuitry with stringent requirements on more robust bus bars, tabs, current collector foils, fuses, disconnect switches, insulation, etc., resulting in increased pack weight and cost. The electric vehicle supply equipment (EVSE) would have to accommodate the higher current as well.

The issues associated with high currents during XFC could be eliminated by increasing the pack voltage. Compared to the existing 400-V packs, an increase in charging voltages to 600 V, 800 V, and 1000 V would reduce the charging current by 33%, 50% and 60%, respectively. The reduced current could significantly decrease the pack weight and cost. Increased voltage would also decrease the pack capacity by approximately the same factor; thus, the effective charging C-rate (or charging time) remains the same. 180 kW/600 V, 250 kW/800 V, and 300 kW/1000 V battery packs would exceed the 300-A charging current limit, which would require sophisticated (e.g., liquid cooled) EVSE cable, plug, and charging pins to keep them thin and flexible.

Another issue in pack design is maintaining cell balance during XFC. It is possible that, with time, the cells will age at slightly different rates. In turn, the capacity of the cells will change at different rates; some cells will have higher capacities than others. This means that some cells will be at a higher state of charge after XFC. Advanced battery management systems (BMSs) and algorithms will be needed to minimize the impact of cell imbalance on pack life and performance. For example, if it were possible to place voltage and temperature sensors on every cell, then the weaker and hotter cells could be easily identified. The BMS would have to limit

the current passing through the weaker cell(s) to prevent over-heating and thermal runaway.

Additionally, the BMS would need to prevent cell overvoltage, which could lead to faster degradation of those already weaker cells [95], exacerbating the unbalance and aging mechanisms. Passive balancing, that is, using resistors as loads to prevent overvoltage and maintain balance by removing excess energy in weaker cell(s), would contribute to the thermal management challenge as the i^2R heating would increase the overall system requirements for heat rejection. Active balancing methods, such as switched capacitor, inductive, or power converter circuits, would improve the thermal management requirements and balancing time, but they would also require higher cost, greater complexity, and more components as well as more sophisticated balancing algorithms [96]. Active balancing would also permit shuffling energy between stronger cells and weaker cells during both XFC and normal operation, improving overall efficiency compared to passive methods.

3.2. Modeling the performance and cost

Let us consider a battery pack for an all-EV rated for a total energy storage capacity of 80 kWh, and capable of delivering a burst power of 300 kW for 10 s. BatPaC, a spreadsheet tool developed at Argonne to design automotive lithium-ion batteries, was used to size batteries and their cost for the various scenarios reported here [97]. For a NMC622 ($\text{LiNi}_{0.6}\text{Mn}_{0.2}\text{Co}_{0.2}\text{O}_2$) positive electrode and a graphite negative electrode, the pack is designed to operate at a nominal voltage of 900 V. The pack is configured with 6 modules (6S-1P), each with 40 cells (40S-1P), for a total of 240 cells. It is assumed that lithium plating or deposition in the negative electrode can be avoided if the current density during charge is limited to less than 4 mA cm⁻² [21]; this limit is called the maximum allowable current density (MACD).

The pack is designed to meet the above specifications and is capable of being charged to increase the SOC from 15% to 95%, so that $\Delta\text{SOC} = 80\%$ can be achieved in 60 min with a negative electrode thickness of 103 μm (the ratio assumed for the thicknesses of the negative-to-positive electrode is 1.12). The designed battery pack is estimated to cost the vehicle manufacturer \$10,945, or \$129 per kWh_{Total}. At the cell level, the cost is \$103 per kWh. The configuration of the baseline pack and some characteristics are shown in Table 1.

For the baseline pack shown in Table 1, the total heat generated

Table 1
Configuration and cost of a baseline pack capable of adding 80% SOC (from 15% to 75% SOC).

Cathode – Anode Chemistry	NMC622-Graphite
Pack Energy, kWh _{Total}	85
Pack Rated Power (10 s burst), kW	300
Pack Voltage, V	900
No. of cells per pack	240
Maximum Allowable Current Density (MACD), mA cm ⁻²	4
Cell Temperature before Charge, °C	10 ^a
Charging Time, $\Delta\text{SOC} = 80\%$, min	61
Charger Power Needed, kW	77
Anode Thickness (does not include current collector), μm	103
Anode/Cathode Thickness Ratio	1.12
Heat Generated during Charging, kWh per pack	1.45
Heat Generated during Charging, Wh per cell	6.0
Post-Charge Cell Temperature $\Delta 80\%$ SOC (no cooling), °C	25
Cell Cost to OEM, \$ per kWh	\$103

^a It is anticipated that, if the cell is cooled to 10 °C with the available battery cooling system, then, in many cases, the thermal mass of the cell will be able to absorb the heat generated during charging and keep the battery at 40 °C or below. This alleviates the cooling requirement.

during the 60 min of charging is 1.45 kWh for the pack, and 6 W for each cell. Assuming adiabatic conditions, the heat can be absorbed by the thermal mass of the cells to raise the cell centerline temperature from 10 °C to 25 °C.

In order to enable faster charging of the battery pack it is necessary that the charging station have adequate capacity to supply the current. The minimum charger power needed to add 80% to the SOC within the specified charge times, increases non-linearly from 77 kW for a 60 min charge to 461 kW for a 10 min charge, as shown in Fig. 7.

Enabling a faster charging rate necessitates a higher current, and with the constraint of the maximum allowable current density the current needs to be distributed across a larger area and a smaller anode thickness. Thinner electrodes and larger surface area translate to more inactive materials such as current collectors, separators, etc. adding to the mass, volume, and ultimately the cost of the cells and the battery pack. Fig. 8 and Table 2 show the effect of the required charging time on the anode thickness, the cell temperature reached at the end of the charge, and the cost of the cell. The baseline (non-fast-charging) cell is shown at the right edge of the curves with a 60 min charging time. At this slow charge rate the electrode thickness is limited by the cathode (92 μm cathode, 103 μm anode) to meet the specification for sustained discharge rate. This constraint prevails for charging times as low as 55 min. At charging rates less than 55 min, the MACD becomes the limiting constraint necessitating thinner anodes (and larger cell area) to prevent lithium deposition during charging. For a 10 min charging design, the anode can be no thicker than 19 μm . The resulting effect on the cell cost is shown to increase sharply to \$196 per kWh. The incremental cost of reducing the charging time from 55 to 10 min is \$126 per kWh.

Faster charging increases the total current which leads to a higher rate of heat generation. This explains the increase in final temperature after the charge seen (Fig. 8) between 60 and 55 min of charging times. The post-charge temperature is calculated assuming adiabatic operations. At less than 55 min, the MACD limits the electrode thickness, which increases the amount of inactive materials and therefore the thermal mass of the cells. Fig. 9 shows the increasing mass of each cell when the charging time is reduced leading to thinner electrodes. The post-charge cell temperature (Fig. 8) shows that at charge times less than 55 min the post-charge cell temperatures are actually lower than that at 55 min.

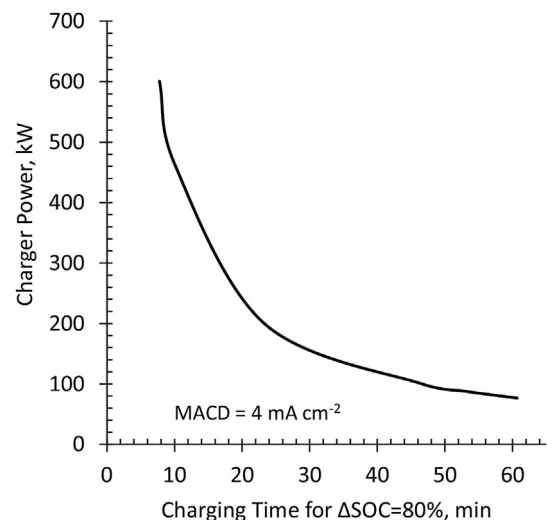


Fig. 7. Charger power needed to recharge a 85 kWh, 300 kW, 900 V battery pack to raise its SOC by 80% (from 15% to 95%) within a specified charging time.

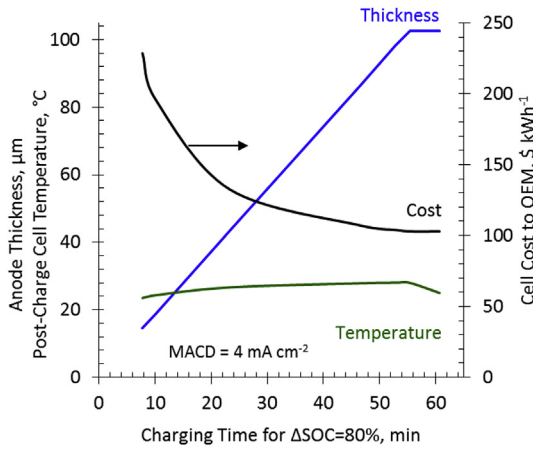


Fig. 8. Effect of charging time on the required anode thickness, the post-charge cell temperature, and the cell cost. Assumptions: No pack cooling, maximum allowable current density to avoid lithium plating (MACD) = 4 mA cm⁻², anode/cathode thickness ratio = 1.12, NMC622-Graphite, 85 kWh pack.

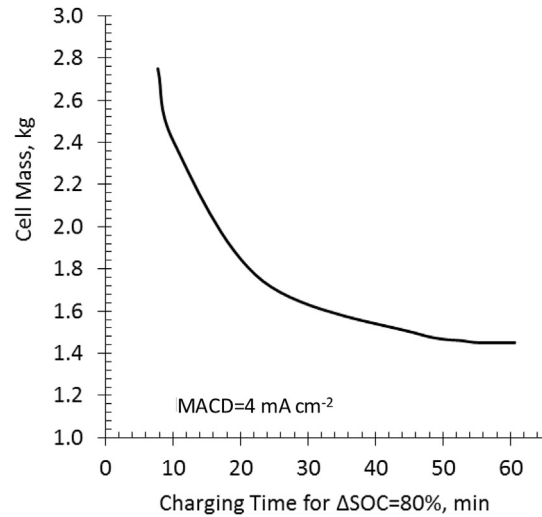


Fig. 9. Effect of charging time on the mass of each cell (NMC622-Graphite, 85 kWh pack, 300 kW, 900 V).

Considering that lithium plating is a key challenge in fast charging and that the deposition is triggered by high current densities, it is worthwhile to quantify the effect of the maximum allowable current density on a given electrode system. Fig. 10(a) shows these effects on the required anode thicknesses to meet the specifications for charging times of 10, 15, and 20 min. As seen earlier, the maximum cathode thickness that can meet the sustained power requirement is 92 μm (anode thickness 103 μm). With faster charge requirements, the anode thickness becomes limiting at larger MACD. Whereas a 20-min charging battery becomes anode-thickness-limited at MACD 11 mA cm⁻² and lower, the 15-min charging battery becomes anode-thickness-limited 14.8 mA cm⁻² and less. The threshold MACD for a 10 min charging battery is outside the limits of the abscissa in the figure.

Fig. 10(b) shows the centerline temperatures of the cells at the end of the charging process, assuming adiabatic operations. The horizontal line represents the boundary above which the cells will need cooling to avoid the maximum allowable cell temperature (assumed at 40 °C). The curves for all three charge times indicate that if the MACD can be increased to 7 mA cm⁻², then the cells will be able to process sufficiently high current such that they will exceed the 40 °C limit (assuming the cells are at 10 °C before the charge) and therefore require cooling during the charge.

The cost of the cells are seen in Fig. 10(c), showing that the combination of slower charge times and higher MACD allows the cost to come down to reach the cost of the non-fast-charging cells (\$103 per kWh), where the electrode thicknesses are limited by the

sustained power requirement. The curve for the 10-min charge indicates that improving the electrode properties to avoid lithium deposition such that the MACD increases from 4 to 6 mA cm⁻², can reduce the cell cost by \$37 per kWh. These results highlight the importance of developing anode materials or electrode morphologies that can avoid lithium plating at high current densities. The results are summarized in Table 3.

Battery and BEV manufacturers seek to improve the pack specific energy (kWh per kg) by reducing the mass of the cell materials. Lighter cells mean lower thermal mass and hence less capacity to soak up the heat generated during fast charging, meaning higher temperature rise for a given heat generation rate. The temperature rise issue can be resolved (a) by improving the heat removal from the cell by increasing the coolant flow, with closer proximity to the coolant, with additional heat transfer area, etc., or (b) by reducing the resistance to ion transfer within the electrodes.

3.3. Usage

The customer's usage pattern needs to be considered during the design and optimization processes of battery cells and packs capable of handling XFC since it is expected that the pattern will affect battery performance, life, and safety. The conventional CCCV charging protocol may not be suitable for XFC due to the high probability of lithium plating toward the end of charging; thus, new fast charging protocols dedicated to XFC should be explored.

Table 2

BatPac simulation comparing the effects of charging time on the required anode thickness, the heat generation in the pack and the resulting temperature rise, the pack cost, and the incremental cost of charging faster than 1-C (60 min) rate. Cell Chemistry: NMC622-Graphite, Pack Energy: 85 kWh; Rated Power (10 s burst): 300 kW; MACD (Maximum Allowable Current Density): 4 mA cm⁻²; No. of cells per pack: 240.

Charging Time, ΔSOC = 80%, min	8	10	23	47	53	61
Charging Time, ΔSOC = 60%, min	5	7	15	30	34	39
Charger Power Needed, kW	601	461	199	100	88	77
Anode Thickness, μm	14	19	43	87	98	103
Heat Generated during Charge, kWh per pack	2.35	2.20	1.89	1.77	1.75	1.45
Post-Charge Cell Temperature (ΔSOC = 80%), °C	22.4	24.4	25.9	26.4	26.4	19.5
Cell Mass, kg	2.75	2.40	1.74	1.49	1.46	1.45
Cell Cost to OEM, \$ per kWh	\$229	\$196	\$132	\$107	\$104	\$103
Cost Difference, \$ per kWh	\$126	\$93	\$30	\$4	\$1	\$0

Italics are independent variables.

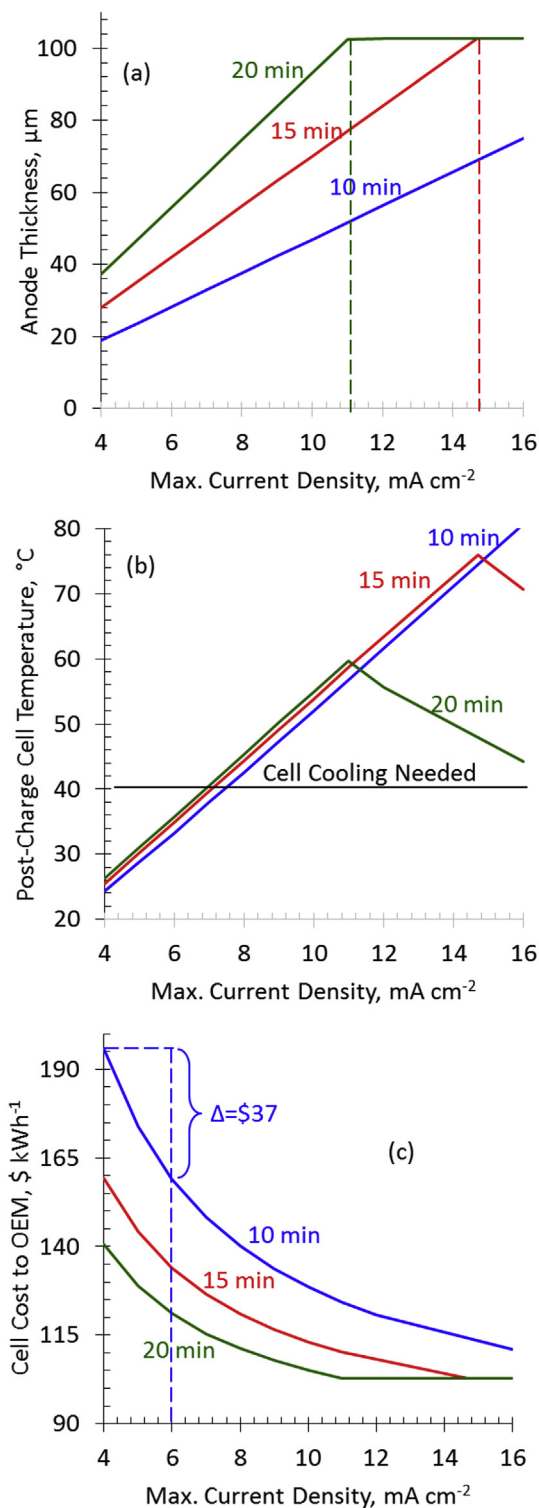


Fig. 10. Effect of the maximum allowable current density on the (a) anode thickness, the (b) post-charge cell temperature (without any cooling) and (c) the pack cost, for recharge times of 10, 15, and 20 min (NMC622-Graphite, 85 kWh pack, 300 kW, 900 V).

Depending on the convenience, availability, and pricing of XFC, EV owners may arrive at recharge stations with battery packs that are anywhere from almost empty to almost full. Thus, the impact of XFC on battery performance, life, and safety may also depend on the initial SOC of the battery pack. Indeed, the frequency of XFC on pack performance, life, and safety must also be understood.

Table 3

The effect of the maximum allowable current density on the anode thickness, the cell temperature after charging, and the cost of the cells designed for 20-min, 15-min, and 10-min charging. (NMC622-Graphite, 85 kWh, 300 kW, 900 V).

Charging Time, $\Delta\text{SOC} = 60\%$, min	20					
MACD, mA cm^{-2}	4	6	10	11	12	16
Anode Thickness, μm	37	56	93	102	103	103
Cell T after Charge, $^{\circ}\text{C}$	26	36	55	60	56	44
Cell Cost to OEM, $\$ \text{ per kWh}$	141	121	105	103	103	103
Charging Time, $\Delta\text{SOC} = 60\%$, min	15					
MACD, mA cm^{-2}	4	6	10	11	14.7	16
Anode Thickness, μm	28	42	70	77	103	103
Cell T after Charge, $^{\circ}\text{C}$	26	35	54	59	76	71
Cell Cost to OEM, $\$ \text{ per kWh}$	159	134	113	110	103	103
Charging Time, $\Delta\text{SOC} = 60\%$, min	10					
MACD, mA cm^{-2}	4	6	10	12	14	16
Anode Thickness, μm	19	28	47	52	56	75
Cell T after Charge, $^{\circ}\text{C}$	24	33	52	57	62	81
Cell Cost to OEM, $\$ \text{ per kWh}$	196	159	129	124	121	111

Italics are independent variables.

Automakers currently assume that EV owners will primarily charge at home. Collection of data from early EV adopters confirms this assumption, where the majority of charging occurs at home followed by workplace charging [98]. However, it is not well understood what the duty cycle is going to look like when large numbers of ICE vehicle owners switch to EVs with XFC capability. From the perspective of the battery, the intentional, repeated XFC corresponds to aggressive use, which, without any balancing between charging events, could raise additional performance and safety concerns. Current knowledge suggests that XFC will accelerate degradation and compromise safety. Further R&D is needed to ensure robust performance capabilities with continued XFC.

4. Safety

4.1. Cell level

The abuse response of a lithium-ion cell during or after XFC is largely unknown. In principle, the abuse response will be affected by the temperature during charge. Since high temperatures typically degrade the performance and, possibly, abuse response of the cell, the abuse response will change. The magnitude of the change will have to be determined experimentally and probably will be a function of cell chemistry and design.

The possibility of “stranded lithium” left after the discharge following XFC will have to be investigated. Here, stranded lithium refers to Li which is plated on the negative electrode and, for some reason, has become electronically or electrochemically isolated from the rest of the cell. Stranded lithium has the potential to become a safety hazard to first responders in the event of a pack casing breach after an automobile accident. Lithium stranded in the battery is typically small but has high effective reactivity. Thus, XFC will not be acceptable without resolving/eliminating the lithium plating issue.

4.2. Pack level

A battery pack capable of XFC has to be scrutinized for maximum safety and stability during charging as well as during normal operation. Some major safety concerns may come from over- and non-uniform heating, inadequate pack balancing, inadequate isolation, and arc flashing. Removing excessive heat generated during XFC with a minimum temperature gradient within the

pack and cell would require redesign of the pack, which, in turn, may produce a larger pack, requiring more space. Without tight temperature control, the battery would age faster and in a non-uniform manner (unbalanced pack), which could raise major safety concerns along with rapid performance decay especially towards the latter half of the battery pack's life.

XFC could magnify the non-uniform aging by overcharging or over-discharging weak cell(s) in a series string (if any). Current production tolerances of cells coupled with loose temperature control within the battery pack could weaken some of cells in a series string. In these situations, the performance of the battery pack would be limited by these weak cells. Charging such an unbalanced pack at a very high rate could be extremely unsafe and may lead to a catastrophic event. Advanced diagnostic techniques to detect internal shorts during and/or after XFC, which would avoid any catastrophic event, would have to be invented and/or developed.

Increasing the battery pack voltage is an alternative and effective way of reducing maximum charging current to achieve the XFC goal. For example, compared to existing 400 V systems, increasing battery pack charging voltage to 800 V and 1000 V can reduce maximum current by 50% and 60%, respectively. A higher voltage system has the potential to offer additional benefits by reducing vehicle weight and cost by, for example, using smaller and less bulky power transistors, smaller gauge wire in the motor winding, and smaller controllers. Finding the most appropriate pack voltage, which will allow the selection of ancillary hardware components for minimum weight and cost penalty (if any), is a key technological challenge and needs an R&D resolution.

Several auto manufactures (Porsche, Volkswagen, etc.) have already started developing battery packs beyond 400 V. Porsche's goal is to recharge 200–225 miles (up to 80% SOC) in 15 min with a 300 + kW DCFC [77]. Porsche has already demonstrated a 220 kW charger (<300 A), which can charge an 800 V battery pack in 19 min [35].

However, unlike conventional, low voltage packs, XFC capable packs would require more safety measures, such as the mitigation of arc and shock, more robust isolation, and thicker insulation. The implementation of these measures would depend on the voltage and current that would be used in the pack and would require an engineering-based mitigation strategy.

Extracting stranded energy safely and efficiently from a high energy and high voltage battery pack following a vehicle crash or emergency situation would raise additional safety concerns to first and secondary responders due to arc flash hazard. The added hazard associated with high pack voltage may even make it less feasible to safely perform onsite stranded energy removal. Protocols and effective measures to dissipate stranded energy would have to be designed into the pack and/or developed.

5. Developmental needs

Based on the previous discussion, the following research and developmental needs are proposed to enable XFC.

5.1. Modeling

- Advanced models are needed to support the work below. This will require updating of existing models, such as BatPaC [97], CAEBAT [89,90], etc., to incorporate fast charge protocols and the constraints of fast charge requirements in the design of cells and battery packs and to estimate the cost of production. These models should include the effects of current, temperature, and temperature distribution on the performance and life of XFC-enabled packs. The most dominant aging and failure

mechanisms pertinent to XFC also need to be identified and incorporated in the models.

5.2. Cell level

- Negative electrode materials. To prevent lithium plating, the negative electrode material must have fast reaction kinetics. This holds true for both intercalation (e.g., graphite) and conversion (e.g., silicon) materials. Even though LTO has sufficiently high reaction kinetics, its potential vs. Li/Li⁺ is too high. To enable high energy content in a cell, the potential of the lithiated negative electrode material should be as low as possible. The potential negative electrode material, thus, would have to possess a blend of two hard-to-obtain properties.
- Electrode design. Electrode designs that accommodate the need for fast diffusion in and out of a reaction site need to be developed.
- Studies of the impact of XFC on materials. The potential effect of XFC on cell materials is known only for a limited number of them. The studies should include the effect of XFC on silicon negative electrodes, lithium metal negative electrodes, positive electrodes, electrolytes, and separators. The studies are needed to elucidate the effect of high reaction kinetics and temperature.
- Studies to understand/detect/prevent lithium plating. Since lithium plating is a safety and performance issue, methods are needed to detect and prevent it.
- Studies to measure cell temperature distributions during XFC and update/validate models.

5.3. Pack level

- Thermal management. Cooling of battery packs during extreme fast charging is an absolute necessity. The cooling system must handle the maximum load during XFC with minimum temperature gradient within the pack and individual cells. Cooling load would depend on the pack size, battery chemistry, design, and maximum allowable temperature during an XFC event for a given charger power. Likely challenges are pack design modification to facilitate better heat transfer from cell to cooling media within the strict volume restriction, ensuring uniform temperature within the pack and cell, and finding the most suitable method of heat rejection outside the pack.
- Electrical safety. At voltages of 1000 V, surface conductivity of the pack is a major concern due to the arc hazard. To combat the possibility of dielectric breakdown and the resulting leakage current, new insulators will need to be developed. In turn, this may have an impact on pack design.
- Effect of XFC on pack life. More understanding is required as to how and in what magnitude individual usage factors (charging protocol, frequency of XFC, travel pattern, duty cycle, intentional abuse, etc.) would affect the durability, reliability, and safety of XFC-enabled battery packs. The effect of some of these usage factors (charging protocol, frequency of XFC, etc.) can be tested in labs (similar to USABC activity or with some modifications) for R&D resolution. Others (travel pattern, customer perception, etc.) would need extensive relevant field data collection and analysis.
- Charging protocol. As a follow-on to the above item, new charging protocols should be explored, such as multi-stage constant current/power charging protocol or other model-based charging protocols optimized to minimize degradation of the battery. These charging protocols may be derived from

experiments or a model-based approach and need to be updated with battery age.

- Safety concerns:
 - High-voltage battery packs that are capable of charging at a high rate would require additional safety measures, such as arc flash mitigation, more robust isolation with reliable all time monitoring, thicker insulation for high current cabling, etc., during normal and off-normal situations such as a collision. Safe and efficient stranded energy extraction protocols following a vehicle crash must be sought out.
 - Abuse (mechanical, thermal, and electrical) response of the battery due to XFC may change significantly, which would raise some safety concerns and requires R&D resolution. New/modified method and standardization (similar to USABC or with some modification) techniques are required to diagnose/evaluate the safety critical issues associated with XFC on batteries at least at their pre-commercial stage, followed by identification of prognostics to eliminate any safety concerns.
- Control and management algorithms. High voltage battery packs would have fewer cells in parallel and more cells in series. Having fewer cells in parallel has the advantage of better control, management, and fault detection capability. Increased cell count in the series string, however, requires more sensors for monitoring and robust battery control and management algorithms. For example, because more cells need to be balanced, more intricate balancing may be needed, which may add additional cost. XFC capable packs should be instrumented with more advanced diagnostics and safety features to monitor and identify any impending short circuit.
- Advanced battery management systems. The battery management system must be sensitive enough to compensate for non-uniform aging (due to thermal gradient or production mismatch) during pack balancing. Repeated XFC without the opportunity of balancing the pack would have potential performance and safety concerns as well. R&D resolution is required to identify a safe envelope concerning these factors beyond which major performance and safety concerns would arise.

Acknowledgment

This work was performed under the auspices of the US Department of Energy, Office of Vehicle Technologies, under Contract Nos. DE-AC02-06CH11357 (Argonne National Laboratory), DE-AC07-05ID14517 (Idaho National Laboratory), and DE-AC36-08GO28308 (National Renewable Energy Laboratory).

The U.S. Government retains for itself, and others acting on its behalf, a paid-up nonexclusive, irrevocable worldwide license in said article to reproduce, prepare derivative works, distribute copies to the public, and perform publicly and display publicly, by or on behalf of the Government.

References

- [1] D. Aurbach, *J. Power Sources* 89 (2000) 2106–2218.
- [2] B. Scrosati, *Nature* 373 (1995) 557.
- [3] From NIST database W.E. Morgan, J.R. Van Wazer, W.J. Stec, *J. Am. Chem. Soc.* 95 (1973) 751.
- [4] From NIST database B.V.R. Chowdari, K.F. Mok, J.M. Xie, R. Gopalakrishnan, *Solid State Ionics* 76 (1995) 189.
- [5] D. Howell, T. Duong, P. Faguy, B. Cunningham, U.S. DOE vehicle battery R&D: Progress update 2011, https://www.hydrogen.energy.gov/pdfs/htac_nov2011_howell.pdf.
- [6] Mitsubishi Motors, i-MiEV charging features, <http://www.mitsubishicars.com/imiev/features/charging> (accessed April 2017).
- [7] Blink, Smart, convenient charging wherever you go, <http://www.blinknetwork.com/drivingelectric> (accessed April 2017).
- [8] BMW USA, BMWi3: Overview, <https://www.bmwusa.com/vehicles/bmw/i3.html> (accessed April 2017).
- [9] Chevrolet, 2017 BOLT EV owner's manual, <https://my.chevrolet.com/content/dam/gmownercenter/gmna/dynamic/manuals/2017/Chevrolet/BOLT%20EV/Owner%20Manual.pdf> (accessed April 2017).
- [10] Tesla, Charging, <https://www.tesla.com/charging> (accessed April 2017).
- [11] M. Inaba, H. Yoshida, Z. Ogumi, T. Abe, Y. Mizutani, M. Asano, *J. Electrochem. Soc.* 142 (1995) 20–26.
- [12] A. Funabiki, M. Inaba, T. Abe, Z. Ogumi, *J. Electrochem. Soc.* 146 (1999) 2443–2448.
- [13] G.-A. Nazri, G. Pistoia (Eds.), *Lithium Batteries: Science and Technology*, Springer Science+Business Media, New York, 2009.
- [14] T. Enoki, M. Suzuki, M. Endo, *Graphite Intercalation Compounds and Applications*, Oxford University Press, New York, 2003.
- [15] S.S. Zhang, *J. Power Sources* 161 (2006) 1385–1391.
- [16] J.C. Burns, D.A. Stevens, J.R. Dahn, *J. Electrochem. Soc.* 162 (2015) A959–A964.
- [17] S.S. Zhang, K. Xu, T.R. Jow, *J. Power Sources* 160 (2006) 1349–1354.
- [18] M. Petzl, M. Kasper, M.A. Danzer, *J. Power Sources* 275 (2015) 799–807.
- [19] S. Tippmann, D. Walper, L. Balboa, B. Spier, W.G. Bessler, *J. Power Sources* 252 (2014) 305–316.
- [20] J. Cannarella, C.B. Arnold, *J. Electrochem. Soc.* 162 (2015) A1365–A1373.
- [21] K. Gallagher, S. Trask, C. Bauer, T. Woehrle, S. Lux, M. Tschech, P. Lamp, B. Polzin, S. Ha, B. Long, Q. Wu, W. Lu, D. Dees, A. Jansen, *J. Electrochem. Soc.* 163 (2016) A138–A149.
- [22] M. Petzl, M.A. Danzer, *J. Power Sources* 254 (2014) 80–87.
- [23] B. Bitzer, A. Gruhle, *J. Power Sources* 262 (2014) 297–302.
- [24] L.E. Downie, L.J. Krause, J.C. Burns, L.D. Jensen, V.L. Chevrier, J.R. Dahn, *J. Electrochem. Soc.* 160 (2013) A588–A594.
- [25] C. Birka, B. Bitzer, M. Harzheim, A. Hintennach, T. Schleid, *J. Electrochem. Soc.* 162 (2015) A2646–A2650.
- [26] M.N. Obrovac, V.L. Chevrier, *Chem. Rev.* 114 (2014) 11444–11502.
- [27] M. Majima, S. Ujiie, E. Yagasaki, K. Koyama, S. Inazawa, *J. Power Sources* 101 (2001) 53–59.
- [28] C.K. Chan, R. Ruffo, S.S. Hong, R.A. Huggins, Y. Cui, *J. Power Sources* 189 (2009) 34–39.
- [29] H.-P. Liu, G.-W. Wen, S.-F. Bib, C.-Y. Wang, J.-M. Hao, P. Gao, *Electrochimica Acta* 192 (2016) 38–44.
- [30] D. Mu, Y. Chen, B. Wu, R. Huang, Y. Jiang, L. Li, F. Wu, *J. Alloys Compd.* 671 (2016) 157–163.
- [31] C. Wang, S. Wang, L. Tang, Y.-B. He, L. Gan, J. Lia, H. Du, B. Li, Z. Lin, F. Kang, *Nano Energy* 21 (2016) 133–144.
- [32] Y.J. Bai, C. Gong, Y.-X. Qi, N. Lun, J. Feng, *J. Mat. Chem.* 22 (2012) 19054–19060.
- [33] Y. Zhang, C. Zhang, Y. Lin, D.-B. Xiong, D. Wang, X. Wu, D. He, *J. Power Sources* 250 (2014) 50–57.
- [34] W. Xu, X. Chen, W. Wang, D. Choi, F. Ding, J. Zheng, Z. Nie, Y.J. Choi, J.-G. Zhang, Z.G. Yang, *J. Power Sources* 236 (2013) 169–174.
- [35] P. Wang, P. Li, T.-F. Yi, X. Lin, Y.-R. Zhu, L. Shao, M. Shui, N. Long, J. Shu, *J. Power Sources* 293 (2015) 33–41.
- [36] P. Wang, P. Li, T.-F. Yi, X. Lin, H. Yu, Y.-R. Zhu, S. Qian, J. Shu, *J. Power Sources* 297 (2015) 283–294.
- [37] H. Ni, W.-L. Song, L.-Z. Fan, Y.-Z. Wang, *Ionics* 21 (2015) 3169–3176.
- [38] P. Zhang, Y. Huang, W. Jia, Y. Cai, X. Wang, Y. Guo, D. Jia, Z. Sun, R. Wang, X. Tang, L. Wang, *J. Electrochem. Soc.* 163 (2016) A1920–A1926.
- [39] Z.W. Zhang, L.Y. Cao, J.F. Huang, S. Zhou, Y.C. Huang, Y.J. Cai, *Ceram. Int.* 39 (2013) 6139–6143.
- [40] Integrity Exports, Mitsubishi chooses super-efficient Toshiba SCiB battery for EVs. <https://integrityexports.com/2011/06/18/mitsubishi-chooses-toshiba-scib-battery-for-evs>, June 2011.
- [41] Green Car Congress, Toshiba's SCiB battery for the fit EV. <http://www.greencarcongress.com/2011/11/scib-20111117.html>, November 2011.
- [42] AA Portable Power Corp., LTO batteries, <http://www.batteryspace.com/Lithium-Titanate-Battery.aspx> (accessed April 2017).
- [43] I. Coweb, All about Batteries, Part 12: Lithium Titanate (LTO), January 2015. http://www.eetimes.com/author.asp?section_id=3638&doc_id=1325358.
- [44] J.O. Besenhard, P. Komenda, A. Paxinos, E. Wudy, *Solid State Ionics* 18/19 (1986) 823–827.
- [45] J.O. Besenhard, M. Hess, P. Komenda, *Solid State Ionics* 40/41 (1990) 525–529.
- [46] C.K. Chan, R. Ruffo, S.S. Hong, R.A. Huggins, Y. Cui, *J. Power Sources* 189 (2009) 34–39.
- [47] J. Yang, M. Winter, J.O. Besenhard, *Solid State Ionics* 90 (1996) 281–287.
- [48] D. Aurbach, E. Zinigrad, Y. Cohen, H. Teller, *Solid State Ionics* 148 (2002) 405–416.
- [49] C.M. López, J.T. Vaughey, D.W. Dees, *J. Electrochem. Soc.* 156 (2009) A726–A729.
- [50] C.M. López, J.T. Vaughey, D.W. Dees, *J. Electrochem. Soc.* 159 (2012) A873–A886.
- [51] B. Song, T. Sui, S. Ying, L. Li, L. Lu, A.M. Korsunsky, *J. Chem. Mat. A* 3 (2015) 18171–18179.
- [52] K. An, P. Barai, K. Smith, P.P. Murkerjee, *J. Electrochem. Soc.* 161 (2014) A1058–A1070.
- [53] J. Christensen, J. Newman, *J. Solid State Electrochem.* 10 (2006) 293–319.
- [54] G. Li, Z. Zhang, Z. Huang, C. Yang, Z. Zuo, H. Zhou, *J. Solid State Electrochem.* 21 (2016) 673–682.
- [55] H. Kim, M.G. Kim, H.Y. Jeong, H. Nam, J. Cho, *Nano Lett.* 15 (2015) 2111–2119.

- [56] D. Wang, X. Wu, Z. Wang, L. Chen, J. Power Sources 140 (2005) 125–128.
- [57] J. Christensen, J. Newman, J. Electrochem. Soc. 153 (2006) A1019–A1030.
- [58] H. Wang, Y.-I. Jang, B. Huang, D.R. Sadoway, Y.-M. Chiang, J. Electrochem. Soc. 146 (1999) 473–480.
- [59] Q. Horn, K. White, Paper 318, presented at the Chicago, IL, Meeting of Electrochemical Society, May 6–10, 2007.
- [60] B.G. Kim, F.P. Tredeau, Z.M. Salameh, Fast chargeability lithium polymer batteries, IEEE on Power and Energy Society General Meeting -Conversion and Delivery of Electrical Energy in the 21st Century, 2008.
- [61] H. Zheng, J. Li, X. Song, G. Liu, V.S. Battaglia, Electrochimica Acta 71 (2012) 258.
- [62] W. Waag, S. Kabit, D.U. Sauer, Appl. Energy 102 (2013) 885–897.
- [63] A.N. Jansen, D.W. Dees, D.P. Abraham, K. Amine, G.L. Henriksen, J. Power Sources 174 (2007) 373–379.
- [64] S.-L. Chou, Y. Pan, J.-Z. Wang, H.-K. Liu, S.-X. Dou, Phys. Chem. Chem. Phys. 16 (2014) 20347.
- [65] J. Xu, S.-L. Chou, Q.-F. Gu, H.K. Liu, S.-X. Dou, J. Power Sources 225 (2013) 172–178.
- [66] Q. Wu, S. Ha, J. Prakash, D.W. Dees, W. Lu, Electrochimica Acta 114 (2013) 1–6.
- [67] P. Prezas, L. Somerville, P. Jennings, A. McGordon, J. K. Basco, T. Duong, I. Bloom, SAE Technical Paper Series, 2016-01-1194.
- [68] D. Aurbach, H. Teller, M. Koltypin, E. Levi, J. Power Sources 119–121 (2003) 2–7.
- [69] L. Somerville, J. Bareño, S. Trask, A. McGordon, C. Lyness, I. Bloom, J. Power Sources 335 (2016) 189–196.
- [70] D. Anseán, M. González, J.C. Viera, V.M. García, J. Power Sources 239 (2013) 9–15.
- [71] G. Sikha, P. Ramadass, B.S. Haran, R.E. White, B.N. Popov, J. Power Sources 126 (2003) 67–76.
- [72] P.H.L. Notten, J.H.G. Op het Veld, J.R.G. Beek, J. Power Sources 145 (2005) 89–94.
- [73] J. Li, E. Murphy, J. Winnick, P.A. Kohl, J. Power Sources 145 (2005) 89–94.
- [74] S.K. Chung, A.A. Andriiko, A.P. Mon'ko, S.H. Lee, J. Power Sources 79 (1999) 205–211.
- [75] Battery Test Manual for Electric Vehicles, U.S. Advanced Battery Consortium, June 2015. Rev. 3.
- [76] P. Arora, M. Doyle, R.E. White, J. Electrochem. Soc. 146 (1999) 3543–3553.
- [77] Information Gathering Meeting, National Renewable Energy Laboratory, Golden, CO, Sept. 21–22, 2016.
- [78] G. Park, N. Gunawardhana, H. Nakamura, Y.-S. Lee, M. Yoshio, J. Power Sources 199 (2012) 293–299.
- [79] J.-W. Huang, Y.-H. Liu, S.-C. Wang, Z.-Z. Yang, IEEE Int. Conf. Power Electron. Drive Syst. (PEDS) (2009) 1547–1551.
- [80] Y.H. Liu, C.H. Hsieh, Y.F. Luo, IEEE Trans. Ind. Electron. 26 (2011) 654–661.
- [81] T.T. Vo, X. Chen, W. Shen, Ajay Kapoor, J. Power Sources 273 (2015) 413–422.
- [82] L.-R. Dung, J.-H. Yen, ILP-based algorithm for Lithium-ion battery charging profile, IEEE International Symposium on Industrial Electronics, July 4–7, 2010.
- [83] W. Shen, T. Tu Vo, A. Kapoor, Charging algorithm of lithium ion batteries: An overview, 7th IEEE conference on Industrial Electronics and Applications, 2012, pp. 1567–1572.
- [84] P.E. De Jongh, P.H.L. Notten, Solid State Ionics 148 (2002) 259–268.
- [85] J. Li, E. Murphy, J. Winnick, P.A. Kohl, J. Power Sources 102 (2001) 302–309.
- [86] L.R. Chen, IEEE Trans. Ind. Electron. 54 (2007) 398–405.
- [87] L.R. Chen, IEEE Trans. Ind. Electron. 56 (2009) 480–487.
- [88] B.K. Purushothama, P.W. Morrison Jr., U. Landau, J. Electrochem. Soc. 152 (2005) J33–J39.
- [89] Computer Aided Engineering for Batteries, Community Battery Simulation Framework, December 2002. <http://batterysim.org>.
- [90] U. S. Department of Energy, Computer Aided Engineering for Batteries, <https://energy.gov/eere/vehicles/downloads/computer-aided-engineering-electric-drive-vehicle-batteries-caebat> (accessed April 2017).
- [91] CHAdeMO, Revolutionizing the way we drive and use our vehicles, <http://www.chademo.com> (accessed April 2017).
- [92] CharIN, Mission and purpose, <http://www.charinev.org/about-us/mission> (accessed April 2017).
- [93] MotorTrend, Tesla supercharger: an in-depth look, <http://www.motortrend.com/news/tesla-supercharger-an-in-depth-look> (accessed April 2017).
- [94] Teslapedia, Understanding charging rates, <http://teslapedia.org/model-s/tesla-drivoer/understanding-charging-rates> (accessed April 2017).
- [95] M. Evertz, F. Horsthemke, J. Kasnatscheew, M. Börner, M. Winter, S. Nowak, J. Power Sources 329 (2016) 364–371.
- [96] M. Daowd, N. Omar, P. Van Den Bossche, J. Van Mierlo, Int. Rev. Elect. Eng. (2011). http://www.superlib.eu/downloads/A%20Review%20of%20Passive%20and%20Active%20Battery%20Balancing_%20based%20on%20MATLAB-Simulink.pdf.
- [97] P. Nelson, K. Gallagher, I. Bloom, BatPaC (Battery Performance and Cost) Software, Argonne National Laboratory, 2012. <http://www.cse.anl.gov/BatPaC>.
- [98] J. Smart, R. Schley, SAE Int. J. Alt. Power 1 (2012) 27–33.

Appendix B



Enabling fast charging – Battery thermal considerations



Matthew Keyser^{a,*}, Ahmad Pesaran^a, Qibo Li^a, Shriram Santhanagopalan^a, Kandler Smith^a, Eric Wood^a, Shabbir Ahmed^b, Ira Bloom^b, Eric Dufek^c, Matthew Shirk^c, Andrew Meintz^a, Cory Kreuzer^a, Christopher Michelbacher^c, Andrew Burnham^b, Thomas Stephens^b, James Francfort^c, Barney Carlson^c, Jiucai Zhang^a, Ram Vijayagopal^b, Keith Hardy^b, Fernando Dias^c, Manish Mohanpurkar^c, Don Scofield^c, Andrew N. Jansen^b, Tanvir Tanim^c, Anthony Markel^a

^a National Renewable Energy Laboratory, 15013 Denver West Parkway, Golden, CO 80401, USA

^b Argonne National Laboratory, 9700 South Cass Avenue, Argonne, IL 60439, USA

^c Idaho National Laboratory, 2525 N. Fremont, Idaho Falls, ID 83415, USA

HIGHLIGHTS

- Aggressive thermal management will be required during extreme fast charging.
- Present high energy density cells will need to increase their charge efficiency.
- Cell design will have an impact on the temperature variation within the cell.
- Battery interconnects will need to be robust and may require a redesign.

ARTICLE INFO

Article history:

Received 21 April 2017

Received in revised form

19 June 2017

Accepted 3 July 2017

Keywords:

Lithium-ion battery

Extreme fast charging

Battery thermal efficiency

Battery thermal management

Cell thermal design

Heat generation

ABSTRACT

Battery thermal barriers are reviewed with regards to extreme fast charging. Present-day thermal management systems for battery electric vehicles are inadequate in limiting the maximum temperature rise of the battery during extreme fast charging. If the battery thermal management system is not designed correctly, the temperature of the cells could reach abuse temperatures and potentially send the cells into thermal runaway. Furthermore, the cell and battery interconnect design needs to be improved to meet the lifetime expectations of the consumer. Each of these aspects is explored and addressed as well as outlining where the heat is generated in a cell, the efficiencies of power and energy cells, and what type of battery thermal management solutions are available in today's market. Thermal management is not a limiting condition with regard to extreme fast charging, but many factors need to be addressed especially for future high specific energy density cells to meet U.S. Department of Energy cost and volume goals.

© 2017 Elsevier B.V. All rights reserved.

1. Introduction

Extreme fast charging (XFC) allows a 200-mile battery pack in a battery electric vehicle (BEV) to be recharged as fast as a conventional vehicle can be refueled. However, XFC will require research and development to address the significant impacts of XFC on the infrastructure, corridor planning, cost of vehicle ownership, battery

chemistry, and deployment economics. While XFC promises to help the adoption of BEVs and curb greenhouse gas emissions and America's need for imported oil, designing high-performance, cost-effective, safe, and affordable energy-storage systems for these BEVs can present challenges, especially in the critical area of battery thermal control. As manufacturers strive to make batteries more compact and powerful, knowing how and where heat is generated becomes even more essential to the design of effective battery thermal management systems (BTMSs).

Enabling XFC requires understanding and controlling the temperature of battery systems. The chemistries of advanced energy-

* Corresponding author.

E-mail address: Matthew.Keyser@nrel.gov (M. Keyser).

storage devices, such as lithium-based batteries, are very sensitive to operating temperature. High temperatures degrade batteries faster while low temperatures decrease their power and capacity, affecting vehicle range, performance, and cost. Understanding heat generation in battery systems—from the individual cells within a module to the interconnects between the cells and across the entire battery system—is imperative for designing effective BTMSs and battery packs.

The 2022 U.S. Department of Energy's (DOE's) battery goals of 350 Wh kg⁻¹, 1000 Wh L⁻¹, and \$125 kWh⁻¹ [1] require battery packs that have higher energy densities, resulting in a very compact system. To meet the specific energy goal, the electrode thickness of the battery will need to increase while decreasing the thickness of the current collectors. Furthermore, the amount of electrochemically inactive material, such as binders, will need to decrease. All of these factors will have a deleterious effect on the thermal performance of the cell. Furthermore, many of the advanced chemistries being developed to attain these goals, such as silicon and lithium metal anodes along with high-energy cathodes, have heretofore suffered from low efficiencies at low to moderate charge and discharge rates. Even if the energy efficiency of the next generation of batteries increases, more heat is being generated per unit volume with a smaller heat transfer area because of the compactness of these batteries. Thus, combining the heat transfer limitations associated with advanced chemistries with XFC will challenge the battery designers to keep the battery temperatures in the “Goldilocks” zone that prevents acceleration of the aging mechanisms within the battery while limiting the cycle life cost.

In 2012, Nissan had to address problems with the battery of its Leaf fully electric vehicle (EV), which was losing capacity in the hot Arizona climate. Many experts in the field attributed this issue to inadequate battery thermal management. Using XFC to enable the penetration of EVs but ignoring their thermal design will negatively affect lifespan, safety, and cost, ultimately resulting in negative consumer perception and reduced marketability.

2. Review of the heat produced in a battery cell and pack

2.1. Battery heat generation

Lithium-ion batteries have very good coulombic cycling efficiencies, as high as 99.5%. The small drop in efficiency is often traced back to a mismatch of properties among the different components (e.g., differences in the rate of transport of electrons versus the ions) and manifests itself in the form of heat. Heat generated within the battery is usually classified into reversible entropic heats and irreversible losses due to low conversion rates for the chemical reactions, or poor transport properties resulting in some polarization losses. Some of these losses are minimized by suitable design changes to the cells. One example is matching the porosity of the electrodes to that of the separator membrane. Mitigation of other types of losses may involve changes to the chemistry of the electrode or the composition of the electrolyte. Tracing back the efficiency losses at the cell level to the relevant contribution from each source will enable battery manufacturers to evaluate tradeoffs between the efficiency improvements and cost of redesigning the cells.

- **Heat Generation from Joule Heating:** Joule heating losses within a cell arise primarily from poor electronic conductivities within the solid phase of the cell, low electrolyte conductivities, contact resistances at the junctions between cell components, or formation of a resistive film on the electrode surface from electrolyte decomposition reactions. Ohmic losses are a function of

the C-rate, size, and age of the cells. Ohmic losses can constitute up to 50% of the heat budget [2].

- **Heat Generation from Electrode Reactions:** Electrochemical reactions taking place within the cells involve transfer of charge at the interface between the electrodes and the electrolyte when the circuit is closed. The mobilities of the bulkier ions are about seven orders of magnitude smaller than those of the electrons, and the difference in the electrochemical potentials for lithium ions within the host lattice at the electrode and within the electrolyte governs the rate of charge transfer. Transfer of charge across the energy barrier at the interface results in loss of a part of the kinetic energy associated with these reactions. Heat losses due to the charge transfer process are measured as the difference in free energies across the two sides of the interface. Whereas sluggish kinetics have been known to limit efficiencies in some chemistries (e.g., in some phosphate-based cathodes), activation barriers usually contribute to 30%–40% of the heat losses under practical operating cases [2].
- **Entropic Heat Generation:** Insertion and de-insertion of lithium ions in and out of the electrodes result in entropic changes within the electrodes. Ideally, such changes are reversible under very slow rates of charge and discharge; however, from a practical perspective, there is some energy loss associated with these phenomena. Usually, the entropic losses in an electrode take place at well-defined voltage windows. Such entropic losses constitute the reversible portion of heat generation. Whereas these changes can be as low as 5%–10% of the total heat budget [2], changes to the entropy of the host lattice are often accompanied by additional limitations such as changes to mechanical properties or phase changes, which complicate the analysis of the impact of such losses on the durability of the cell.

2.2. Heat generation of high energy density cells

Fig. 1 shows the heat efficiency of two cells—energy and power—tested in a large volume isothermal calorimeter. The graph shows a full discharge from 100% to 0% state of charge. The data are limited due to the discharge limitations for the energy cell under test. The maximum continuous discharge rate as specified by the manufacturer was 2C. The power cell in Fig. 1 has a capacity of 6 Ah whereas the energy cell has a capacity of 20 Ah. The thermal heat efficiency is representative of most energy and power cells tested in the calorimeter. Due to the thickness of the coatings (cathode and

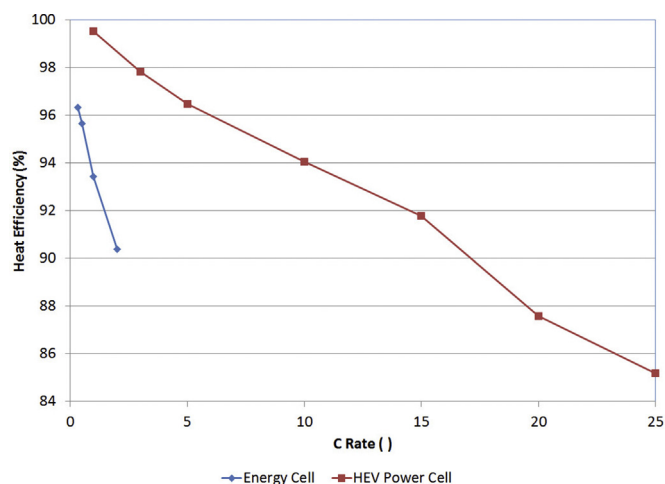


Fig. 1. Discharge efficiency of an energy cell and a power cell at 30 °C.

anode) and the thickness of the current collectors, the efficiency of the energy cells is well below that of the power cell – both cells are of the same chemistry, NMC/graphite. As a rule of thumb, the charge efficiency for graphitic cells is typically 2%–8% less than the discharge efficiency. In the end, the state-of-the-art energy cells have efficiencies that will limit them from being used in XFC scenarios.

To attain DOE's goals of 350 Wh kg^{-1} and $\$125 \text{ kWh}^{-1}$, new cathodes and anodes need to be investigated. On the cathode side, nickel or manganese rich nickel-manganese-cobalt (NMC) has the potential to help with the energy density of the cells; however, cathodes and anodes both have issues with dissolution of the excess metal used in their chemistry. We are also investigating both silicon and lithium anodes to meet the specific energy density goals. Silicon has expansion/contraction issues when cycling as well as irreversible capacity loss after the first cycle, and a pure lithium anode comes with many safety challenges. Both advanced cathodes and anodes were tested in an isothermal calorimeter. Their discharge efficiencies as a function of C-rate are shown in Fig. 2. The advanced NMC cathode with a graphitic anode was tested at 30°C and has a capacity of approximately 20 Ah. The discharge efficiency for this cell at a 2C rate is about 81%. Fig. 2 also shows a lithium anode cell with a solid electrolyte. The solid electrolyte helps to address safety concerns but has poor ionic diffusivity at room temperature, so the test was run at an ambient temperature of 80°C . The efficiency for the lithium anode under a constant current discharge approaches 94%, but only for a C/2 discharge rate. In comparison, present high-power lithium-ion cells used in EVs have a discharge efficiency of about 99% under a C/2 discharge and at an ambient temperature of 30°C . The solid electrolyte limits the rate and temperature at which the cell can be used, which limits their present use in EVs. Improvements to both the cathode and anode need to be made to meet the DOE's energy and cost goals, and the efficiency of these advanced cells will also need to be improved to meet the demands of XFC.

2.3. Cell temperature study under XFC

To better understand the heat transfer limitations with regards to extreme fast charging, a lumped heat transfer analysis and a 3-D simulation for a standard lithium ion cell were performed. The specification and heat transfer conditions of battery pack are shown in Table 1 and Table 2, respectively.

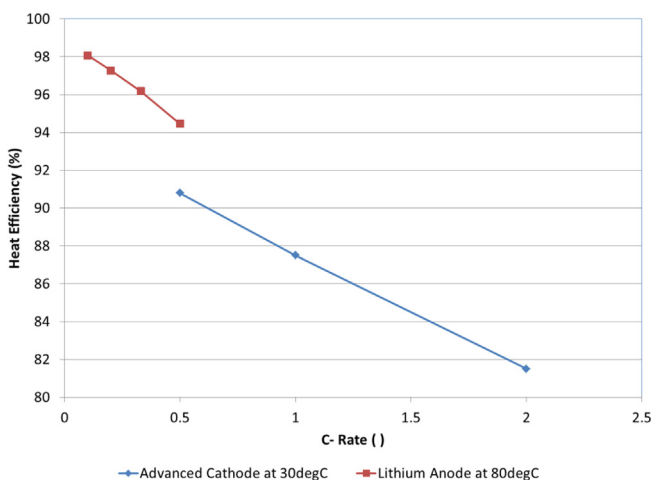


Fig. 2. Discharge efficiency of a cell with an advanced NMC cathode and a cell with a lithium anode.

Table 1
Battery pack specification.

Performance Characteristics	Typical	Unit
Maximum Range Provided	200	Miles
Energy Used Mile ⁻¹	0.33	kWh mile ⁻¹
Pack Energy	66	kWh
Charger Power	350	kW

Table 2
Battery pack heat transfer conditions.

	Lower Limit	Upper Limit
Battery Regen/Charge Efficiency (%)	70	90
Pack Heat Generation (kW)	116	39
Heat Transfer Coefficient ($\text{W m}^{-2} \text{K}^{-1}$)	10	100
Cooling Provided (kW)	2	15
Energy Density (Wh kg^{-1})	175	300

In this study, we modeled a single cell within the battery pack. The specification and geometry of battery cell are shown in Table 3.

To understand the effects of heat transfer conditions and energy density of the battery on temperature of single battery cell, four cases were selected for this study as shown in Table 4. At the beginning of each simulation, the heat transfer coefficients specified in Table 4 are the limiting condition for heat transfer. As the cell heats and the available cooling power increases, the limiting condition is the total thermal power removed per cell.

The 3-D simulation was performed using the commercially available ANSYS/Fluent software. For the 3-D simulation, the heat transfer coefficient and cooling are being provided to the large surfaces of the cell, not to the terminals or edges; all other surfaces of the battery cell are assumed to be under adiabatic conditions. The ambient temperature and initial cell temperature were assumed to be 23°C .

The battery cell was divided into 31 sets of layers. Each layer includes the aluminum current collector, cathode, separator, anode, and copper current collector. The properties for these cell components are shown in Table 5.

Fig. 3 shows the cell temperature rise for the four individual cases during the 350-kW XFC. The figure shows that Cases 2 and 4 have the lowest temperature rise, and the temperature rise for Cases 1 and 3 are approaching abuse levels—greater than 200°C after 750 s. For Cases 1 and 3, the charge efficiency of the cell is 70% (typical charge efficiency for high energy density cells), and the thermal management system is only providing 2 kW of cooling to the pack. When comparing Cases 2 and 4, the cell energy density for Case 4 is the lowest, which leads to the maximum number cells needed to provide a 200-mile range for the EV. Thus, the heat generation per cell is much lower for Case 4 with the largest available surface area to remove the heat: more cells leads to more surface area. It should be noted that both Cases 2 and 4 have the same total pack cooling power, 15 kW, which is substantially oversized as compared to the cooling systems for most EVs presently on the market. In summary, when heat transfer conditions for the battery packs are the same, the cell with the lower energy density yields an overall lower cell temperature.

This simplified study yields a few interesting conclusions. With

Table 3
Cell geometry and mass.

	Typical	Unit
Mass of Single Cell	0.78	kg
Dimensions of Single Cell (T × W × H)	$7.9 \times 225 \times 190.5$	mm

Table 4
Case conditions under a constant 350-kW charge.

Case 1			Case 2		
Energy Density	175	Wh kg ⁻¹	Energy Density	300	Wh kg ⁻¹
Number of Cells	484	cells	Number of Cells	282	cells
Cell Efficiency	70	%	Cell Efficiency	90	%
Pack Heat Removed	2	kW	Pack Heat Removed	15	kW
Heat Generation per Cell	239.9	W	Heat Generation per Cell	138.3	W
Cooling Provided per Cell	4.14	W	Cooling Provided per Cell	53.2	W
Heat Transfer Coefficient	10	W m ⁻² K ⁻¹	Heat Transfer Coefficient	100	W m ⁻² K ⁻¹
Case 3			Case 4		
Energy Density	300	Wh kg ⁻¹	Energy Density	175	Wh kg ⁻¹
Number of Cells	282	cells	Number of Cells	484	cells
Cell Efficiency	70	%	Cell Efficiency	90	%
Pack Heat Removed	2	kW	Pack Heat Removed	15	kW
Heat Generation per Cell	411.3	W	Heat Generation per Cell	80.7	W
Cooling Provided per Cell	7.1	W	Cooling Provided per Cell	31	W
Heat Transfer Coefficient	10	W m ⁻² K ⁻¹	Heat Transfer Coefficient	100	W m ⁻² K ⁻¹

Table 5
Properties of battery cell with multiple layers.

Properties	Thickness (μm)	C _p (J kg ⁻¹ K ⁻¹)	Density (kg m ⁻³)	K-cross plane (W m ⁻¹ K ⁻¹)	K-in plane (W m ⁻¹ K ⁻¹)
Al current collector	20	889	2700	235	235
Cathode	43	973	3611	1.03	19.15
Separator	22	2057	1107	0.31	0.31
Anode	46	1111	1907	2.36	28.18
Cu current collector	14	378	8880	400	400

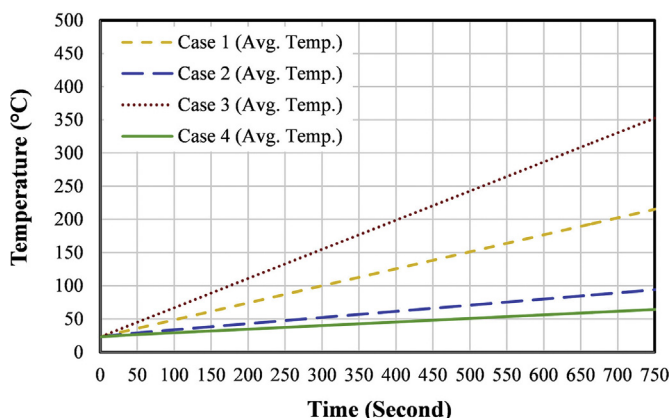


Fig. 3. Average temperature rise of a single battery cell for Cases 1, 2, 3, and 4.

an oversized BTMS of 15 kW and low energy density cells (power cells), it is possible to design a system that may be able to charge at 350 kW without hitting the DOE's maximum operating temperature goal of 52 °C. From the Case 4 scenario above, the end temperature of the cell would be around 56 °C from a starting temperature of 23 °C after charging for 600 s or at a 6C rate. However, when using a cell with an energy density of 175 Wh kg⁻¹ as in the Case 4 scenario, the penalty to the vehicle would be increased mass, volume, and cost. The typical power cell has thinner material coatings on the cathode and anode as well as thicker aluminum and copper current collectors. All of these contribute to higher power cells but also increase the battery pack cost due to the loss of active material. The typical lithium ion power cell costs between \$400–\$600 kWh⁻¹. In the end, we can come close to meeting the thermal targets of charging at 350 kW by using power cells but with a cost, volume, and mass penalty. However, we need to take other factors into consideration before making such a sweeping generalization.

2.4. Battery temperature variation and design

The 3-D study described above assumes that all the heat generation within the cell is spread equally across the volume of the cell, which is obviously an over-simplification. Furthermore, Section 2.3 assessed how the average temperature of the cell varies as a function of energy density and heat transfer characteristics but the temperature variance within the cell also needs to be evaluated, especially for XFC conditions. NREL previously performed an empirical study [3] on varying the length scales and tab designs for a lithium cell to determine the temperature effects of a fast rate discharge. The models used for the discharge study were modified here to simulate a fast rate (6C) charge. Fig. 4 summarizes the four different cell designs investigated during the study.

In the fast charge study, the cell design was varied to assess the volumetric temperature variation and these results are presented in Fig. 5. In Fig. 5, temperature contours at nine cross-sectioned surfaces of each cell are presented to show details of the spatial temperature imbalance at the end of charge. The average charge efficiency for each of the cell designs was calculated to be approximately 90%, which is the typical efficiency of a power cell under a high rate charge. The results clearly show how the tab and cell design affects the temperature distribution within the cell but also how the interior cell temperature varies across its volume. The most thermally uniform cell is the counter tab design, a 2.9 °C difference across the cell, whereas the least thermally uniform is the small tab design, a temperature difference of 4.4 °C. The maximum temperature of the cell needs to be limited during XFC, but the temperature difference across the cell will also impact the cell cost and life.

The cell thermal contour study was performed using high-power cells where the battery material and design were optimized for today's hybrid electric vehicles. As a counter point, Fig. 6 shows the thermal image of a high-energy NMC/graphite advanced chemistry 18-Ah cell that was designed exclusively for EV applications. The figure contains a thermal image of the cell at the end of

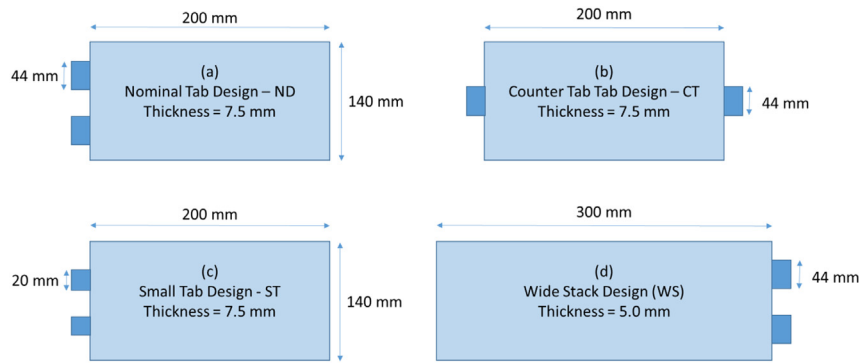


Fig. 4. Schematic description of the 20-Ah stacked pouch cell designs.

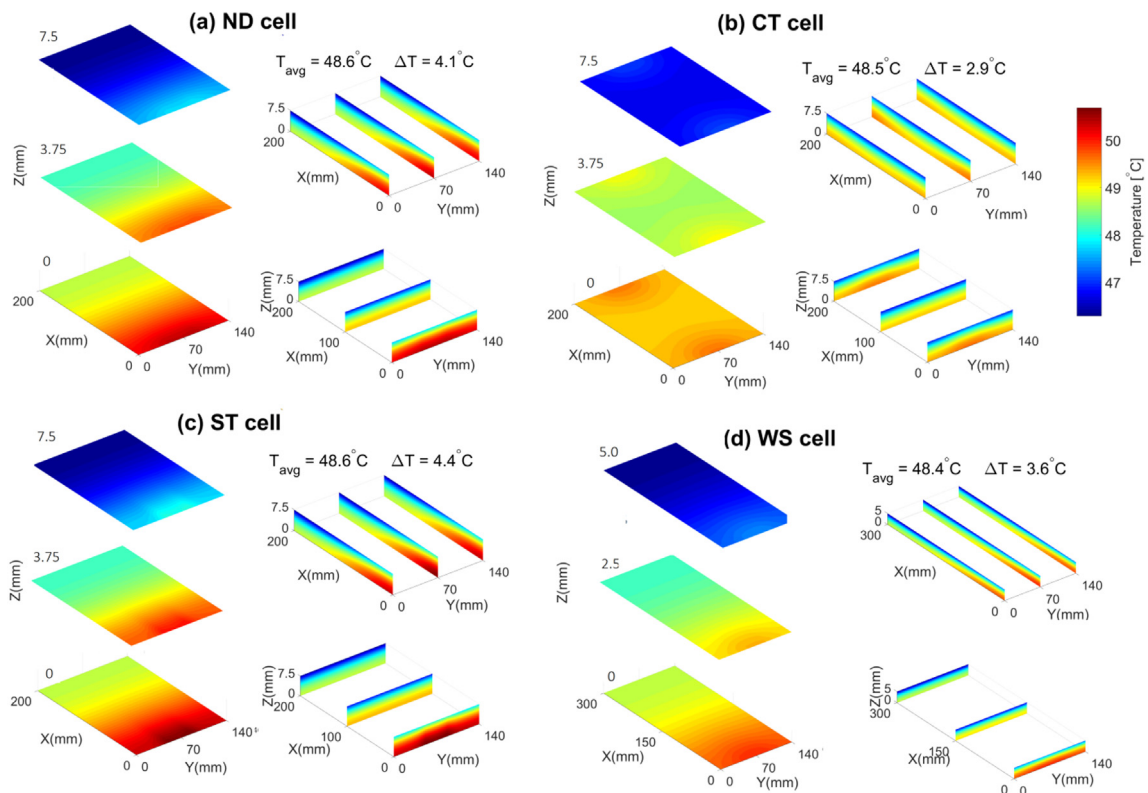


Fig. 5. Contours of temperature at nine cross-sectioned surfaces in cell composite volume at the end of 6C constant current charge: (a) ND cell, (b) CT cell, (c) ST cell, (d) WS cell. (Dimensions in Z direction of the contour surfaces are exaggerated for a clearer view of quantity variation in Z direction.)

a 2C constant current discharge as well as a plot showing horizontal contour lines across the face of the cell – L01, L02, L03, and L04. The cell had an initial temperature of 23 °C. Fig. 6 shows a hot spot in the upper left corner of the thermal image of the cell as well as a wide spread in temperature across the face of the cell from top to bottom and left to right – the active area surface temperature varies by about 6 °C. When the cell temperature is non-uniform and inconsistent, areas within the cell age at different rates, leading to poor cycle life: areas of the cell that are higher in temperature are more efficient and therefore age faster due to higher power loads [4]. It should be noted that the high-energy NMC cells are prone to gassing during cycling, and further research and development will be necessary to incorporate these cells in BEV and XFC applications.

To enable XFC, cell designs may need to be modified to minimize the time constant for the heat generated within the cell to get to the

primary cooling plate, liquid, etc., during XFC. If the time constant is large, the heat will not be able to get from the cell interior to the cooling system. Methods to adjust the cooling path may include:

- Increasing the amount of carbon black or other conductive material in the cathode and anode [5].
- Increasing the thickness of the current collectors.
- Incorporating low temperature phase change material within the cell to absorb heat where it is generated. However, it may not be feasible to modify the cell with an electrochemically inert material.
- Continuous current collectors have a more optimal heat conductive path but would limit the cell design options.

All of the above suggestions will have an impact on the energy

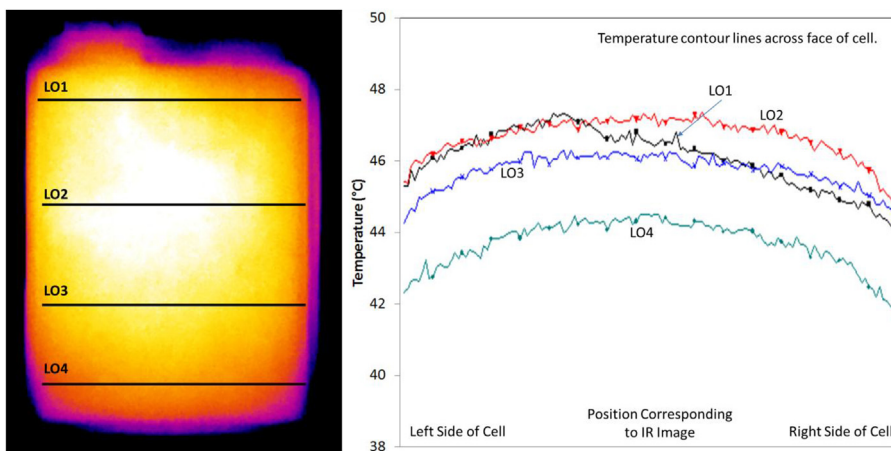


Fig. 6. Thermal image and temperature plot of a high-energy NMC/graphite cell at the end of a 2C constant current discharge from 100% to 0% state of charge.

density of the battery and will therefore affect the range of the vehicle. However, they may be necessary to keep the battery cool during XFC.

2.5. Module interconnect design

To understand the heat generation in a module due to the battery interconnects, the heat generation of a lithium-iron-phosphate/graphite cell was measured individually and when incorporated into a 10-cell module. The module was designed for a hybrid electric vehicle application, and the cells were considered to be power cells with a power-to-energy ratio of greater than 10 – the power-to-energy ratio is defined as the maximum battery power for a known period of time divided by the overall energy stored in the battery. Fig. 7 shows a comparison of the heat generation of a single lithium-iron-phosphate/graphite cell and the heat generation per cell for the module at various discharge currents – the difference in heat rate/cell is due to the interconnects between the cells in the module. The root mean square current for the relevant HEV application was calculated to be approximately 35 A. At this current, the heat generation normalized per cell in the module is about 22% greater than for an individual cell. Thus, even with a design optimized for high power/current, the interconnects can contribute a substantial amount of heat above and beyond the cells. For XFC applications, the heat contributed by the interconnects will need to be considered in order to mitigate potential safety

concerns.

3. Thermal management system

3.1. Battery thermal management design

During our previous 3-D temperature study in Section 3.2, we considered two BTMSs with cooling powers of 2 kW and 15 kW. The 3-D study showed that the cooling power during XFC will need to be increased beyond today’s BTMSs for BEVs, perhaps to levels greater than 15 kW, to limit the temperature rise of the cells within the pack. In the end, the BTMS ensures that the battery pack can deliver the specified load within the temperature constraints set by battery performance and life requirements across a wide range of operating conditions for the battery pack. The temperature distribution within a battery module is usually controlled tightly and is often as low as 2 °C. There are additional specifications on weight, volume, cost, energy budget, and reliability that are closely tied to the application. There are different classifications of thermal management techniques for battery packs based upon the working fluid (an air-cooled versus a liquid-cooled system) or functionality (an active cooling system with a heating or cooling source versus a passive system). A BTMS for an XFC system should carefully consider the tradeoffs between the energy budget for thermal management and the heat loads under fast charge, since an XFC system will have very different heat loads compared to conventional battery packs. Design of an optimal BTMS is often a tradeoff among the following constraints [6]:

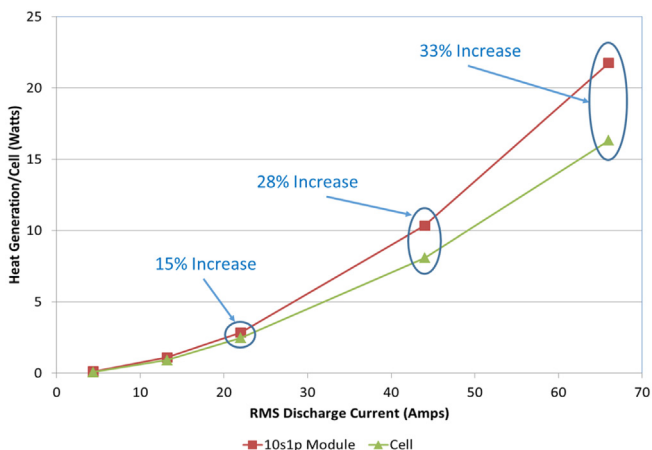


Fig. 7. Heat generation normalized on a cell basis for a single cell and a 10-cell lithium-iron-phosphate module.

- The BTMS should balance the desired thermal performance for the modules and packs under various operating conditions (e.g., specifications on the average temperature for the battery pack, minimum or maximum temperatures) with constraints on size or weight of the BTMS.
- Interfaces between the cells, as well as those between the battery and the rest of the vehicle, are important, but often overlooked aspects of thermal management.
- Safety requirements (e.g., structural specifications to sustain pressure drop for a given flow rate of the coolant) for battery packs are often different from those for other passive components within the vehicle.

3.2. Battery thermal management strategies

Today’s BTMSs typically use air, liquid, or refrigerant cooling to

manage the temperature of the cells. The air-cooling technique circulates ambient or actively cooled air through the battery pack, and the heat is rejected to the surroundings, which requires large surface areas to extract the heat. Air is typically the least expensive thermal management option, but due to its low thermal conductivity and heat capacity, it requires large flow channels and high fan power. The high fan power may also irritate some drivers due to the noise.

Liquid cooling is the preferred thermal management strategy for most BEV systems on the market today. It typically involves a combination of ethylene glycol and water as the working fluid due to the low cost. Liquid cooling systems benefit from high heat capacity and thermal conductivity as compared to air systems. However, the liquid flow channels are typically more complex and require an extensive number of connections leading to a higher potential for failure. If the liquid cooling system were to fail, then there is the potential that the liquid could short out adjacent cells within the battery pack which could lead to thermal runaway. To address this concern, a dielectric coolant could be utilized instead of an ethylene glycol/water mixture, but at a significant cost penalty. Also, dielectric fluids tend to lose their ability to insulate over time, which may require costly regular maintenance or a filtration system.

The third option is to actively cool the batteries using a vapor compression system. The typical design shunts heat from the cells in the battery pack to the evaporator of the vapor compression system using a thin metal plate. The evaporator consists of a flat plate through which the refrigerant circulates in channels or tubes. This system is more complex and with a higher initial cost and it also has reliability issues—the refrigerant will have to be contained within a hermetically sealed system for the life of the battery pack. One net positive of the system is that the evaporator plate can be cooled to sub-ambient temperatures, allowing for more thermal power to be dissipated due to the higher temperature difference between the battery cells and the cold plate. However, since the refrigerant is not in direct contact with the cells, the temperature difference across the surface of the cell may be increased.

3.3. Cooling fluid provided at direct current fast charging station

If XFC is to be utilized in vehicles, new cooling strategies may need to be developed such as jet impingement, submersion of the battery pack in a dielectric coolant, or perhaps incorporating phase change material as a buffer for XFC. External cooling provided to the vehicle at the direct current fast charging (DCFC) station should also be considered. However, what type of standardized cooling should be provided by the charging station? If chilled air is provided at the charging station, the cooling power would be limited, as indicated above, by the low heat capacity of air. The air volume required for the needed cooling power would be extremely high, limiting the use of most internal heat exchangers presently used in today's EVs. Active cooling in the form of vapor compression—i.e., providing a low-pressure refrigerant to the vehicle and integrated with the battery heat exchangers—will not be feasible. The potential for release of refrigerant would be a difficult to approve/handle from an environmental health perspective. The only feasible option would be to provide chilled water/coolant to the vehicle. If the onboard system has a different type of cooling strategy, would that mean that two heat exchanger systems are required? What would be the temperature of the cooling liquid? Would this only exacerbate the cell temperature imbalance and affect the cycle life cost of the battery. In summary, there are many thermal management questions that need to be answered before XFC will be a reality.

4. Temperature effect on battery lifetime and capacity

4.1. Temperature effect on life of battery

Lithium-ion battery life also varies greatly with cell temperature, maximum and minimum SOC, all of which are impacted by XFC. Charging C-rate is also a factor in aging; however, in test data that exists to date, it is difficult to decouple the impact of charging C-rate from coupled factors of elevated cell temperature and accelerated frequency of charge/discharge cycles per day. It would be possible to design experiments that decouple each of these factors. Different cell chemistries and power-to-energy ratio designs would respond differently to these factors.

Previous work at the National Renewable Energy Laboratory [7–9] has developed aging models of lithium-ion cells that consider the impact of temperature and charge/discharge cycle on battery life. The dominant factor, temperature, is well captured by the models. Fig. 8 shows the influence of cell yearly average temperature on battery life. Lifetime roughly doubles for each 13 °C reduction in average battery temperature. While average temperature dominates calendar life, minimum and maximum temperature extrema will also influence lifetime. It should also be noted that the critical point in the curve at approximately 80% DOD delineates the transition between calendar and cycle aging effects—below approximately 80%, the calendar ageing effects dominate whereas above 80%, the cycle ageing effects dominate [10].

Another issue related to battery temperature and lifetime is cell-to-cell capacity imbalance growth. Passive electrical cell balancing is the norm in today's BEVs due to the lower cost of those electrical controls compared to active cell balancing. With a passive balancing system, the overall battery pack's capacity is limited by the weakest cell in the series string of cells. Cells age differently, both due to manufacturing non-uniformity and cell-to-cell temperature differences across a multi-cell pack. Large packs with cells spread across the vehicle platform will experience relatively large cell-to-cell temperature differences. Depending on the thermal management design, fast charging may exacerbate cell-to-cell temperature imbalance and drive weak cells in hot locations of the pack to premature end of life. This factor remains to be quantified for XFC.

4.2. Effect of 50-kW DCFC on battery life and capacity

Although the effects of XFC have not yet been studied by the

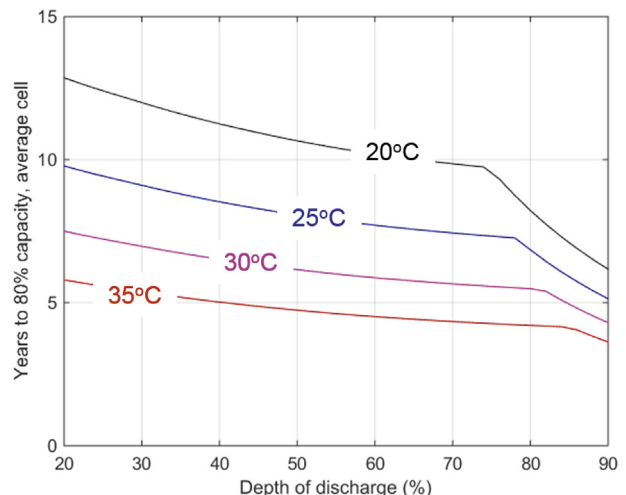


Fig. 8. Capacity fade of a NMC/Gr. cell at different average temperatures [10].

authors, the Battery Lifetime Analysis and Simulation Tool (BLAST) [11] has been used to investigate the impact of 50-kW DCFC on simulated battery degradation. The analysis also reviewed the effects of three different BTMSs (passive, active, and active with standby cooling) in two climates (Seattle, Washington (cool/wet), and Phoenix, Arizona (hot/dry)) using a simulated single-cell battery model of a nickel-cobalt-aluminum cathode and graphite anode with a power-to-energy ratio of 6.1. The study showed that the vehicles with the most extreme travel history and the largest time-averaged battery temperature had a time-averaged battery temperature increase of 2°C–3°C in the presence of a passive BTMS. Where an active BTMS is present, this effect is largely unnoticeable. As shown in Table 6, there is little impact from 50-kW DCFC on capacity loss in either Seattle or Phoenix; however, the BTMS has a significant impact on capacity in Phoenix. Past studies [12] have shown that BEV battery life is often dependent on calendar fade mechanisms rather than cycling fade mechanisms; thus, the time-averaged battery temperatures directly relate to battery capacity loss.

While the nearly negligible impact of 50-kW DCFC use on battery capacity fade may be surprising to some, it is important to point out that most drivers will use DCFCs quite sparingly. Most drivers use a DCFC less than once per month, and when DCFCs are used, they typically increase the charge of the battery by less than 60%. Further, recent tests where DCFCs are used twice per day to charge Nissan LEAFs driving in Phoenix [13] have shown that the difference in capacity loss is less than 3% due to fast charger use (as compared to an otherwise identical case using Level 2 charging) after 50,000 miles of driving. Thus, the results employing more realistic, less aggressive fast charging habits are to be expected. However, it is possible that alternative battery chemistries outside of this study could sustain considerable losses in capacity or increases in resistance due to such low frequency DCFC use (e.g., via particle fracture). Clearly, it would not be advisable to recommend fast charging such chemistries, and thus analysis of such cases is not addressed herein.

Where the effect of DCFC use is most noticeable is in the maximum achieved battery temperature. As shown in Table 7, comparison of cases with and without DCFC availability shows that maximum battery temperatures are ~15 °C higher for the median driver when fast charging is employed with a passive BTMS. In the presence of fast charging, our simulated maximum battery temperatures regularly exceed 45 °C in Seattle and 60 °C in Phoenix, so high that they could pose a safety risk if charging and/or driving are not impeded by onboard vehicle control systems. The addition of active battery cooling, however, can significantly moderate maximum battery temperatures, especially when employed while driving and charging.

Finally, the variation in cell state of health within packs following 10 years of automotive service was studied for 50-kW DCFC. The study employed a multi-cell model only with the active BTMS operated during driving and standby, having recognized its necessity in the previously describe work. Results for maximum thermal gradients show that such gradients regularly

exceed 11 °C in the presence of fast charging. Such gradients, if sustained for long periods of time, would be expected to create large variations in cell state of health within a pack, which would then limit the utility of the vehicle.

The 50-kW DCFC study showed that battery capacity fade will be highly dependent on how often the fast charging stations are used by the consumer as the fade is directly related to the mean temperature of the battery. However, the maximum temperature under certain ambient conditions (Phoenix) and the cell-to-cell temperature variation across the pack were of more concern at the 50-kW level of fast charging. It should also be noted that the power-to-energy ratio of the battery simulated was 6.1, and most 200 + mile BEVs will have a much lower power-to-energy ratio. The cells will therefore be less efficient, and the temperature maximum and variation will be increased. Obviously, each of these parameters will be magnified when utilizing XFC stations on a regular basis. Further studies on cooling strategies will be needed to determine how to keep the batteries below the operational maximum temperature limit during XFC and still be able to provide the driving range desired by consumers.

5. Conclusions

Extreme fast charging will allow the consumer to charge the vehicle battery by 80% in an 8- to 10-min period, which is on par with the refueling time of conventional gasoline-powered vehicles. The ability to charge the BEV this rapidly will decrease the range anxiety of many consumers and will aid in the adoption of BEVs. However, there are many battery thermal considerations that need to be addressed before XFC can become a reality, including:

- A robust BTMS will be required and will be independent of the energy density of the cells; even with high power cells, an oversized BTMS will be needed.
- The size of the BTMS will have to increase from today's BEV average size of 1–5 kW to around 15–25 kW.
- The heat efficiency of high energy density cells will need to improve by 10%–20% at high rates of charge.
- New thermal management strategies like jet impingement or immersion of the battery in a dielectric fluid may need to be investigated to keep the battery below the maximum operational temperature limit.
- The cell-to-cell imbalance due to XFC will affect the longevity and cycle life cost of the cells. New passive and/or active battery management systems will need to be investigated to ensure that the batteries meet the original equipment manufacturer's warranty obligations.
- Cell design will have an impact on the temperature variation within the cell and the temperature imbalance within the pack.
- The mean average temperature of the battery directly affects the cycle life of the battery. High XFC use by the driver will have a strong influence on this metric.
- Additional cooling at the XFC station may be required to ensure a complete charge of the battery pack.

Table 6
Effect of DCFC and BTMSs on battery capacity loss in Seattle and Phoenix [9].

Seattle Climate 10-Year Capacity Loss, %			Phoenix Climate 10-Year Capacity Loss, %		
Strategy	No Fast Charge	Fast Charge	Strategy	No Fast Charge	Fast Charge
Passive Cooling	17.6	18.1	Passive Cooling	27.0	27.6
Active Cooling	17.3	17.5	Active Cooling	24.4	24.5
Active + Standby	17.1	17.3	Active + Standby	21.0	21.2

Table 7
Effect of DCFC and BTMS on maximum battery temperature in Seattle and Phoenix [9].

Seattle Climate Maximum Battery Temperature, °C			Phoenix Climate Maximum Battery Temperature, °C		
Strategy	No Fast Charge	Fast Charge	Strategy	No Fast Charge	Fast Charge
Passive Cooling	32.8	47.2	Passive Cooling	47.8	63.5
Active Cooling	31.2	37.2	Active Cooling	46.3	46.7
Active + Standby	29.6	29.8	Active + Standby	42.5	42.7

XFC from a thermal perspective will be challenging, but it is not an improbable barrier to overcome. Presently, we can address many of the thermal issues by using low energy density or power cells in combination with an oversized BTMS. However, the system will not meet DOE's cost, mass, and volume goals for a BEV, and the cost alone will not allow for large market penetration. To meet DOE's goals, we will need to investigate new thermal management strategies for cell and pack cooling and will need to greatly improve the thermal efficiency of many of the advanced cathodes and anodes presently under development. The cell thermal design for these advanced chemistries will also need to be optimized to limit the life cycle effects on the battery pack associated with XFC.

Acknowledgements

This work was performed under the auspices of the U.S. Department of Energy Office of Vehicle Technologies, under Contract Nos. DE-AC02-06CH11357 (Argonne National Laboratory), DE-DE-AC07-05ID14517 (Idaho National Laboratory), and DE-AC36-08GO28308 (National Renewable Energy Laboratory). The U.S. Government retains for itself, and others acting on its behalf, a paid-up nonexclusive, irrevocable worldwide license in said article to reproduce, prepare derivative works, distribute copies to the public, and perform publicly and display publicly, by or on behalf of the Government.

Acronyms

BEV	battery electric vehicle
BTMS	battery thermal management system
C-Rate	Rate at which a battery is discharged relative to its maximum capacity
DCFC	direct current fast charging

DOE	U.S. Department of Energy
XFC	extreme fast charging (between 150 and 400 kW)
EV	electric vehicle
NMC	nickel, manganese, and cobalt cathode

References

- [1] D. Howell, B. Cunningham, et al., Overview of the DOE VTO Advanced Battery R&D Program, Annual Merit Review, June, 2016.
- [2] V. Srinivasan, C.Y. Wang, Analysis of electrochemical and thermal behavior of Li-ion cells, *J. Electrochem. Soc.* 150 (2003) A98–A106.
- [3] G.-H. Kim, K. Smith, K. Lee, S. Santhanagopalan, A. Pesaran, Multi-domain modeling of lithium-ion batteries encompassing multi-physics in varied length scales, *ECS 158* (2011) A955–A969.
- [4] Smith, K.; Shi, Ying; Santhanagopalan, Shriram. (2015). Proceedings of the 2015 American Control Conference (ACC), July 1-3, 2015, Chicago, Illinois; pp. 728–730.
- [5] Y.-H. Chen, C.-W. Wang, G. Liu, X.-Y. Song, V.S. Battaglia, A.M. Sastry, Selection of conductive additives in Li-Ion battery cathodes, *ECS 154* (2007) A978–A986.
- [6] S. Santhanagopalan, K. Smith, J. Neubauer, G.-H. Kim, A. Pesaran, M. Keyser, Design and Analysis of Large Lithium-Ion Battery Systems, Artech House, 2014.
- [7] K. Smith, Y. Shi, E. Wood, A. Pesaran, Optimizing battery usage and management for long life, Advanced Automotive Battery Conference, Detroit, Michigan, June 16, 2016.
- [8] J. Neubauer, E. Wood, E. Burton, K. Smith, A.A. Pesaran, Impact of fast charging on life of EV batteries, EVS28, Kintex, Korea, May 3–6, 2015.
- [9] J.S. Neubauer, E. Wood, Will your battery survive a world with fast chargers? SAE World Congress, Detroit Michigan, April 21–23, 2015.
- [10] K. Smith; Y. Shi; E. Wood, A. Pesaran. Advanced Automotive Battery Conference (AABC), Detroit Michigan, June, 14–17, 2016.
- [11] J. Neubauer, Battery Lifetime Analysis and Simulation Tool (BLAST) Documentation, December, 2014.
- [12] J. Neubauer, E. Wood, Thru-life impacts of driver aggression, climate, cabin thermal management, and battery thermal management on battery electric vehicle utility, *J. Power Sources* 259 (2014) 262–275.
- [13] INL/MIS-13–29877, DC fast Charge Effects on Battery Life and Performance Study – 50,000 Mile Update, April, 2015.

Appendix C



Contents lists available at ScienceDirect

Journal of Power Sources

journal homepage: www.elsevier.com/locate/jpowsour

Enabling fast charging – Vehicle considerations



Andrew Meintz^{c,*}, Jiucai Zhang^c, Ram Vijayagopal^a, Cory Kreutzer^c, Shabbir Ahmed^a, Ira Bloom^a, Andrew Burnham^a, Richard B. Carlson^b, Fernando Dias^b, Eric J. Dufek^b, James Francfort^b, Keith Hardy^a, Andrew N. Jansen^a, Matthew Keyser^c, Anthony Markel^c, Christopher Michelbacher^b, Manish Mohanpurkar^b, Ahmad Pesaran^c, Don Scofield^b, Matthew Shirk^b, Thomas Stephens^a, Tanvir Tanim^b

^a Argonne National Laboratory, 9700 South Cass Avenue, Argonne, IL 60439, USA

^b Idaho National Laboratory, 2525 N. Fremont, Idaho Falls, ID 83415, USA

^c National Renewable Energy Laboratory, 15013 Denver West Parkway, Golden, CO 80401, USA

HIGHLIGHTS

- BEV refueling time requires 4–6 C-rate charging and large battery capacities.
- Peak charge rate less important than average rate for 150–200 mile range recharge.
- XFC significantly impacts BEV voltage design, which may impact other EVs.
- BEV-charging infrastructure coordination must provide consistent charge experience.

ARTICLE INFO

Article history:

Received 28 April 2017

Received in revised form

17 July 2017

Accepted 25 July 2017

Keywords:

Direct current fast charging (DCFC)

Battery electric vehicles (BEV)

Extreme fast charging (XFC)

Power electronics

Long-distance travel

ABSTRACT

To achieve a successful increase in the plug-in battery electric vehicle (BEV) market, it is anticipated that a significant improvement in battery performance is required to increase the range that BEVs can travel and the rate at which they can be recharged. While the range that BEVs can travel on a single recharge is improving, the recharge rate is still much slower than the refueling rate of conventional internal combustion engine vehicles. To achieve comparable recharge times, we explore the vehicle considerations of charge rates of at least 400 kW. Faster recharge is expected to significantly mitigate the perceived deficiencies for long-distance transportation, to provide alternative charging in densely populated areas where overnight charging at home may not be possible, and to reduce range anxiety for travel within a city when unplanned charging may be required. This substantial increase in charging rate is expected to create technical issues in the design of the battery system and the vehicle's electrical architecture that must be resolved. This work focuses on vehicle system design and total recharge time to meet the goals of implementing improved charge rates and the impacts of these expected increases on system voltage and vehicle components.

© 2017 Elsevier B.V. All rights reserved.

1. Introduction

Presently, plug-in battery electric vehicles (BEVs) are not capable of charging at rates that allow for a recharging time similar to refueling conventional internal combustion engine vehicles (ICEVs). Charging BEVs at a higher power should enable more travel and allow the driver to take advantage of lower electric fuel costs,

thus improving the economics of BEV ownership. This work will explore the vehicle design considerations that require research, development, and deployment (RD&D) activities to meet the challenge of providing BEVs with similar performance to that of ICEVs. This work will include analysis of the drivetrain and auxiliary components of the vehicle with the exception of the battery cell- and pack-level considerations, though the battery system capacity and system thermal performance will be explored. In addition to this article, battery cell and pack design RD&D are described in the companion articles “Enabling Fast Charging – A Battery Technology

* Corresponding author.

E-mail address: andrew.meintz@nrel.gov (A. Meintz).

Gap Assessment” and “Enabling Fast Charging – A Battery Thermal Management Gap Assessment.” The economic and infrastructure challenges of charging stations to support these vehicles are discussed in “Enabling Fast Charging – Infrastructure and Economic Considerations.”

In the current market, Tesla vehicles offer the fastest recharge rates with 120 kW from most of its Supercharger stations [1], though it is believed that some of these chargers can support up to 145-kW charging [2]. Porsche has demonstrated the Mission E concept vehicle, which can support up to 350 kW from a d.c. fast charger (DCFC) that operates at a d.c. voltage of 800 V. Porsche has plans to go into production with a vehicle based on this concept in 2020 [3]. Other BEVs in today’s market, such as the Nissan Leaf and BMW i3 [4], have been designed around the prevailing 50-kW DCFC infrastructure [5]; however, the Chevrolet Bolt is reported to extend this power up to 55 kW [6] utilizing a DCFC with 150 A capability (or a 60-kW rating at 400 V). Meanwhile, BEVs are expected to continue supporting home and workplace charging with a.c. on-board chargers where DCFC infrastructure is expected to expand charging coverage and convenience for BEV drivers. It remains to be seen what impacts, in terms of cost to the vehicle and battery system, would be incurred to exclusively provide DCFC for refueling. However, to provide a refueling time comparable to that for an ICEV, it has been proposed that charging power will need to increase from the existing maximum of 120 kW to at least 400 kW, which we will refer to as extreme fast charging (XFC). This XFC will likely require an increased battery voltage rating from the existing 400-V consensus of passenger vehicles to reduce charging current and manage the cable size of the charger. A detailed discussion around this voltage change for the charging connector cable is included in the infrastructure and economics paper “Enabling Fast Charging – Infrastructure and Economic Considerations.” In this paper, we will consider an 800- to 1000-V range as the design criterion for XFC. Table 1 defines future BEVs and compares differences between current or existing BEVs and future BEVs. The defined future BEV characteristics will be used for the analysis in this paper.

The objective of this work is to assess the impact to the vehicle due to the transitions of charging power, battery pack voltage, and battery pack capacity as proposed in Table 1. To assess this impact, the work will (1) evaluate the technical factors that limit XFC with respect to the BEV, (2) identify the factors that limit the operation of BEVs with respect to ICEVs, and (3) define key areas where the U.S. Department of Energy can play an active role in performing RD&D support for advancing the implementation of XFC capability in BEVs. In addition to surveying literature and the expertise at the Department of Energy’s national laboratories, the team engaged industry to identify the key questions that need to be addressed to successfully implement XFC. These include understanding the XFC use cases and the effect on BEVs, how the BEV electrical architecture will be impacted by XFC, and finally understanding how XFC will impact the vehicle charging system design.

2. XFC use cases and effect on BEVs

Primarily, existing BEVs are charged with low power (1.4–7.2 kW) level 1 and level 2 electric vehicle service equipment (EVSE) at home and in the workplace. However, XFC can be a supplement for unplanned trips or for daily charging in regions without home or workplace access to level 2 EVSE, such as multi-unit dwellings and dense urban environments [1]. Further, XFC can benefit other use cases such as long-distance travel or for taxis, commercial vehicles, and other shared fleets. We have identified the following design considerations that need to be addressed for XFC and will examine intercity travel impacts on battery capacity in the subsequent sections.

- How will these differing use cases (taxis, fleets, urban, rural, etc.) impact the frequency and duration of XFC events, and what effect will this have on vehicle design?
- How will the price of an XFC event affect whether drivers choose to charge at an XFC given no immediate travel need when level 2 EVSE is an alternative, and how does this impact vehicle design for battery life constraints and charging component design?
- Does XFC present an opportunity to allow a high level of electrification for autonomous vehicles and shared taxis?
- How can XFC handle regional differences such as electric vehicle (EV) credit, climate, and urban design in the Northeast, high commute miles in California, and rural applications?
- How does XFC affect the desired range and battery capacity of a BEV?

2.1. Intercity travel analysis for XFC

Intercity travel has been noted as the driving rationale for XFC as a means to enable BEV travel that is comparable to ICEV travel. The analysis in this section will examine the travel time of existing BEVs as illustrated in the example shown in Fig. 1 for a trip from Salt Lake City, Utah, to Denver, Colorado. The methodology used for determining the charging time required for each BEV scenario in this analysis is detailed following the description of all travel scenarios, which are summarized in Table 2.

As a baseline, the trip is approximately 525 miles and takes about 8.4 h by an ICEV with one refueling stop that lasts 15 min. This stop is assumed to take about 10 min for setup, which includes activities such as taking a detour to a fueling station, waiting in a queue, setting up the dispenser, and paying, plus five minutes for fueling of the ICEV [9]. The travel times for the ICEV and all BEV scenarios in this analysis are calculated using an average travel speed of 65 mph. If the same route is driven with a 200-mile BEV, at least two charging stops would be needed to account for the shorter range of the BEV.

Starting with the 50-kW DCFC and 200-mile BEV scenario, it will take more than one hour to fully recharge a nearly empty battery. This is generally not acceptable to drivers on long trips where there

Table 1
Comparison between existing and future BEVs.

	Existing BEVs	Future BEVs
d.c. charging power	50–120 kW	>400 kW
Battery pack voltage	400 V for passenger vehicles [7] 800 V for some commercial vehicles [7,8]	800–1000 V
Battery pack capacity	20–90 kWh	>60 kWh
Vehicle range	80–300 miles	>200 miles
Charging connector	SAE J1772 CCS, CHAdeMO, Tesla	Revised CCS and CHAdeMO or a new XFC connector

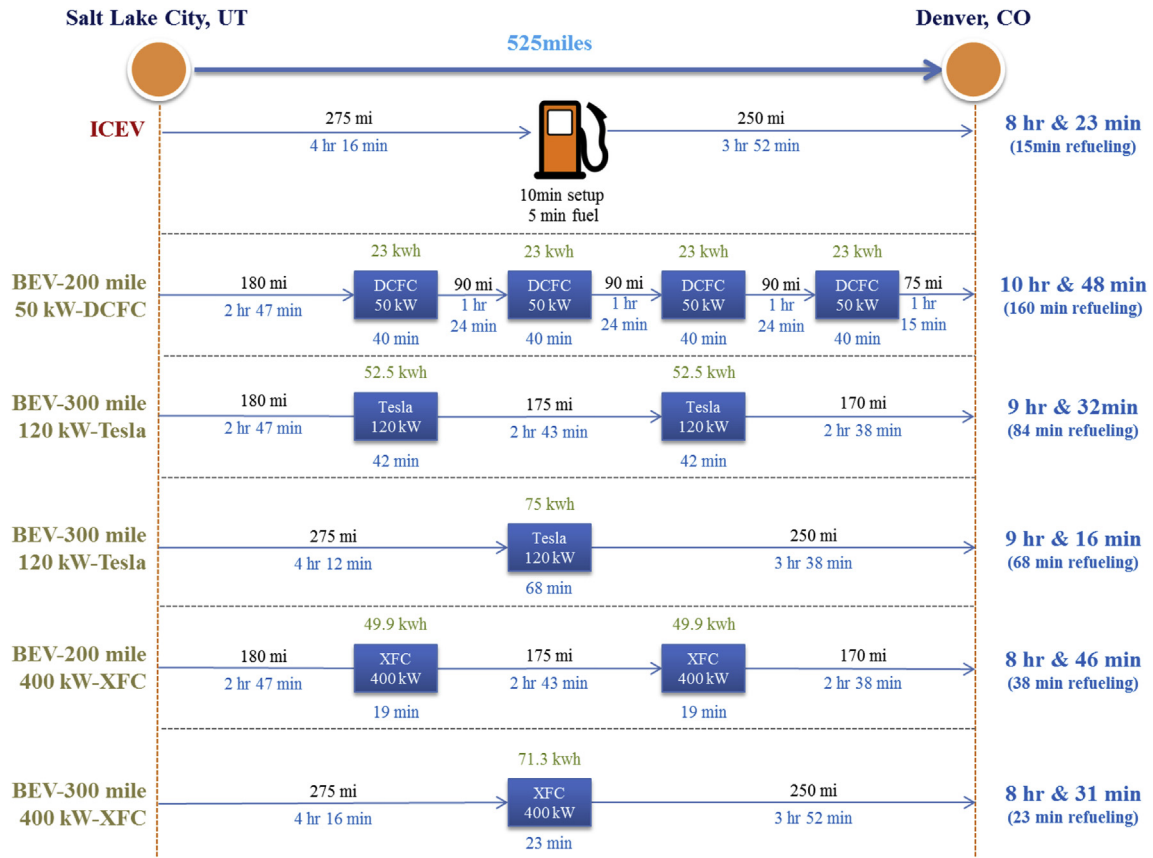


Fig. 1. Intercity travel from Salt Lake City to Denver.

Table 2
Summary of intercity travel analysis.

Vehicle Type	Drive Efficiency (Wh/mi)	Range Charged (mi)	Charge Event Time (min)	Charged Capacity (kWh)	Capacity Charged (% of rated)	Time Driving (% of total)	Travel Time (% increase)	Total Travel Time (h:m)
ICEV	N/A	300	5	N/A	N/A	97.0	0.0	8:23
DCFC BEV 200	256	90	30	23.0	38.3	75.3	28.8%	10:48
Tesla BEV 200	300	175	32	52.5	58.3	85.3	13.7	9:32
Tesla BEV 300	300	250	58	75.0	83.3	87.8	10.5	9:16
XFC BEV 200	285	175	9	49.9	76.7	92.8	4.6	8:46
XFC BEV 300	285	250	13	71.3	75.0	95.5	1.6	8:31

is an expectation to keep moving. Therefore, we adopt a 30-min charge with an additional 10-min penalty for setup in this analysis. The DCFC replenishes only 90 miles of range, so there would need to be four charging stops. The driving time between successive recharging events is 1 h and 24 min, which is much less than the expected driving time for ICEVs. The limited recharge capability of the 50-kW DCFC and this vehicle range impact the average driving speed over the entire route drastically. The total charging time would be 2 h and 40 min, which requires 28.8% more time to travel the same route than in the ICEV case. The following example is of a 300-mile BEV that can charge at 120 kW using the Tesla DCFC but maintains a 200-mile range for comparison to the 200-mile BEV. The 175-mile recharge, which takes 32 min, allows for two recharge stops and would result in the trip finishing in 9 h and 24 min. The total travel time would be about 13.7% longer for the

Tesla DCFC solution than with an ICEV. However, if the 300-mile BEV were to use its full range for only one recharge stop, as shown in the next example, then the total trip time is reduced to 9 h and 8 min with a total charging stop time of 68 min. This results in a modest improvement of 16 min in travel time over the 200-mile range case or about 10.5% longer than the travel time with an ICEV.

The proposed 400-kW XFC would allow for a 200-mile BEV to reduce the travel time even further, but would still require two recharge stops. These stops would take about 19 min for the same 175-mile refuel as the Tesla DCFC but with 9 min of charging instead of 32 min. The total travel time becomes 8 h and 46 min, which is 4.6% longer than the ICEV. A higher BEV range is required to reduce the number of charging stops and further decrease the total travel time as the time penalty for exiting the travel path and starting the charge becomes a greater proportion of the total

refueling stop time. A 300-mile BEV requires one recharge stop in this example and is expected to replenish 250 miles in 13 min of charging. The travel time would be 8 min longer than the ICEV or about 1.6% longer. Table 2 summarizes the parameters used in this analysis of intercity travel as well as some travel results.

Charging times for the DCFC BEV and Tesla BEVs used in this example trip from Salt Lake City to Denver have been calculated based on the published charging time for the Chevrolet Bolt [10,11] and Tesla 90D [12] by the manufacturers. These published charging times and recharge ranges have been translated into stored energy using the vehicle efficiency [13,14] and compared against the total energy transfer possible at the maximum rated power of the DCFC equipment for both vehicles as illustrated in Fig. 2. For comparison, charging times for the Kia Soul EV [15], Chevrolet Spark EV [16], and Volkswagen eGolf EV [17] have been included to represent the performance of existing 80-mile BEVs with 50-kW DCFC capability. The data have been collected for multiple vehicles of each model utilizing a 50-kW DCFC rated at 100 A of d.c. current and with charging tests that start from a low state of charge (SOC) (3–8%) after the vehicle has rested in a controlled 25 °C soak condition.

The triangle markers indicate the selected charge time and energy transfer for each stop in the analysis above. These charge times are greater than that indicated by the dashed lines, which specify the energy that could be transferred at the respective 50-, 120-, and 400-kW constant power rates. This increase in charge time is expected based on battery charge rate limitations, battery charge efficiency, battery thermal constraints, and d.c. current limitations of the DCFC. Lithium chemistries are restricted by an upper voltage limit to prevent oxidation of the electrolyte solvents which can occur at high cathode over-potentials. Exceeding this over-potential can lead to further oxidative side-reactions that may involve gas generation and overpressure of the cell. As a result, the vehicle battery management system will control the DCFC to modify the charge current to avoid these conditions. Charge control methods are devised by the vehicle manufacturer and more detail on the many aspects of the possible methodologies are found in Refs. [18–22]. The effect of this control is an upward bend in stored energy versus charge time from the constant power line when each vehicle model reaches the end of its charge as shown in Fig. 2.

The power of the chargers in the analysis above are indicated at

50 kW for the DCFC and 120 kW for the Tesla DCFC instead of the rating of 60 kW and 145 kW as the charging time curves in Fig. 2 show that the charging times of the Chevrolet Bolt and Tesla 90D are more consistent with these lower constant power rates. This difference illustrates that the time-averaged charging capability will be less than DCFC capability which is typically defined by the maximum charging current but using a voltage beyond the typical charge voltage of a connected vehicle. However, vehicle manufacturers may recommend charging with a higher power-rated DCFC, as seen in the Chevrolet Bolt user manual with an 80-kW DCFC [11], to ensure sufficient d.c. charging current during the beginning of the charge when charging voltages are lower.

Charging times of 9 and 13 min have been adopted for the hypothetical XFC 200-mile and 300-mile BEVs based on an assumed 20-mile per minute charge capability target for these vehicles. This equates to an average charged energy of 5.7 kWh per minute, which is effectively a 342-kW charge rate. This is a significant improvement over the Tesla vehicle, which achieved an average charged energy of 1.6 kWh per minute (98.4 kW) for the 175-mile recharge and an average charged energy of 1.3 kWh per minute (77.6 kW) for the 250-mile recharge. It is expected that an XFC vehicle will not be capable of charging at the full rated 400-kW power for the entire charge period due to battery life and thermal limitations. However, calculation of the exact limitations will require additional work to understand the battery chemistry and thermal cooling performance for the battery systems in these future XFC vehicles. Further, the XFC infrastructure design has been proposed to this point as a current-limited device at 350 A with a peak of 400 A. This means that it will only be able to transfer the full power rating at the 1000-V maximum rating and will have reduced power transfer performance based on the inherent voltage window of the battery system unless higher current ratings are considered.

2.2. Range and battery capacity for XFC vehicles

There is tradeoff between maximum charging rate and battery capacity as alluded to in the intercity travel example. Assuming that XFC at 400 kW is available, driving on highway corridors can be estimated to be as described below. BEVs with various battery sizes (30 kWh, 60 kWh, 90 kWh, and 140 kWh with 85% usable energy)

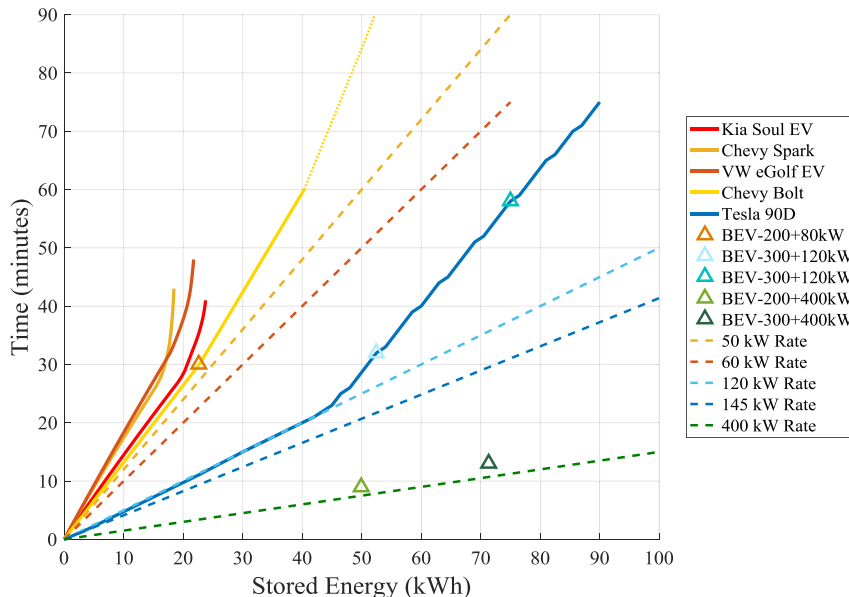


Fig. 2. Charging time and energy comparison [2,10–17,23].

are considered on the 525-mile corridor. They may need one or more stops for charging during this trip.

Argonne's simulation tool, Autonomie [24], was used to examine the energy consumption of a midsize BEV at steady high-speed operation of 80 mph. The relatively high cruising speed was used to get a more conservative estimate. An auxiliary electric load of 460 W was also considered to represent the real-world electric loads in a vehicle.

The Autonomie analysis results indicate that a midsize BEV consumes approximately 34 kW for a BEV100, and 38 kW for a BEV300. However, as a preliminary analysis to evaluate the number of charging events and the impact of charging time, the electric consumption is kept constant at 35 kW for all analysis in this section.

For a BEV with a 30-kWh battery pack and an 85% usable SOC window, the effective range will be approximately 60 miles, before which the vehicle will have to stop traveling to recharge. Similar to the previous example, we assume a 10-min penalty for activities such as taking a detour to a charging station, paying, waiting, and setting up the charger. Once connected, we assume that the charger can charge the vehicle at a constant rate of 400 kW. For the sake of comparing the effect of energy capacity on a BEV, this analysis assumes that there is no limitation from the battery or thermal system that prevents charging at the full power rate of the XFC infrastructure. For a relatively small (30 kWh) EV battery pack, this would mean a full charge in a little over 3 min and a charge rate in excess of a 12 C-rate. Although it achieves a very quick charge, the distance that can be driven with a full charge is also smaller with smaller battery pack. A BEV with a 30-kWh pack will have to stop for charging again after another 45 min of driving. Apart from the inconvenience of frequent stops, this adds to the overall driving

time as shown in Fig. 3. Further, as the battery pack size increases, the frequency of charging decreases, along with the overall time taken by the trip.

From the feedback received during the XFC meeting with industry representatives, it is believed that for extended travel with a BEV, a stop after every 2 h might be an acceptable limitation. This 2-h minimum points to the need for a battery size greater than 60 kWh. However, with the price differences in battery, gasoline, and charging costs, we might also see changes in consumer behavior.

As we see in Fig. 4, the increase in battery size and higher charging power can bring down the overall trip time. This lowered trip time is achieved by reducing either the number of charging events or the duration of such events. The 140-kWh pack needs only one stop for charging, but the 30-kWh pack will need as many as 8 stops for charging. If the charging is planned to end the drive with a fully depleted battery, we might be able to reduce the overall charging time a little bit for all vehicles, but the penalty associated with stopping for charging remains the same.

If we measure long distance driving by the trip time alone, then a BEV with a 140-kWh battery pack capable of charging at 150 kW could be comparable to one with a 90-kWh battery pack with a 250-kW charging capability. Similarly, a BEV with the same 140-kWh battery capable of charging at 250 kW achieved a 5 min advantage to one with a 90 kWh battery pack with a 400 kW charging capability.

The battery size selection will vary based on the assumptions. If we assume a lower driving speed 65 mph, and an electrical power consumption of 285 Wh (mile)⁻¹ to be consistent with a more moderate driving requirement, the driving time for the same 525-mile drive will be different. Fig. 5 shows the estimated trip time

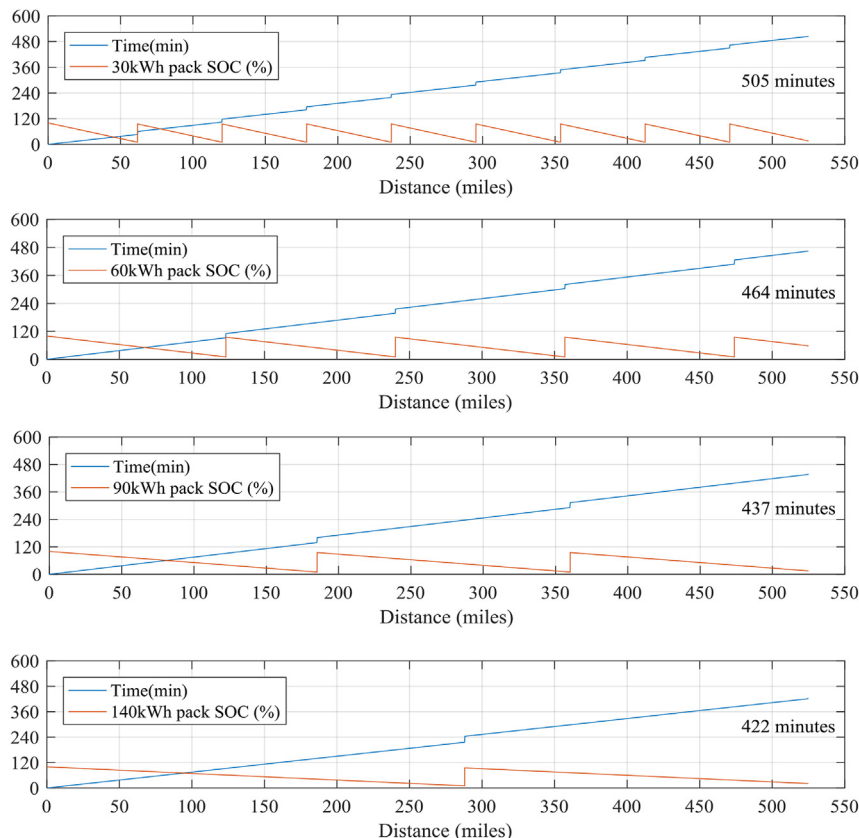


Fig. 3. Battery capacity and travel distance simulation.

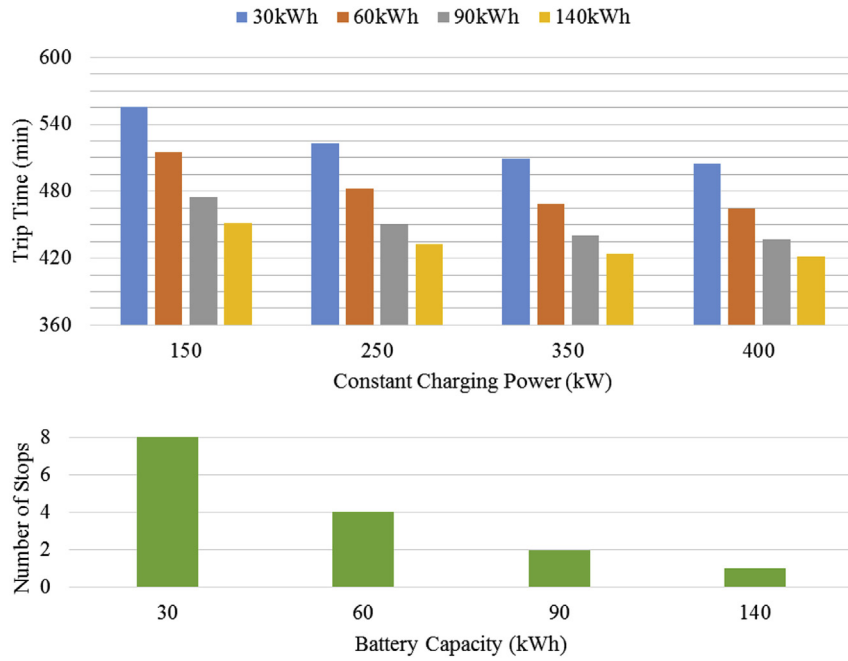


Fig. 4. Estimated 525-mile trip at 80 mph for different capacity and charging power.

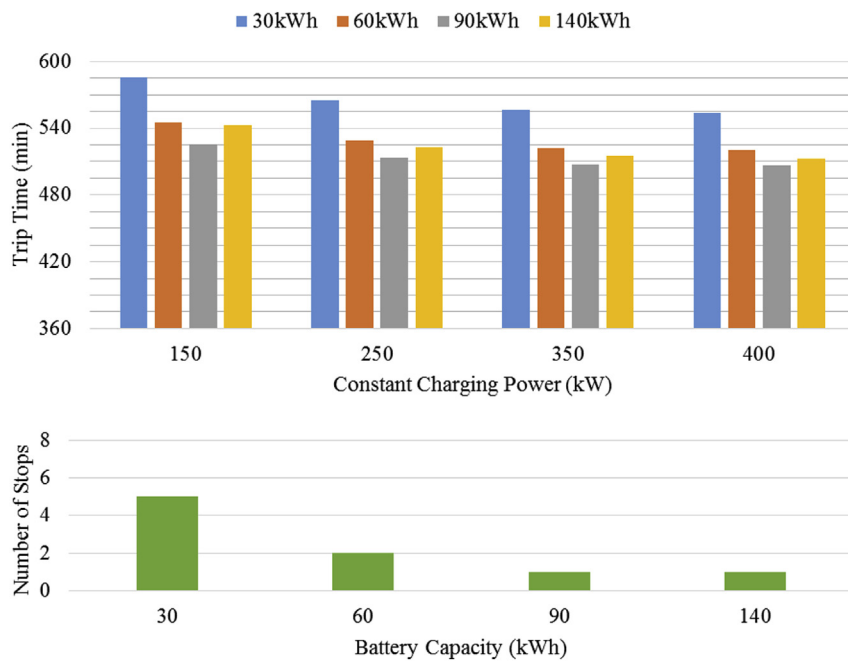


Fig. 5. Estimated 525-mile trip at 65 mph for different capacity and charging power.

with these assumptions. It is interesting to note that if vehicle energy consumption is lower, both a 90-kWh pack and 140-kWh pack can complete the trip with just one stop for charging. The larger pack takes longer to charge, hence this results in a slightly longer trip time. While the 90-kWh pack finishes the trip almost fully depleted, the 140-kWh pack will still remain almost full. Based on the assumptions made for vehicle usage, performance, component cost, and convenience costs, an optimum choice could be made for the battery size.

An economically optimum choice could be found with the right-

sized battery and charge rate, once more is understood about the estimated cost of XFC at these power levels and the cost of advanced batteries. The analysis presented here assumes the battery capacity and charging rate are independent of each other for simplicity. However, the maximum charging rate for a given battery will have some dependence on the battery capacity. This may result in a situation where larger-capacity vehicles are a byproduct of designing battery systems to meet the high-power rating of the charging infrastructure.

3. BEV electrical system impacts for XFC

Electrified vehicles for the light-duty passenger vehicle market have powertrain systems with voltages in two stratified regions: that of relatively low 12- to 48-V systems for mild or “start-stop” hybrids, and around 400 V for full hybrid EVs and BEVs [7,8]. These voltage ranges have been driven by the relative power level required of the powertrain. XFC has the potential of creating an additional voltage class for EVs in the 800- to 1000-V range, in this case based on the need to reduce current for charging the battery. However, this increase in voltage may benefit the application of BEVs in the light-duty truck class of passenger vehicles with increased power capability, which is an area that BEVs have seen limited exposure. We have identified the following considerations that will need to be addressed for XFC. The subsequent sections will examine electrical architecture approaches and the impact on power electronic components.

- What are the impacts of higher battery voltage on powertrain component volume, mass, efficiency, and cost given the duty cycle of the vehicle?
- Does increased voltage impact considerations of personal safety and first response, and are the existing design approaches sufficient to mitigate these concerns?
- What are the impacts to hybrid EVs, plug-in hybrid EVs, and existing BEVs that use a lower voltage than new XFC-enabled vehicles?

3.1. Electrical architectures to support XFC

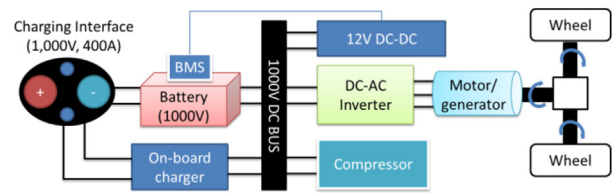
A higher charging voltage will reduce the cable size between the charger and the vehicle; however, this requires an innovative power electronics architecture and component changes inside the XFC-capable BEV. There are at least four options for XFC voltage-capable BEV architectures as shown in Fig. 6. For simplicity, the 800- to 1000-V range considered in this work will be shown at the system maximum of 1000 V.

The first option as shown in Fig. 6(a) adopts the existing BEV architecture, but upgrades each component to support 1000-V and 400-kW charging. A discussion of the impact to the power electronic component design for this voltage change is included in the following section.

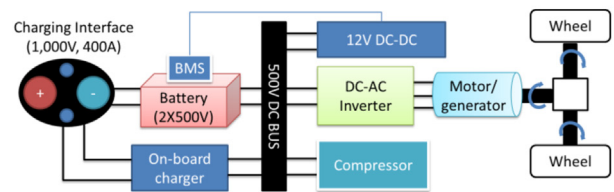
The second option, shown in Fig. 6(b), is to design a configurable battery that can connect in series to provide 1000 V for charging and connect in parallel to provide a 500-V d.c. bus for driving. This architecture requires a complex battery management system and electronics to flexibly convert the battery connection from series to parallel and vice versa. Implementing a flexible series and parallel connection can be challenging as two series battery strings will have different impedance and temperature conditions, which could result in SOC imbalances. Charge imbalances might appear while the vehicle is being driven in the parallel configuration and while it is charged in the series configuration. After a charge event, the series-to-parallel configuration change would require balancing of each string before the vehicle is ready to be driven. This will require development in a novel battery integration, control, and management method to make this architecture feasible [25,26].

The third design, in Fig. 6(c), is to add an additional d.c./d.c. converter between the charge interface and the battery to allow for existing 400-V power electronic components. The converter between the charge port and the battery would need to be capable of 400 kW to maximize the benefit of XFC infrastructure. A converter of this rating would likely negate the benefits of XFC in that the vehicle would be burdened with the additional volume, mass, and

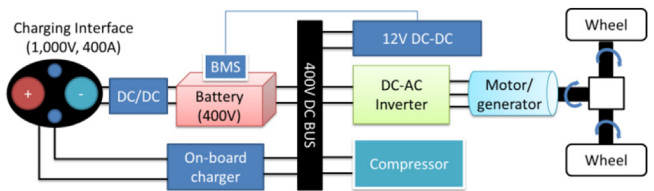
A. 1,000-V battery



B. Two 500-V configurable battery



C. d.c./d.c. converter +400-V battery



D. 1,000-V battery + d.c./d.c. converter

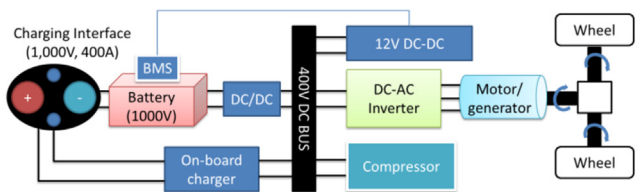


Fig. 6. Options for 1000 V BEV architectures.

cost constraints of a converter that only provides benefit for use with XFC infrastructure.

The final design, in Fig. 6(d), is to add an additional d.c./d.c. converter between a 1000-V battery and the 400-V d.c. bus to allow for the power electronic components to remain at their existing rating. This concept would allow for a reduced peak power rating of the converter to be around 150–200 kW for a typical non-performance car BEV. However, this design adds additional conversion inefficiencies that would impact total range and vehicle efficiency. A variant of this architecture where the traction inverter is rated at 1000 V and directly tied to the battery, but the auxiliary components reside on a second 400-V bus formed by a converter that is rated at a lower power level, may be more realistic. This variant would allow for continued use of common auxiliary components across a manufacturer's hybrid EV, plug-in hybrid EV, and BEV vehicle models.

While these four design options of BEV architectures will have

many advantages and disadvantages that make it unclear at first approach which is the best option, the first option is the most similar approach to existing design practices. Further, options 6(a), 6(c), and 6(d) require the use of 1000-V power electronics hardware on the vehicle; therefore, in the following paragraphs we use the first option (Fig. 6(a)) as an example to identify the potential challenges for the design of power electronics and other components in the electrical system:

- Existing power electronics at the 1000-V level have proven industry-standard components and technologies; however, there is limited exposure to automotive applications in this work.
- Increased voltage will require increased insulation and creepage requirements [27] that may add volume and mass to the vehicles' electrical components, cabling, and connectors.
- Higher battery voltage will require a battery pack with more cells connected in series. This will require additional sensing and balancing circuits to monitor and balance the battery pack.
- Fusing in the vehicle from the main pack line to the sensing lines will require increased clearing ratings. This may require new materials and fuse designs to meet the low resistance requirements for high-accuracy measurements.
- Charging power of 400 kW will require battery management systems that have been designed to support high current charging while maintaining accurate SOC prediction. Further, the balancing circuit design may need to change to better manage more cells connected in series and greater imbalances due to the higher charging and discharging rates.

System voltage levels will have different impacts depending on the use case and performance level of the BEV. For example, a high-performance BEV with the associated high power levels during driving could greatly benefit from a higher overall system voltage given that energy moves into and out of the battery at high power levels more often. A common 1000-V rating throughout the BEV will likely offer lower overall weight because lighter and smaller cables are sufficient for the higher power transport and counter the greater insulation requirements. At higher power levels, optimized 1000-V power electronics architecture may offer improved driving efficiency by providing a much larger reduction in typical operating current. However, this will be specific to the use and duty cycle of the BEV. Similarly, BEV designs for more typical commuting and slower travel through cities may not see as much benefit from the higher voltage throughout the vehicle design. Analysis is needed to understand which electrical architecture and corresponding component design will provide the most effective overall design that enhances the value of XFC charging and driving efficiency given the use of the vehicle.

3.2. XFC voltage impacts on power electronics and electric machines

A higher XFC voltage rating will impact the design of the internal electronics for inverters which support the traction motor and refrigerant compressor as well as for the converters that support the 14-V electrical, on-board charger, and battery management systems. Switches for these devices could be replaced by 1700-V insulated gate bipolar transistors or 1700-V silicon-carbide metal-oxide-semiconductor field-effect transistors which are both available. However, the maturity of the metal-oxide-semiconductor field-effect transistors is not as far along as the insulated gate bipolar transistors. Further, film capacitors for the d.c. bus also exist in the 1400- to 1700-V range and could be substituted for existing components. However, the design of gate

drivers and other sensing and control components would need to be modified to account for the higher isolation requirements.

The higher voltage in these power electronic components should reduce conduction loss of the switch, but the higher voltage could result in higher switching loss in the entire operating region. This could result in a situation where the higher switching loss cancels the benefit of lower conduction loss, but this effect will be dependent on the type of switches chosen, operating frequency, and the type of design for the converter or inverter. Overall it is possible that the efficiency of the drive inverter could be improved due to lower current levels for the same power level. However, the efficiency of the on-board charger and 14-V d.c./d.c. would likely decrease due to the higher turns ratio for an isolated transformer design.

Similarly the design of the electric machines in the vehicle would need to change as a result of higher operating voltages. This would impact the traction motor design and refrigerant compressor motor depending on the auxiliary component design for the BEV. These motor designs would need new insulation, winding, and magnetic designs that account for the higher system voltage. The higher voltage should improve power density of the motor and allow for higher base-speed operation in their design. However, changes to the insulation material or thickness could impact the thermal performance of the motor, which may lead to lower power density to achieve adequate cooling performance.

Higher voltage is expected to allow better utilization of silicon-carbide devices, and they should outperform current state-of-the-art silicon devices. Effort is needed in applying these devices to automotive systems. Specifically, package stack thermal resistance may increase, leading to reduced heat transfer and increase the need in research for thermal management and thermal reliability to meet quality and life targets. Research into materials, packaging, thermal management for the reliability of inverters, converters, and motors is needed for systems operating at these higher voltages.

4. XFC impact on BEV charging system design

XFC has the potential to provide a significant improvement in the flexibility of charging to alleviate travel uncertainty issues with the long charging duration of existing BEVs. However, this places new constraints on how XFC is incorporated into the design of vehicles to account for the diversity of charging capabilities of both XFC EVSE and vehicles. Coordination will be needed to remove consumer uncertainty around charging type, duration of an event, and other factors. We have identified the following considerations that will need to be addressed for XFC in the design of a BEV charging system. The subsequent sections will examine vehicle thermal system impacts, charging interface considerations for existing and XFC BEVs, and the cybersecurity implications for XFC.

- How should the charging rate of XFC be managed based on the environment and condition of the vehicle?
- What standards are needed to enable an XFC EVSE to share in the calculation of charge rate and charge duration? What is the need for certification of pairing process and function due to too much uncertainty in both d.c. and a.c. charging today?
- Are additional standards needed to enable a BEV/battery management system to share control signals and provide display data to the station and driver?
- Will the design of an interface to support XFC allow for automated refueling?
- Could cooling on the infrastructure connector eliminate the need for cooling on the vehicle inlet? Will new material development be needed to cool down connector pin temperatures?

4.1. Vehicle thermal system impacts of XFC

Implementation of XFC is expected to have a significant impact on vehicle thermal system design. Existing EV thermal systems must meet many design criteria, including requirements for the thermal management of the traction battery, power electronics, and electric motor, all under dramatically varying environmental conditions. Thermal system architectures vary in their complexity, from numerous independent thermal subsystems to a fully integrated combined system. Representative EV thermal systems use a vapor compression cycle and chiller combined with a water/ethylene glycol secondary loop to perform the critical functions of traction battery, power electronics, electric motor, and vehicle cabin thermal management. Existing design capacities for these systems are based on peak power electronics, electric motor, and battery heat rejection demands. At 70%–90% charging efficiency for the XFC event, depending on the battery cell type selected, thermal losses and subsequent battery cooling demands are expected to far exceed existing design capacities. Therefore, to meet the cooling demands of the XFC event, either the onboard thermal system capacity will need to increase significantly, or an independent cooling system associated with the XFC charging infrastructure will be necessary. Modifications to the thermal system design or incorporation of an external independent cooling system will be driven by the battery selection and associated thermal management needs.

If thermal management of XFC can be accomplished through an onboard thermal system, increased capacity will be necessary for the radiator and air conditioning compressor, as well as the battery thermal subcircuit. For the battery thermal design alone, the elevated heat rejection requirements could force implementation of direct refrigerant-based cooling of the traction battery, replacing existing water/ethylene glycol cooling designs. Alternatively, if thermal management of XFC requires an independent cooling system, it will have to function alongside the normal battery thermal management system. Therefore, redundant or shared systems would be necessary, which would require significant changes to design and control strategies.

While XFC will require changing the thermal system design, and either increasing onboard or adding independent cooling capacity, intelligent thermal system design provides an opportunity to recover charging losses during the XFC event. During cold weather conditions, EV range reduction due to cabin heating can be over 50% due to the need to operate a resistive heater with the traction battery. However, stored thermal energy in the battery during and after an XFC event could be used for cabin heating with a thermal system design that utilizes this heat through a heat pump. As an example, for a 300-kg battery with heat capacity of $800 \text{ J (kg-K)}^{-1}$, a $20 \text{ }^\circ\text{C}$ increase in battery temperature above the target operating temperature from the XFC event displaces the equivalent of 16 min of continuous operation of a 5-kW vehicle cabin resistive heater that would otherwise be powered from the battery, increasing the effective range of the vehicle. Additional intelligent thermal system design could enhance XFC performance, including opportunistic preconditioning of the thermal circuit prior to the XFC event. Further research on a thermal management system incorporating XFC is necessary to incorporate the unique demand while meeting existing component requirements and optimizing the system for varying operating conditions.

4.2. Charging interface for existing and XFC BEVs

There is a need to select appropriate cables and connectors to support 1000-V and 350-A XFC. The connector shapes should be standardized to assure interoperability with new and existing BEVs. The existing connectors that manufacturers are offering have a

maximum current rating of 250 A with convective cooling and cannot support 400-A XFC [28]. One option is to integrate a cooling circuit into the cables and connectors as a new liquid-cooled cable system [29,30]. The integrated cooling controller allows the system to detect when cooling is needed and activates the system as necessary. With liquid-cooled cables and connector systems, charging current of 350 A and short-term events up to 400 A d.c. maximum are possible while still providing a flexible, small-diameter and low-weight cable solution [3]. Manufacturers of these cables are developing prototypes of CCS-2 (1000 V) and CHAdeMO (500 V) cables [29,30]. A summary of the existing and proposed connectors with voltage and current ranges is included in Fig. 7.

Further research is needed to develop new materials to reduce the cable and connector sizes, cool the cables and connectors with liquid or other technologies, and develop a safe and light charging cable and connector for XFC. The existing cable and material design for temperature rise of these cables may result in heavy and difficult-to-use connector solutions. Further, it may be an option to use automatic docking, where a robot arm can automatically connect and disconnect the charger to the vehicle charge interface with no input required from the driver, making it easier to operate and potentially safer. Automatic charging solutions via overhead connections have been considered in electric bus applications with charging power rates at 500–600 kW [31,32]. Further complicating the design of the charging connector is the concept of the extreme DCFC infrastructure providing cooling to the vehicle during charging.

Since each BEV model has a unique battery chemistry, battery pack size, and rated voltage, each BEV model will require a unique charging method. Even if the BEV models are the same, different battery SOCs, states of health, and battery temperatures require different charging rates and charging voltages. Future charging infrastructure will need to be more flexible than existing chargers in terms of the voltage and current to meet both new and existing vehicles as shown in Fig. 7. A requirement for new XFC EVSE will be interoperability with existing BEVs to allow them to initiate and properly control charging voltage and current. This will require that the power electronics of the new XFC EVSE operate in the existing voltage and current range and that the communication methods remain the same.

Further, BEVs should allow the EVSE to negotiate and respond to changes in the charging power level to allow charging to be effectively and efficiently shared at an XFC charging depot. The unused power from one vehicle can be dispensed to charge other vehicles. On the other hand, allowing power level negotiation also enables charging depots to respond to charging demand to reduce, and perhaps avoid, peak demand charges. While this may increase overall charging time, the upstream utility cost will be affected, and thus the business model for XFC charging may challenge the notion of constant fuel prices throughout a refueling event or during a business day.

4.3. Cybersecurity of BEV for XFC

XFC and existing d.c. charging require critical communication between a BEV and the charging infrastructure to coordinate charging voltage and current. Unlike a.c. charging, d.c. charging creates a vulnerability because the onboard charge controller must communicate important battery constraints to the off-board battery charger. Enabling BEVs to support 1000-V and 400-kW XFC charging could give hackers an enticing vulnerability to exploit. The higher power level could be used more easily to impact the grid than with other components. Further, if XFC allows for a larger portion of the transportation fleet to become electrified, then a

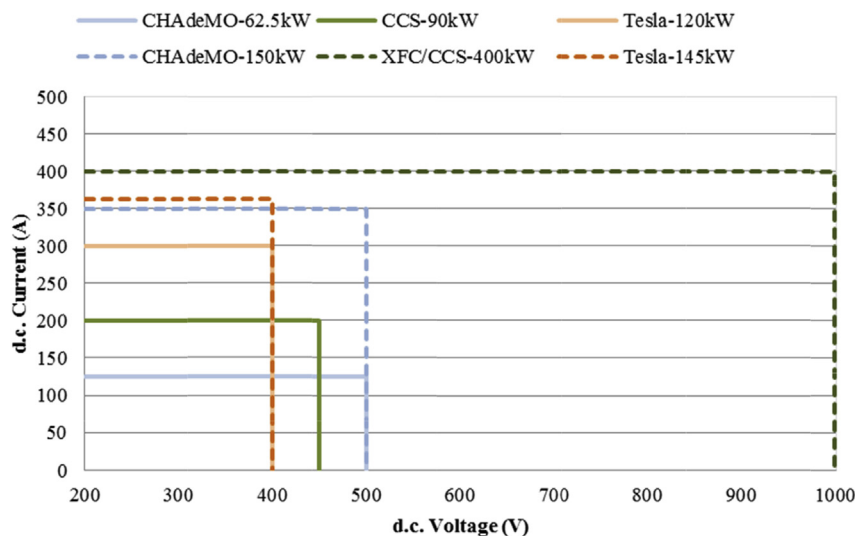


Fig. 7. Charging connector voltage and current range for new and existing vehicles.

larger disruption to the transportation system could be affected by attacking this infrastructure.

Effective deployment of XFC will require that the new infrastructure is capable of charging existing vehicles. This means that the new XFC infrastructure, which is capable of applying higher voltage and current to charge new XFC-capable BEVs, will interact with less capable existing BEVs. This represents a scenario in which the existing vehicle could be exploited to request the XFC infrastructure to apply more power than it is capable of receiving. This may result in damage to the vehicle and potentially the XFC infrastructure. XFC vehicles would also be subject to the same sort of vulnerability in which the compromised XFC BEV may request power for longer than it is capable of supporting a higher XFC charge rate. Other vulnerabilities from the vehicle side exist, such as the locking mechanism, which could be vulnerable to erroneously unlocking while charging the vehicle. If the user then tried removing the connector, he or she could be exposed to a shock or arc flash hazard.

The nature of XFC and existing d.c. fast chargers where vehicles may move from one charger to the next creates an interesting cybersecurity situation. As has been suggested in Ref. [33], it may be possible for a vehicle infected with malicious code to infect a charger that then proceeds to infect other vehicles. The drivers of these newly infected vehicles could then unknowingly spread the malicious code to other chargers and infect the d.c. charging network. Therefore, there is a critical need for consistent security for BEVs to ensure safe, secure, and resilient d.c. charging. The point where the vulnerabilities could be used to gain access and exploit infrastructure beyond that of the BEVs to XFC should be identified. Cybersecurity must be built into the BEV architecture, battery management systems, and XFC infrastructure.

5. RD&D considerations for XFC BEVs

Driven by a push toward both higher-power XFC and higher battery voltage, both new and existing BEVs are facing new technical challenges and technical development opportunities. The success of this transition will be heavily dependent on their interoperability to bridge the gap between BEVs and EVSE in terms of charging voltage and current ratings. Securing this interoperability is essential to succeed in promoting adoption of BEVs and XFC.

Existing energy-dense battery technology supports charging at a 1.5 to 2.0 C-rate. BEVs charge with a power of 50 kW for most BEVs and 120 kW for Tesla BEVs. There are two fundamental methods to transition the voltage rating of BEV architecture from 400 to 1000 V. The first approach is to upgrade the BEV charging voltage directly to 1000 V, but gradually increase the allowed charging current based on the battery technology. Another approach is to move to a 400-A system charging current, but to step up the BEV system voltage with the change in battery technology. There are advantages and disadvantages to each approach for the BEV architecture; however, new EVSE designs to accommodate both approaches can be the same as shown in Fig. 8.

Identification and prioritization of research and design challenges and opportunities have the potential to lead to more rapid generation of subsequent research to address those gaps. Table 3 summarizes the challenges of BEVs and EVSE to support 400-kW XFC and higher battery voltage.

The main challenge is how to provide interoperable BEVs and EVSE given their different voltage and current ratings. To resolve these challenges, research opportunities lie in developing new power electronic architecture, components, and interoperable interfaces to bridge BEVs and EVSEs together. Innovative system optimization methods are also needed to effectively integrate all components together to improve charging and driving efficiency. Data-sharing methodologies and cybersecurity strategies should also be developed to protect the drivers' privacy and ensure safe operation of BEVs and XFC.

6. Conclusions

If BEVs are to make a significant increase in the market share of passenger vehicles, it is expected that XFC will be needed to improve the range that BEVs can travel and to allow these vehicles to be charged with as much convenience as fueling an ICEV. This faster recharge will require significant changes in the design of BEVs to increase their charging power to at least 400 kW to allow 200 miles of charging in a time of 10 min to be consistent with the 5 min in which an ICEV can refuel. The changes required to meet this challenge for the vehicle design necessitate RD&D to address the following:

	Today		Future	
Charger Voltage	400V		400 - 1000V	
Charge Inlet	CHAdeMO, SAE J1772 CCS, Tesla		XFC Designed Inlet (s) for 1000V@400A	
Vehicle	400V, 125A, 50kW 400V, 350A, 140kW	600V, 400A, 240kW 1000V, 210-280 A, 210-280 kW	800V, 400A, 320kW	1000V, 400A, 400kW
Battery	1.5 – 2C	2.0 – 3.3C	3.3 – 4.6C	4.6 – 6C

Fig. 8. Timeline of BEVs and battery C-rate to support XFC.

Table 3
Challenges and opportunities to support XFC.

		New BEVs	Existing BEVs
Extreme Fast d.c. Charging	Challenge	<ul style="list-style-type: none"> • Durability of high current inlet and cable in a range of environments • Higher system voltage design may impact the mass and volume of vehicle hardware • Development of a new inlet/connector standard that is backward compatible • Cybersecurity and safety risks may increase with higher voltage • High cost of XFC may result in a large discrepancy in charging rate within the market, leading to consumer confusion • Vehicle thermal design for XFC may be costly while rarely used for some cases • Battery charge estimation and cell balance management could be more difficult 	<ul style="list-style-type: none"> • Interface interoperability issues could require software updates • Low battery voltage requires greater XFC range • Cybersecurity and safety concerns may increase with higher voltage/current and exposure
	Opportunity	<ul style="list-style-type: none"> • New material and methodology for designing high-current cable and connectors • High-voltage power electronics may improve vehicle efficiency • Integrated cabin and vehicle thermal designs may improve on-road efficiency • A new charging method for XFC could be automated to improve accessibility and help with automated vehicles 	<ul style="list-style-type: none"> • Higher current capability could be exploited on older vehicles • Increased infrastructure if backward compatible would increase utility of existing vehicles
Existing d.c. Fast	Challenge	<ul style="list-style-type: none"> • The d.c. voltage operating range of DCFC is likely too low for new XFC vehicles • New charge interface may not be backward compatible and may strand existing infrastructure 	
	Opportunity	<ul style="list-style-type: none"> • Existing equipment voltage range could be upgraded with lower installation costs • Some vehicle electrical architectures could allow for voltage compatibility 	
Existing a.c.	Challenge	<ul style="list-style-type: none"> • Higher d.c. voltage will impact onboard charger design • Larger battery capacity may take too long to charge, especially with level 1, though level 2 may still be a challenge 	
	Opportunity	<ul style="list-style-type: none"> • XFC could spur increased a.c. infrastructure as more vehicles are introduced into the market • New material and cooling technology development may benefit a.c. charging 	

- Battery charging power density must be increased while maintaining energy-dense cells such that long distance travel does not require excessive recharge events.
- The desired use cases for XFC, whether primarily for intercity travel or for everyday refueling, should be understood as it will impact the tradeoffs for BEV design.
- Increased system voltage will impact the design of power electronics and electrical architecture designs. This could increase the volume, mass, and cost of components and should be optimized in conjunction with vehicle duty cycle.

- Interoperability of XFC charging systems with vehicles will be required to provide consistent charging experiences for BEV owners. Charging capabilities of different vehicle models and charging infrastructure should be classified in a way that allows XFC to be commonly understood by the public.

While it is expected that the design changes to support the challenges of XFC represent a significant shift in the design of the vehicle electrical architecture and battery system. The benefits of XFC on the operation of BEVs should bring these vehicles much

closer to accepted refueling norms and increase the adoption of BEVs in the market.

Acknowledgements

This work was performed under the auspices of the U.S. Department of Energy, Office of Vehicle Technologies, under Contract Nos. DE-AC02-06CH11357 (Argonne National Laboratory), DE-DE-AC07-05ID14517 (Idaho National Laboratory), and DE-AC36-08GO28308 (National Renewable Energy Laboratory). The U.S. Government retains for itself, and others acting on its behalf, a paid-up nonexclusive, irrevocable worldwide license in said article to reproduce, prepare derivative works, distribute copies to the public, and perform publicly and display publicly, by or on behalf of the Government.

Acronyms

a.c	alternating current
BEV	plug-in battery electric vehicle, includes both battery and plug-in hybrid electric vehicles
CCS	combined charging system, also called combo coupler
d.c	direct current
DCFC	d.c. fast charger or d.c. fast charging
EV	electric vehicle
EVSE	electric vehicle supply equipment
ICEV	internal combustion engine vehicle
RD&D	research, development and deployment
SOC	state of charge
XFC	extreme fast charging (20 mile/minute recharge)

References

- [1] Tesla, Supercharger, (n.d.). <https://www.tesla.com/supercharger> (Accessed 30 November 2016).
- [2] F. Lambert, Tesla quietly upgraded its Superchargers for faster charging, now capable of 145 kW | Electrek, Electrek (2016). <https://electrek.co/2016/07/20/tesla-supercharger-capacity-increase-145-kw/> (Accessed 7 March 2017).
- [3] Porsche, e-mobility: new possibilities with 800-volt charging, Porsche (2016). <https://newsroom.porsche.com/en/technology/porsche-engineering-e-power-electromobility-800-volt-charging-12720.html> (Accessed 30 November 2016).
- [4] H. Boeriu, BMW and Nissan are joining forces to offer public DC Fast charging, BMWBlog (2015). <http://www.bmwblog.com/2015/12/21/bmw-and-nissan-are-joining-forces-to-offer-public-dc-fast-charging/> (Accessed 30 November 2016).
- [5] Zach McDonald, A simple guide to DC fast charging, Fleetcarma (2016). <http://www.fleetcarma.com/dc-fast-charging-guide/>. Accessed 11 March 2017.
- [6] Acquisition De Données D'une Recharge Rapide Ccs-combo Sur Une Bolt 2017-Suite, 2017. Québec, http://www.ivosolutions.ca/wp-content/uploads/2017/05/AcquisitionRechargeBolt_5Mai_2017.pdf. Accessed 8 July 2017.
- [7] L. Kostal, L. Schmidhauser, L. Kabel, R. Bosch, Voltage classes for electric mobility voltage classes for electric mobility. www.zevi.org, 2013. Accessed 7 March 2017.
- [8] K. Küpper, T. Pels, M. Deiml, A. Angermaier, T. Bürger, A. Weinzerl, G. Teuschl, Tension 12 V to 800 V; efficient powertrain solutions, FISTA (2015). <http://siar.ro/wp-content/uploads/2016/01/2.-Kupper-K.-AVL-Tension-12-V-to-800-V-2015.compressed.pdf> (Accessed 7 March 2017).
- [9] NACS, fuels resource center. http://www.nacsonline.com/YourBusiness/FuelsCenter/Basics/Articles/Pages/The-US-Petroleum-Industry-Statistics-Definitions.aspx#_WestQHrN7hE, 2016 (Accessed December 4, 2016).
- [10] S. Weintraub, The very good Chevy Bolt reviews are in but everyone forgot to ask the most important question | Electrek, Electrek (2016). <https://electrek.co/2016/09/14/the-very-good-chevy-bolt-reviews-are-in-but-everyone-forgot-to-ask-the-most-important-question/> (Accessed 30 November 2016).
- [11] General Motors, Bolt EV Owner's Manual, 2016. Plymouth, MI, https://my.chevrolet.com/content/dam/gmownercenter/gmna/dynamic/manuals/2017/Chevrolet/BOLT_EV/Owner's_Manual.pdf (Accessed 31 March 2017).
- [12] Tesla, model S: charging estimator, Tesla. <https://www.tesla.com/models>, 2017 (Accessed 11 March 2017).
- [13] 2017 Tesla Model S AWD - 90D, (n.d.). <http://www.fueleconomy.gov/feg/Find.do?action=sbs&id=38569> (Accessed 2 April 2017).
- [14] 2017 Chevrolet Bolt EV, (n.d.). <http://www.fueleconomy.gov/feg/Find.do?action=sbs&id=38187> (Accessed 2 April 2017).
- [15] Idaho National Laboratory, 2015 Kia Soul EV: DC fast charging at temperature test results, Ida. Falls (2016). <http://dx.doi.org/INL/MIS-16-38450>.
- [16] Idaho National Laboratory, 2015 Chevrolet Spark EV: DC fast charging at temperature test results, Ida. Falls (2016). <http://dx.doi.org/INL/MIS-16-38450>.
- [17] Idaho National Laboratory, 2015 Volkswagen eGolf EV: DC fast charging at temperature test results, Ida. Falls (2016). <http://dx.doi.org/INL/MIS-16-38450>.
- [18] A. Abdollahi, X. Han, N. Raghunathan, B. Pattipati, B. Balasingam, K.R. Pattipati, Y. Bar-Shalom, B. Card, Optimal charging for general equivalent electrical battery model, and battery life management, J. Energy Storage 9 (2017) 47–58, <http://dx.doi.org/10.1016/j.est.2016.11.002>.
- [19] M.F. Hasan, C.-F. Chen, C.E. Shaffer, P.P. Mukherjee, Analysis of the implications of rapid charging on lithium-ion battery performance, J. Electrochem. Soc. 162 (2015) A1382–A1395, <http://dx.doi.org/10.1149/2.0871507jes>.
- [20] P.H.L. Notten, J.H.G.O. het Veld, J.R.G. van Beek, Boostcharging Li-ion batteries: a challenging new charging concept, J. Power Sources 145 (2005) 89–94, <http://dx.doi.org/10.1016/j.jpowsour.2004.12.038>.
- [21] R. Klein, N.A. Chaturvedi, J. Christensen, J. Ahmed, R. Findeisen, A. Kojic, Optimal charging strategies in lithium-ion battery, Proc. 2011 Am. Control Conf. IEEE (2011) 382–387, <http://dx.doi.org/10.1109/ACC.2011.5991497>.
- [22] Y.-H. Liu, J.-H. Teng, Y.-C. Lin, Search for an optimal rapid charging pattern for lithium-ion batteries using ant colony system algorithm, IEEE Trans. Ind. Electron 52 (2005) 1328–1336, <http://dx.doi.org/10.1109/TIE.2005.855670>.
- [23] A. Balogh, P. Evci, EV charging infrastructure intelligent charging solutions. http://eszk.org/docs/sae/Lectures/SAE_SAE_e_mobility_ABB_Balogh_2014_08_26.pdf, 2014 (Accessed 7 March 2017).
- [24] Autonomie - Home, (n.d.). <http://www.autonomie.net/> (Accessed 17 July 2017).
- [25] H. Kim, K.G. Shin, On dynamic reconfiguration of a large-scale battery system, in: 2009 15th IEEE real-time embed, Technol. Appl. Symp. IEEE (2009) 87–96, <http://dx.doi.org/10.1109/RTAS.2009.13>.
- [26] S. Ci, N. Lin, D. Wu, Reconfigurable battery techniques and systems: a survey, IEEE Access 4 (2016) 1175–1189, <http://dx.doi.org/10.1109/ACCESS.2016.2545338>.
- [27] Insulation Coordination for Equipment within Low-voltage Systems. Part 1, Principles, Requirements and Tests, second ed., International Electrotechnical Commission, Geneva, 2007.
- [28] Phoenix Contact, E-Mobility DC quick charging with up to 350 A, 2016. (n.d.). https://www.phoenixcontact.com/assets/downloads_ed/global/web_dwl_promotion/52007586_EN_HQ_E-Mobility_LoRes.pdf (Accessed 30 November 2016).
- [29] RealWire, HUBER+SUHNER cooled cable and connector puts super-fast charging of electric cars within reach, 2016. (n.d.). <http://www.realwire.com/releases/HUBERSUHNER-cooled-cable-and-connector-puts-super-fast-charging-of-electric> (Accessed 30 November 2016).
- [30] Efavec, main challenges of high power DC charging, in: EPRI Infrastruct. Work. Counc. 2016. San Francisco, <http://www.epri.com/Documents/InfrastructureWorkingCouncilMeeting1611/DayOnePresentations.pdf> (Accessed 30 November 2016).
- [31] Proterra, proterra catalyst overview, in: International Drive Business Improvement District, 2016. Orlando, http://www.iridetrolley.com/editorFiles/Presentations/20160831_DAB_Proterra_Presentation.pdf (Accessed 19 March 2017).
- [32] ABB, TOSA: An e-bus charging innovation from ABB for sustainable urban transport, (n.d.). <http://new.abb.com/grid/technology/tosa> (Accessed 19 March 2017).
- [33] J. Chugg, R. Condit, A. Keith, K. Rohde, B. Wheeler, Cyber security research and development: CAN bus security research across multiple sectors, Ida. Falls (2016). <http://dx.doi.org/INL/CON-16-37908>.

Appendix D



Enabling fast charging – Infrastructure and economic considerations



Andrew Burnham^a, Eric J. Dufek^{b,*}, Thomas Stephens^a, James Francfort^b, Christopher Michelbacher^b, Richard B. Carlson^b, Jiucui Zhang^c, Ram Vijayagopal^a, Fernando Dias^b, Manish Mohanpurkar^b, Don Scofield^b, Keith Hardy^a, Matthew Shirk^b, Rob Hovsopian^b, Shabbir Ahmed^a, Ira Bloom^a, Andrew N. Jansen^a, Matthew Keyser^c, Cory Kreuzer^c, Anthony Markel^c, Andrew Meintz^c, Ahmad Pesaran^c, Tanvir R. Tanim^b

^a Argonne National Laboratory, 9700 South Cass Avenue, Argonne, IL 60439, USA

^b Idaho National Laboratory, 2525 N. Fremont, Idaho Falls, ID 83415, USA

^c National Renewable Energy Laboratory, 15013 Denver West Parkway, Golden, CO 80401, USA

HIGHLIGHTS

- Management of intermittent, high power demand is crucial.
- Planning is needed for XFC including siting future corridors.
- Planning needs to include cost of charging equipment, operation and installation.
- Increased coordination needs to occur between governing authorities.
- Safety, cyber physical security, interoperability and compatibility will impact use.

ARTICLE INFO

Article history:

Received 29 April 2017

Received in revised form

20 June 2017

Accepted 25 June 2017

Keywords:

Extreme fast charging (XFC)

Electric vehicle infrastructure

Battery electric vehicles

Demand charges

Total cost of ownership

Economics

ABSTRACT

The ability to charge battery electric vehicles (BEVs) on a time scale that is on par with the time to fuel an internal combustion engine vehicle (ICEV) would remove a significant barrier to the adoption of BEVs. However, for viability, fast charging at this time scale needs to also occur at a price that is acceptable to consumers. Therefore, the cost drivers for both BEV owners and charging station providers are analyzed. In addition, key infrastructure considerations are examined, including grid stability and delivery of power, the design of fast charging stations and the design and use of electric vehicle service equipment. Each of these aspects have technical barriers that need to be addressed, and are directly linked to economic impacts to use and implementation. This discussion focuses on both the economic and infrastructure issues which exist and need to be addressed for the effective implementation of fast charging at 400 kW and above. In so doing, it has been found that there is a distinct need to effectively manage the intermittent, high power demand of fast charging, strategically plan infrastructure corridors, and to further understand the cost of operation of charging infrastructure and BEVs.

© 2017 Elsevier B.V. All rights reserved.

1. Introduction

The push to reduce the charging time needed for plug-in battery electric vehicles (BEVs) creates a suite of intertwined research, development and deployment (RD&D) challenges. In addition to the RD&D challenges for vehicles and battery technologies that have been described elsewhere [1][2][3], there is a distinct need to

understand how extreme fast charging (XFC) with powers of 400 kW and above will impact the electrical grid, the use of electric vehicle supply equipment (EVSE), corridor planning and ultimately how the cost of ownership and deployment economics evolve.

Both BEVs and internal combustion engine vehicles (ICEVs) require specific and unique forms of infrastructure for refueling. In the case of ICEVs, there is an expansive network of refueling stations that already exists. For BEVs, the options are more disparate including residential charging, work place charging, and the use of a still emerging public charging infrastructure including both

* Corresponding author.

E-mail address: eric.dufek@inl.gov (E.J. Dufek).

alternating current (AC) Level 2, and direct current (DC) fast charging (DCFC) [4]. The range of charging options present both challenges and opportunities as the adoption of BEVs continues to increase [5]. One distinct opportunity that exists is the ability to logically plan the infrastructure for the BEV fleet including the placement of DCFC above 50 kW and up to 400 kW in metro areas and travel corridors.

Higher power charging systems which operate up to 400 kW and could replace 320 km (200 miles) in 10 min of recharging, look to address what some perceive as limitations with BEVs including: length of time to charge and overall BEV range [6]. Public fast charging could increase BEV market penetration by allowing consumers who do not have access to either residential or workplace charging to use it as their primary means of charging. The use of BEVs in commercial applications such as taxi, ride-share, or car-share services, where vehicles are heavily utilized could be enabled due to the added convenience of fast charging. In addition, higher power charging would make long-distance, intercity travel more practical for BEVs by making refueling times similar to ICEVs.

Presently most BEV users charge at home followed by work place charging [7]; however, early evaluations of the impact of DCFC up to 50 kW highlights the added flexibility that the faster charging gives to BEV users. One example of the positive impact on travel distance was identified in a study that followed Nissan Leafs which either used or did not use DCFC (up to 50 kW) [8]. With the use of DCFC (up to 50 kW), it was observed that longer range trips using BEVs have occurred in the northwestern portion of the United States. Indeed, the use of DCFC has increased the number of trips that extend beyond the centralized metropolitan centers of Seattle, Washington and Portland, Oregon. The extended range provided by DCFC allowed more trips to the Oregon and Washington coast and into the Cascade mountain range. While the data is not presently available it is expected that similar impacts would be observed for other regions of the country and the world. The ability to use DCFC

XFC stations.

2. Review of key considerations of XFC infrastructure and economics

2.1. Overview of XFC cost drivers

In this section, we detail the cost drivers of XFC from both a vehicle owner and EVSE provider standpoints. The total cost of ownership (TCO) for a vehicle owner is shown in Equation (1).

$$\begin{aligned} \text{TCO} = & \text{Vehicle (Depreciation)} + \text{Maintenance \& Repair} + \text{Fuel} \\ & + \text{Insurance} + \text{License \& Registration} \\ & + \text{Public support cost} + \text{Value of Travel Time} \end{aligned} \quad (1)$$

As shown in Fig. 1A, the cost of BEVs using XFC will be heavily influenced by battery costs, while other vehicle costs, such as power electronics and thermal management, may be important as well. Additionally, battery lifetime can impact maintenance and repair costs. For BEVs fuel cost is directly tied to the cost of electricity at the point of sale, which depends on the cost of EVSE infrastructure, demand charges, and station utilization. Indirect costs should also be accounted for including opportunity costs relating to travel time.

The TCO of XFC-capable BEVs can be compared with that of different vehicles to assess the economic feasibility from the owner's perspective and to examine how XFC influences the magnitude of each cost component. Examples of TCO for gasoline ICEVs, gasoline hybrid electric vehicles (HEVs), BEVs solely using DCFC, and BEVs solely using XFC are given in section 2.6.

The simple payback of owning and operating an EVSE are the ratio of upfront costs to total annual costs, as illustrated in Equation (2).

$$\text{Simple Payback} = \frac{\text{Private Capital Costs} - \text{Public Incentives}}{\text{Point of Sale Revenue} + \text{Indirect Revenue} - \text{Operation \& Maintenance Costs}} \quad (2)$$

for longer trips, combined with automotive manufacturers producing a greater number of BEVs with range above 160 km, can help minimize, but not fully remove the 'range anxiety' gap that exists, for some users, between ICEVs and BEVs.

Current DCFC systems do not offer BEV consumers nearly the same refueling experience as gasoline ICEV consumers. Replacement of more energy in a shorter period of time is one of the ways that the gap between ICEVs and BEVs can be further bridged. Extreme fast charging with powers at 400 kW or higher would enable a significant replacement of driving range in a period of 10–25 min. For the present work XFC is defined as the replacement of at least 32.2 km min^{-1} . At these rates it is conceivable that 320 km of range could be replaced in 10 min of charging. In addition to replacing significant driving range, for XFC to be viable it must be at price that customers are willing to pay. As such, it is necessary to understand a host of interactions for XFC that occur at the grid and EVSE level as well as the business case of XFC infrastructure. In the discussion below key uncertainties and the related RD&D needs are highlighted including; installation and operational cost of XFC EVSEs, the purchase and operational cost of XFC-capable BEVs, market opportunities, planning and stakeholder education, and management of intermittent load profiles likely to arise from

As shown in Fig. 1B, the economics of an XFC station heavily depend on the cost of EVSE equipment and installation, electricity costs, demand charges, station utilization, point of sale revenue, and indirect revenue. The key cost drivers for both XFC infrastructure and BEVs are discussed in detail in the following sections.

2.2. Infrastructure costs and considerations

Due to the complex nature of the infrastructure needed for XFC, three different areas were defined for analysis. These include grid and utility needs, charging station needs and EVSE needs. For each area, an issue tree was constructed that defines key areas for consideration that need to be addressed for the successful implementation of XFC. Overarching each issue tree is the need for safety and well-defined codes and standards. Ultimately, for the successful development of codes and standards there needs to be a concerted effort on the part of multiple organizations that include industry and codes and standards bodies such as the National Fire Protection Association (NFPA). To address the safety of XFC, coordination between industry, local authorities and various authorities

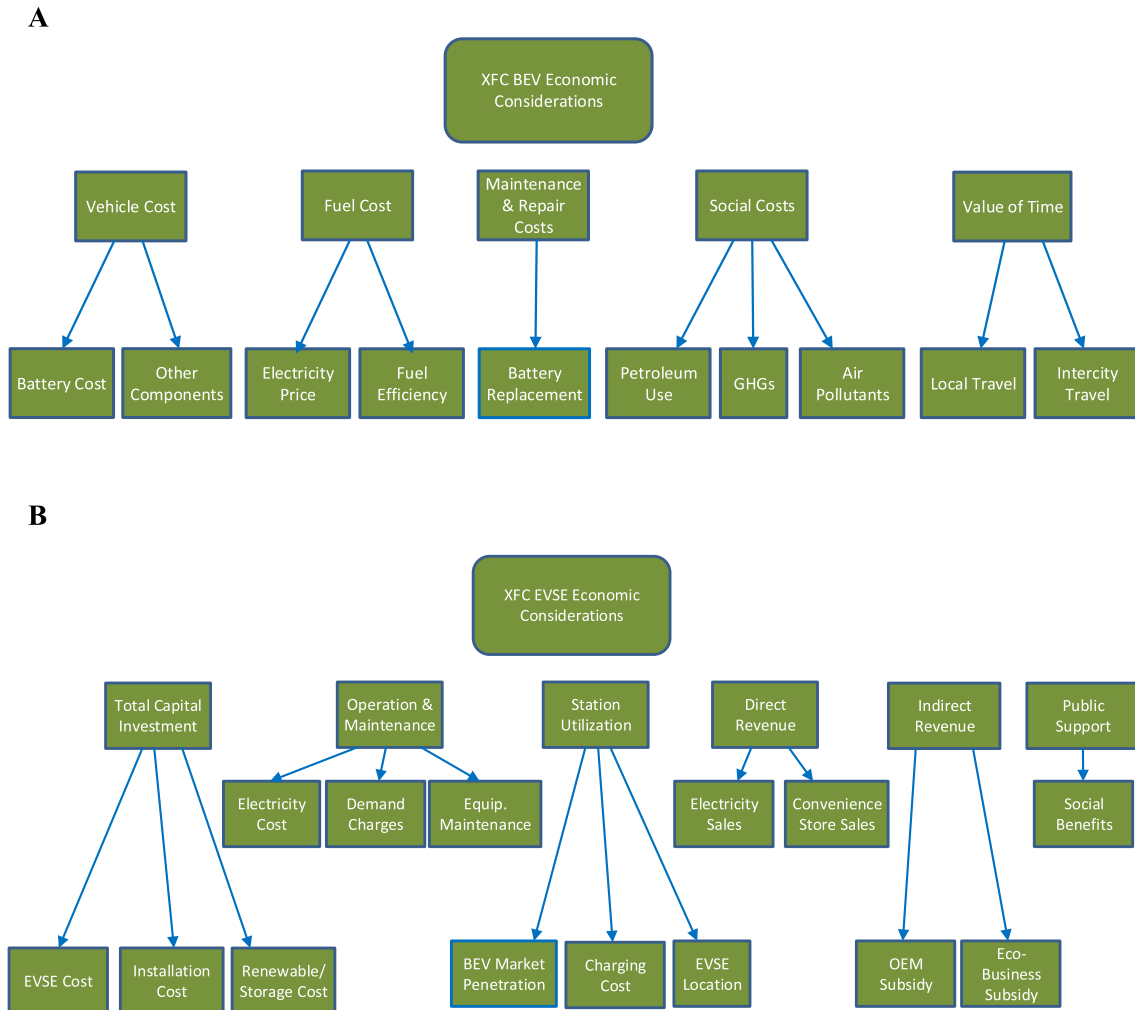


Fig. 1. Cost per km of cash flow or payback of XFC BEVs issue tree.

having jurisdiction (AHJs) and public utility commissions (PUCs) will become important. In conjunction with planning, will be the need for sufficient stakeholder education and engagement.

2.2.1. Utility and planning

2.2.1.1. XFC station siting. Presented in Fig. 2A are the potential impacts to grid and utility operation with the implementation of XFC. While extensive fast charging networks are only now starting to emerge, there have been a few isolated studies that hint at the potential grid issues that may arise from larger scale implementation. First, a key concern is that the addition of multiple charging stations will increase the overall power demand and that the hardware will create grid instabilities. Some support of this concern has been found where current BEV fast charging stations have been seen altering the steady state voltage stability of the grid [9] [10]. Others studies have found that harmonic limits need to be considered as much as the limits set on power to the EVSE [11]. Additional grid stability issues associated with high BEV adoption have also been identified, including enhanced aging of transformers related to the shortened life of insulation, though the study did not specifically look at impacts associated with fast charging [12].

The ability of the power grid to support XFC is a key area for consideration. The chief concern being that the addition of multiple charging stations and the associated overall power demand will

increase stress to localized portions of the grid that have aging infrastructure. As an example, an XFC station with multiple, simultaneous charging events at a single location could result in power levels well over 1 MW. At these levels, the power demands surpass most buildings including large hotels and medium office buildings across the country [13].

Early studies of fast charging have shown that grid harmonics and voltage stability can both be impacted even at levels near 50 kW [10] [11]. These impacts coupled with high power demands highlights the need to develop control schemes that provide sufficient localized control. Examples to minimize the power quality and delivery impacts include the ability to effectively manage non-abrupt initiation and discontinuation of the charging protocol. Additionally, implementing smoothed ramping up and down and coordination between different charge equipment at the same XFC station may be needed to minimize non-ideal grid behavior.

Power quality is not the only issue that needs to be addressed at the utility scale. In addition to voltage and harmonic issues that could arise, there are also key issues that need to be addressed associated with both siting and the appropriate power feed to an XFC location. While at the base level, many of the specific XFC station needs will be location specific, there are a few commonalities that will arise. These include the need to have an adequate distribution feeder and the inclusion of an appropriately sized transformer. For XFC operation, this will likely entail the use of a

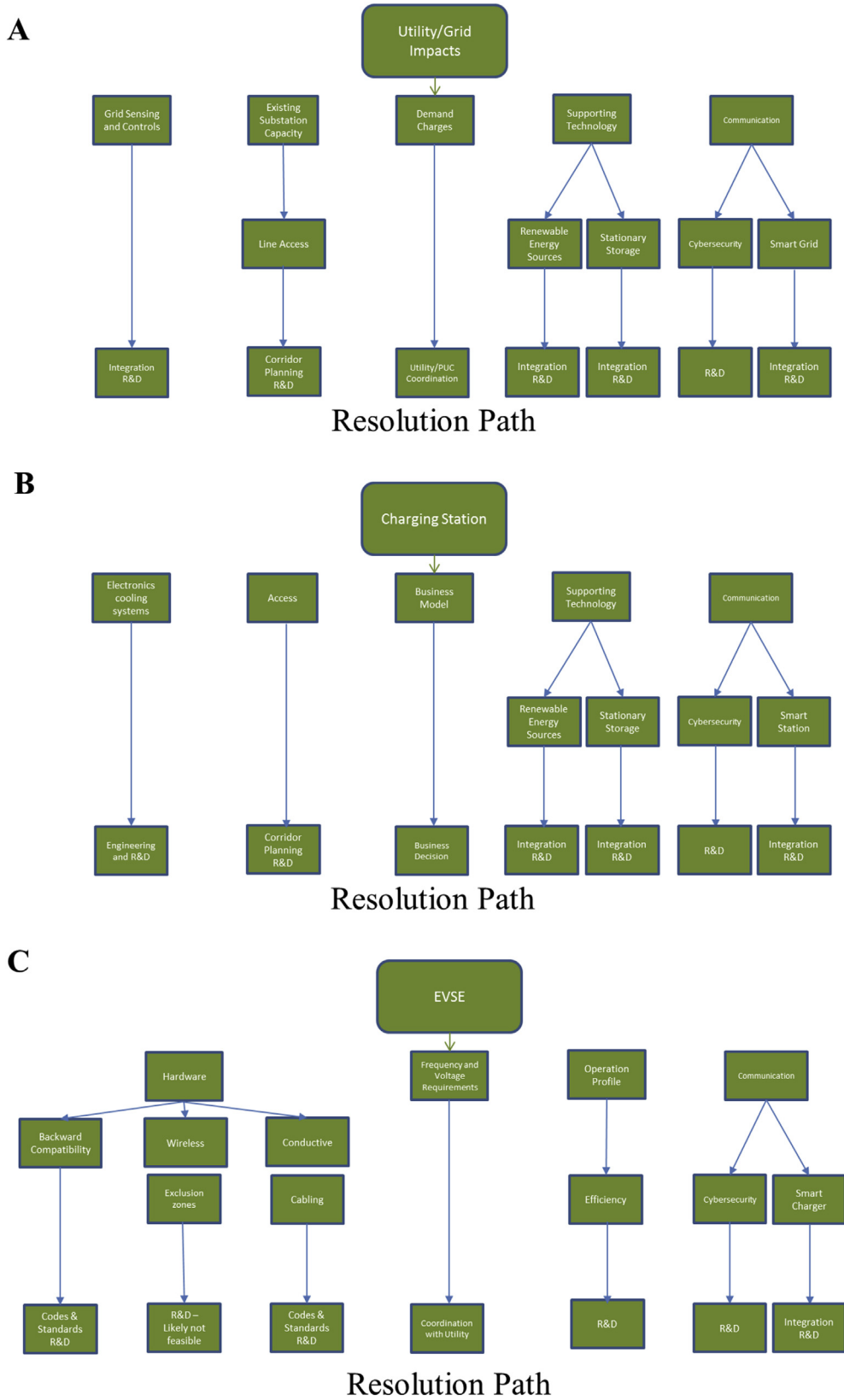


Fig. 2. Grid (A), Charging station (B) and EVSE (C) issue trees for the implementation of XFC.

pad mounted transformer such as a 2500 kVA transformer. With respect to the distribution feed, an XFC station would typically require an underground service and an associated switch cabinet, as is common for many commercial and light industrial locations with public access. Lastly, each station will need to follow the established codes for the specific location as well as for other governing bodies such as the NFPA and the Americans with Disability Act (ADA) requirements.

Coordination of an XFC network will also need to balance the needs of location specific charging stations with implementation across a broad geographic area, as their power surge has enough magnitude to propagate through the distribution and transmission network [14] [15] [16]. To alleviate propagation impacts, a proper system protection design needs to be implemented. This will likely require direct interaction with multiple public utilities and coordination with multiple PUCs. Across the United States, individual PUCs have different requirements for the sale of electricity and on overall cost structure. Additionally, there are other AHJs which impact the siting and requirements needed for the permitting and registration of charging infrastructure. The broad variability across the country currently stands as a possible impediment to widespread implementation of XFC infrastructure. A key to addressing this possible issue is a broad strategy to involve stakeholders from across the country to look at more uniformity as it concerns XFC infrastructure.

2.2.1.2. Demand charges and management. The cost of providing electricity for an EVSE at high power will be a crucial factor in the success of XFC. The components of delivered electricity cost broadly include electricity generation, transmission, and distribution. Utilities often use demand charges, which are based on peak power usage, as a tool to accommodate the delivery of electricity to customers during high demand periods. As such, demand charges are typically used for large electricity users that have high variability to provide compensation for the additional hardware and capacity that is needed to provide periodic high rates of power to the customer. This can require the installation or upgrading of distribution lines, transformers, and other equipment, and increased operation and maintenance costs.

XFC is expected to be intermittent during its initial implementation and even after initial implementation some rural stations that are part of corridors may see low utilization. Distribution equipment for irregular loads is usually oversized relative to that for more continual loads to mitigate the effects of intermittency. The costs associated with distribution network capacity upgrades must be recovered by the utility. Often, when utilities install a new service such as an XFC station, a connection fee is charged that covers a portion of the cost of the upgrade. The remainder of the cost is recovered through an energy charge (per kWh delivered), and/or a combined energy and demand charge that is calculated based on the peak kW delivered. Each utility has a differing rate structure for commercial users, some with proportionally high energy costs and others with high demand charges. For example, demand charges can range from \$2/kWh in Seattle to \$8/kWh in New York and more than \$30/kWh in Hawaii [17].

The impact of demand charges for fast charging is highly dependent on station utilization. When utilization is low, the energy provided is low, and the demand charge per kWh delivered is high. For EVSEs with low utilization providing high power charging, such as some DCFC locations from the EV Project, demand charges can account for a significant portion of the cost of operating the station and can make these stations unprofitable [17]. With XFC, the peak power demands will be significantly higher, so understanding how to mitigate high demand charges will be very important.

With higher utilization, an EVSE's profitability becomes less

dependent on demand charges as shown below. If XFC stations are sited in locations with a sufficient BEV population that uses the stations frequently, high utilization will not be an issue. However, in corridors and other sites that have lower utilization, demand charges will be a larger issue. Therefore, an analysis of what XFC station utilization is needed to make a station viable would be very useful. The development of sample rate structures for XFC stations could be useful for utility outreach. For example, a high energy charge and low demand charge for low utilization (early stations) and a low energy charge and high demand charge for a high utilization (mature stations).

Demand side management (DSM) has been used to mitigate impacts of peaky loads, through the control, including curtailment, of power demanded during times when the grid is operating near peak capacity. A key feature of DSM is that high power loads are typically impacted at lower rates than low power loads [18]. As mentioned in section 2.2.1.1, an XFC station is likely to have instantaneous power demands, which are on the order or greater than what is seen for many mid-sized buildings in the United States. This level of power would suggest that XFC may not be an optimal choice for DSM and is counter to many discussions suggesting that BEVs could be a prime use case for DSM [19] [20]. Where XFC differs from standard DSM for BEVs is that for its optimal utilization and to ensure consumer confidence there needs to be ready access to full power. Curtailing power to XFC stations, even briefly may decrease utilization of XFC stations by BEV drivers.

Key technological possibilities to reduce the impact of demand charges include on-site renewables that could minimize the total load needed from a utility and stationary energy storage that could be used to supplement grid demand and as a result smooth the use of energy. A side benefit of implementing demand response capable XFC on a distribution feeder, is that it would provide means to absorb excess renewable penetration either through charging events or when combined with stationary energy which could directly supplement charging needs. Both means could help mitigate negative ancillary effects of renewable variability and uncertainty, improving grid reliability and maximizing the renewable generation and revenue [21].

2.2.1.3. Integration of renewable generation and stationary energy storage. Use of stationary storage to effectively minimize or remove demand charges requires that the storage be capable of operating during the high power portions of charging events and also be able to remain in operation for extended periods of time. Recent work has shown that there is some ability to use energy storage options to minimize the full impact of power demand during a fast charging event [22]. During high use times, multiple XFC events may occur either simultaneously at a single location or back-to-back at the same location. At an example station that has six charging ports, the power supplied by the energy storage could be greater than 1 MW and the overall capacity may exceed 500 kWh. An effective energy storage solution would need to be able to buffer both the power and energy demands of such a station. The other key consideration for stationary energy storage is that it would need to be charged at a sufficiently fast rate or be sufficiently oversized for a specific location to facilitate many events in a short time frame such as during a rush hour period. The inability to meet the demands of all XFC events would lead to increased demand charges and partially negate the benefits of the stationary energy storage.

The side benefit of stationary energy storage is that during low use times it may be possible to use the storage to provide ancillary services for grid operation. However, the extent of benefit would be very much dependent on location and services needed, as significant peak load shifting would not be feasible due to the need to retain availability for possible XFC events. Other ancillary services

such as frequency regulation may be feasible. Storage systems (both Li-ion and flow batteries) which could meet these demands are already being integrated into other grid and microgrid settings often in conjunction with renewable energy generation assets. However, there are challenges in providing ancillary grid services. Two that are distinctly apparent are market size and market risk. With respect to size, the demand aggregator needs to be able to provide at least some minimum demand to the ancillary services market, but the market size is limited, so the market can saturate quickly. Market risk is also important, as prices for ancillary services are volatile. Thus, the key to incorporation of storage with XFC is the combination of appropriate control schemes, and economic considerations for installation, maintenance and replacement due to performance fade of the installed storage or changes in use conditions for the XFC location.

Analysis of when DCFC are used during the work week has found that for current installations the highest use rates were closely aligned with the evening commute between the hours of 5 and 7 pm [23]. The same study found very little use between midnight and 6 am. This data, while dating to 2013, suggests that it is probable that the enhanced implementation of other fast charging options such as XFC would have high use rates during the same time period. With such a use scenario, it is feasible that the integration of localized renewable generation, especially solar, at the XFC station could curb demand during the day with an additional buffer from stationary energy storage. The storage could then be charged from either excess renewable energy during the day or from the grid during off-peak nighttime hours.

However, other issues could arise for the inclusion of XFC in areas that have high renewable generation, but which lack sufficient storage. A key example of this is California, which has mandates for high penetration of renewable power generation. California ISO has projected there will be a need for sufficient ramping of generation during the evening hours, especially in the spring and fall to account for renewables going off-line and the increase in power consumption as residents go home at the end of the work day [24]. This projection, which takes into account high renewable penetration, especially from solar, includes the assumption that more renewables are added to the system, but that overall energy use does not increase, shows the need for ramping of close to 13,000 MW over a three hour period. What it does not take into account is that if transportation becomes more electrified there will likely be a net increase in grid energy demand. If patterns for XFC use during the work week mirrors the use of early adopters of DC fast chargers [23], the increased demand during and just after the evening commute from 5 to 8 pm could exacerbate issues associated with ramped generation or require additional storage capability.

As an example in 2015 there were just over 24 million registered light duty vehicles in California [25]. If adoption of XFC-BEVs advances to encompass 10% of the vehicles (2.4 million vehicles) and if 5% of those vehicles (120,000) fast charge during the 5–8 pm rush hour peak period [23], between 6500 and 7700 MWh of additional total generation would be needed if each charging event replenished close to 320 km of driving range (57 kWh). The variation being due to efficiencies in chargers and variation in the energy needed per km of driving distance replaced. Regardless of extent of renewable integration into the grid, this level of ramping needs to be accounted for in areas where it is foreseen that high levels of adoption of XFC capable vehicles are possible.

2.2.2. Charging stations

The implications of XFC on infrastructure extends beyond just grid and utility operation. The ability to effectively provide XFC for BEVs will require the implementation of charging stations at

specific locations which are capable of providing the power and also being readily accessible to a populace with a higher adoption of BEVs. The design of these charging stations needs to take into account a host of different issues as shown in Fig. 2B. The stations also need to be part of corridor planning, which takes into account the human psychological perspective to allow consumers to feel unburdened by the distance between XFC stations. Satisfying this condition may require some overbuilding of infrastructure or better education and distribution of pertinent information such as range to consumers [26].

Regional variation in acceptance may also be a key consideration during the planning process. This combined corridor optimization will require advanced understanding of BEV use patterns which are expected to change as BEV adoption rates increase, as BEV range increases and as BEVs become more viable for those that do not have access to home charging. In parallel with understanding BEV use, the corridor planning effort must be cognizant of grid issues such as anticipated changes in generation mix and aging substations, distribution and transmission lines. Much like the integration of renewables and localized stationary energy storage, the other area that must be part of corridor planning efforts is understanding how XFC EVSEs impact the overall functioning of the grid and if there are any issues which could emerge due to high use of XFC infrastructure.

The flow of vehicles presents a possible challenge that does not exist for refueling ICEVs. The general layout of a XFC station would entail multiple charging ports that would be situated to optimize flow of vehicles. For XFC, flow pattern is crucial due to the less consistent amount of time needed for charging when compared to ICEVs. Much like refueling stations for ICEVs, a key area of interest is how to get new, low charge BEVs into open ports as they become accessible. This is especially pertinent as the likely scenario, based on prior data obtained from the use of DCFC, is that most cars will be arriving with a state-of-charge below 40% [27]. Current BEVs have charge ports in more disparate locations (i.e. the side versus the back of the vehicle), which does not readily lead to the easy movement of vehicles into and out of an XFC station. Facilitation of XFC station throughput could be aided by standardization of the location of vehicle charge ports across manufacturers or the development of longer cables. However, as discussed below in section 2.2.3.1, cable weight could become a key concern.

2.2.3. Electric vehicle supply equipment (EVSE)

2.2.3.1. EVSE technical issues (cable, voltage, connector).

Fig. 2C defines the key issues associated with the implementation of EVSE for XFC purposes. Among the most significant challenges are those associated with the type of charger and its compatibility with existing BEVs. These issues are much less focused on development of new technologies, but more so on the joint understanding of how technologies can be used and how codes and standards for multiple organizations can be unified. Of particular impact is the unification of codes and standards put out by the Society of Automotive Engineers (SAE), and the National Electrical Code (NEC) put out by the NFPA, while still meeting the needs of the Occupational Safety and Health Administration (OSHA).

An example of the interplay between the different governing bodies can be found in comparing what type of cabling limits arise when following both the NEC cable sizing requirements and the OSHA limits for lifting (Fig. 3). A 50 kW DCFC cable is the closest example that currently exists that can be compared to a future XFC cable. The DCFC cable is typically 3.7 m long and comprised of 2 AWG (American Wire Gauge) conductors for the DC charging current up to 125 A. A 3.7 m long CHAdeMO cable mass is 10.4 kg including the connector. Since most cabling systems suspend half of the cable, the driver/operator only has to lift half of the mass since

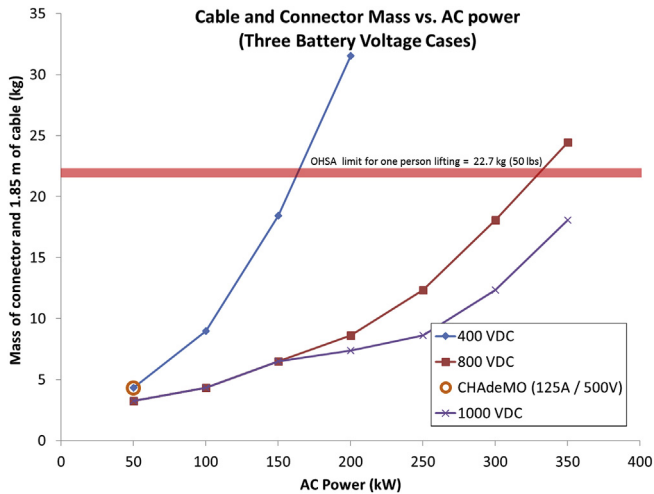


Fig. 3. Comparison of uncooled cabling for EVSE operating at 400, 800 or 1000 V. Calculations using different copper cables which meet the National Electric Code (NEC) capacity ratings and use the current weight of a CHAdeMO connector.

the other half is supported by the DCFC.

For XFC systems without a significantly higher voltage than what is currently used for DCFC, the current requirement of the cabling increases to nearly 900 A. This requires wire gauge sizing that weighs over 14.7 kg m^{-1} . With a higher battery voltage, the current requirement significantly decreases but cable wire gauge size is still a concern. The issue of using standard cabling is shown in Fig. 3. The figure shows how with increasing power levels there is a distinct increase in cabling weight. At a battery voltage of 800 V, the current requirement is over 400 A, which requires MCM 350 wire gauge that weighs over 11.8 kg m^{-1} , where MCM is an abbreviation for a thousand circular mils. Again assuming a cable management system that only requires the driver or XFC station operator to move 1.85 m of cable, the resulting mass is 25.9 kg. This cable mass exceeds the OSHA lifting limit for a single person. Indeed for both 400 and 800 V systems the cabling exceeds the OSHA limit well below 400 kW minimum charger power needed for the defined XFC charge. Only when the voltage level increases to 1000 V does the cable weight remain near the 22.7 kg OSHA limit.

The use of liquid cooling could significantly reduce the overall cable mass and allow the average consumer the ability to charge using an XFC EVSE. However, there is currently no set agreement on how to accommodate liquid cooled cables within the National Electric Code (NEC). Another option would be the use of robotic or automated charging stations. A third option to not have heavy cables for conductive XFC is the use of high power wireless charging. To date high power wireless charging has been demonstrated at 50 kW with plans for expansion to 200 kW and beyond for buses [28]. To enable wireless charging either large single coils or multiple coils are paired together (side by side in parallel) with the size of the coil dictating the overall power capability. One current issue is that with existing technology the size of the coils needed for wireless XFC would be greater than the underside of a typical sedan. Additionally there are potential safety concerns with respect to electromagnetic field emissions surrounding such a high power wireless charging system. Thus, while a possibility, the overall feasibility of using high power wireless charging for light duty vehicles is questionable.

The need for greater uniformity in the location of charging ports to facilitate XFC has been put forth in section 2.2.2 relating to charging stations. With respect to the EVSE a similar enhancement in uniformity to a standard, high power connector would

significantly improve XFC planning. Currently with three primary DC fast charging connectors in the United States (SAE J1772 CCS, CHAdeMO and Tesla) harnessing a single station for quick XFC purposes is something which will require direct codes and standards involvement on the part of industry (both vehicle and EVSE manufacturers) and independent specialists such as those located within the Department of Energy national laboratory system. This is similar to what occurred for other EVSE codes and standards efforts, such as those associated with SAE J1772 and SAE J2954.

2.2.3.2. EVSE installation and equipment costs. The cost of XFC installation and equipment is an important factor in understanding the business case of this technology. Current DCFC installation costs vary significantly and often depend on how close the EVSE is to existing power infrastructure. Analysis from the Recovery Act EV Project, found that 111 DCFC installations ranged from \$8500 to over \$50,000, with a median of \$22,600 [29]. The addition of new electrical service was the largest cost driver. For example, if the DCFC location did not have adequate service nearby, a transformer, switches, and long conduits would need to be installed and would increase costs. The cost to purchase and install a transformer is around \$18,000 [30]. The surface type where wiring and conduit were installed was the second largest cost driver. For example, if a significant amount of concrete or asphalt needed to be removed and replaced a substantial increase in installation cost would result. The least costly installations were at retail shopping centers that had adequate electric service and that required either short, hand-shoveled underground or surface-mounted conduit service.

As XFC will require locations with excellent electrical service, the cost of installations could be more expensive than those for DCFC. Understanding the installation and interconnection cost of XFC at an “optimal” versus “non-optimal” site is necessary for planning XFC locations. Francfort et al. performed a rough order of magnitude analysis of the costs of a charging complex with six EVSEs, comparing DCFC (at 50 kW) and XFC EVSEs at rural and urban corridor locations. The installation cost estimate per XFC EVSE ranged from \$40,300 to \$42,000 or about \$7300 to \$9400 more than the cost per DCFC [29].

Currently DCFC systems are available that provide 145 kW charging (Tesla), with plans in the near-future to deploy 225 kW systems (Porsche). Dual-port DCFC hardware costs for chargers rated at 50–60 kW are estimated to be between \$20,000 and \$36,000. Francfort et al. estimated the equipment cost per XFC EVSE to be \$245,000 as compared to the \$30,000 DCFC EVSE [29]. While initial experience by OEMs developing these high power systems found that the equipment costs may be significantly higher, the expectation is that they will be similar in cost to current systems once they are beyond the prototype development phase.

A distinct difference between lower power DCFC and XFC equipment is the cabling that is necessary for higher power. As charge power increases the current, the conductor size and weight increases as discussed above in 2.2.3.1. In order to reduce the size of the charging cable, cooling is likely required. The addition of liquid cooling increases the complexity of an EVSE due to the need for pumps and a reservoir of coolant. Cables guided by robotics could also be used instead of vehicle operators but again this would increase the overall complexity of the EVSE. Both routes to deal with increased cable weight are likely to increase the equipment and maintenance costs.

2.2.3.3. Subscription options. XFC stations will need to be installed in sufficient numbers and in appropriate locations to influence adoption of BEVs that are capable of XFC. This requires investment in charging infrastructure that may not be fully utilized until the

BEV market grows, making the investment risky. Fleets owners of centrally recharged XFC BEVs might be able to support the fleet with a predictable and affordable number of XFC stations, with locations known before installation. However, the numbers and locations of public XFC stations needed to promote adoption of XFC BEVs will be difficult to predict. Public XFC infrastructure may require a phased deployment in conjunction with an XFC BEV adoption campaign. First, by deploying XFC chargers in locations to support early adoption of XFC BEVs, then expanding to additional locations as adoption increases. Public EVSE network providers and operators will need to consider different business models and rate structures. Several models exist, including: per kWh, per minute, and subscription.

It is difficult for a public charging station to realize sufficient revenue from electricity sales (per kWh charging), as has been documented by several studies [31] [32] [33]. Some networks charge on a time-basis (per minute) or charge a subscription fee, for access to chargers in their network, or a combination. Charging on a time-basis is often done for Level 1 and 2 EVSEs in locations where parking is at a premium and turnover for charging access is desired. A subscription fee compensates the EVSE network provider for making the EVSE available, independent of the utilization, and subscribers realize the value of the availability of EVSE stations “just in case”, even if they charge mostly at home or elsewhere.

2.2.4. Cyber and physical security

One area that crosses all three levels of infrastructure needs for XFC is the combination of physical and cyber security. Due to the high rate of energy transfer needed for XFC there has to be private and secure communication between the vehicle and the EVSE. Likewise, communication between the grid and the charging station is expected. This tiered communication presents the possibility that significant cyber security issues could arise with an expansive XFC network. The risk is that breaches in security could impact not just individual vehicles or charging stations, but could cascade to impact broad swaths of transportation infrastructure or the grid.

It is important to continuously assess the resiliency of a physical system such as an XFC station by using scientifically sound techniques. The impact of maloperation of XFC on the power systems needs to be assessed and control actions to counter impact should be designed in advance. The use of different techniques including real-time simulation can identify unfavorable operating conditions that result from cyber and cyber-physical attacks on physical systems. With the use of different simulation and actual device assessments, proactive insights can be leveraged to prevent malicious operating conditions from occurring, or minimize damages if they do happen.

2.3. Battery and vehicle costs and considerations

Battery costs are a critical driver of BEV price and ultimately the total cost of ownership of a vehicle. Li-ion batteries for BEVs have seen significant reductions in costs in the past 10 years with some 2016 battery pack costs publicized near or below \$200 kWh⁻¹ [34] [35]. While Tesla battery packs are capable of charging to 120 kW, the cost implications for XFC-capable batteries are not clear [36]. XFC could impact factors such as battery lifetime, chemistry adopted, cell design, and thermal management and these issues require analysis [1,2]. Fast charging can have implications on battery degradation, so understanding the cycle life implications of BEVs using XFC at different frequencies is needed. For drivers who only use XFC occasionally this may not be an issue, but for multi-unit dwellers or commercial fleets who use them frequently, performance degradation could be a concern.

Battery chemistry and cell design changes made to improve

battery charging performance and lifetime, will impact production costs [1]. If XFC-capable BEVs (XFC-BEV) are warranted as are current BEVs (battery life warranted for 8 years or 161,000 km), whichever occurs first [37], and the cost to automakers of warranty battery repairs and replacements are included in the BEV price, then reduced battery lifetimes would impact the vehicle price.

It is likely that XFC-BEVs would not have different vehicle energy efficiency from standard BEVs, therefore the energy costs will be driven more by the cost of electricity per kWh than the amount of electricity consumed per km, assuming losses in the XFC EVSE are not much higher than losses in DCFC EVSE. Since vehicle costs, amortized per km depend on the distance driven, the enhanced usability of BEVs provided by XFC may enable users to drive BEVs greater distance, making BEVs more economical than conventional vehicles on a per-km basis if the electricity cost per km is less than that of gasoline. XFC-BEVs may be economically advantageous for users who drive many km per year. However, uncertainty in battery lifetimes due to potential battery degradation might reduce resale value. Some BEVs are reported to depreciate faster than comparable conventional vehicles, but high-performance/luxury BEVs appear to retain value well [38] [39]. It is unknown how XFC-BEVs would depreciate, but if introduced in the luxury-performance segment (and if batteries do not degrade), XFC-BEVs may hold their value well.

2.4. Value of time

Travel demand is typically generated from the activities at the destinations of trips. Travel time has a negative utility; it is something private and commercial users have a willingness to pay to have less of. The value-of-travel-time-savings (VTTS) is often used in government cost-benefit analyses of regulatory actions and investments in transportation to make sure resources are used appropriately. The VTTS varies depending on multiple factors including the individual traveling and the type of travel. The U.S. Department of Transportation (DOT) has analyzed this topic and provided guidance on how to use VTTS in economic analyses [40]. However, analysis of VTTS for both consumer and fleet BEV drivers would help determine the economic viability of XFC.

Research has typically found VTTS for personal travel to be lower than the hourly earning rate. For local personal travel, the DOT estimated the VTTS at 50% of hourly median household income [40]. In 2015, the median hourly income was \$27.20 per hour, resulting in a local VTTS of \$13.60 [41]. The DOT examines intercity personal travel separately as estimates of VTTS rises with distance of a trip. For intercity personal travel, the DOT estimated the VTTS at 70% of hourly median household income, which was \$19.00 per hour in 2015 [40] [41]. An analysis of the VTTS for various consumer segments would help determine the cost limits that XFC would need to meet to provide consumer value.

There is wide agreement that the VTTS for business travel should equal the gross hourly cost of employment, including payroll taxes and fringe benefits. For local and intercity business travel and commercial vehicle operators, the DOT assumed the VTTS to be equal to a nationwide median gross compensation, defined as the sum of the median hourly wage and an estimate of hourly benefits. Following the DOT approach to calculate business VTTS, we estimate the value to be \$26.00 [40] [42] [43]. Using the latest data on long-distance travel from the National Household Travel Survey and total light-duty vehicle mileage the Bureau of Transportation Statistics, we estimate the percentage of vehicle travel for the DOT VTTS categories: local personal (66%), intercity personal (25%), local business (5%), and intercity business (4%) [44] [45]. Using these percentages and the values for each of the four VTTS, we estimate the weighted average VTTS to be \$16.00 per

Table 1
Summary of key inputs for ICEV, HEV, and BEV TCO analysis for a single XFC port.

	ICEV	HEV	DCFC-BEV	XFC-BEV
Fuel Economy (MPGGE)	33.0	46.1	115.4	115.4
CD Electricity Use (kWh/100mi (160.9 km))			28.5	28.5
Purchase Price (\$/Vehicle)	\$20,000	\$23,000	\$35,000	\$36,000
Vehicle Lifetime (yr)	15	15	15	15
Vehicle Annual (km)	19,950	19,950	19,950	19,950
EVSE Hardware Cost			\$30,000	\$245,000
EVSE Installation Cost			\$33,000	\$41,000
Charging Time (min/user)			80	10
Charge Sessions (#/day)			5	12
EVSE Charging Power (kW)			50	400
EVSE Efficiency (%)			92%	90%
EVSE DC Electricity Dispensed (kWh/session)			67	67
EVSE Lifetime (yr)			15	15
Demand Charge (\$/kW/month)			\$8	\$8
Base Electricity Rate (\$/kWh)			\$0.10	\$0.10
EVSE Cost Amortization (\$/kWh)			\$0.09	\$0.24
Total Electricity Cost (\$/kWh)			\$0.19	\$0.34
Gasoline Price (\$/gal)	\$3.00	\$3.00		
Value of Time Travel Savings (\$/hr)				
Gasoline Fueling Rate (gal/min)	10	10		
Vehicle Lifetime (hours fueling)	9	7	1060	133

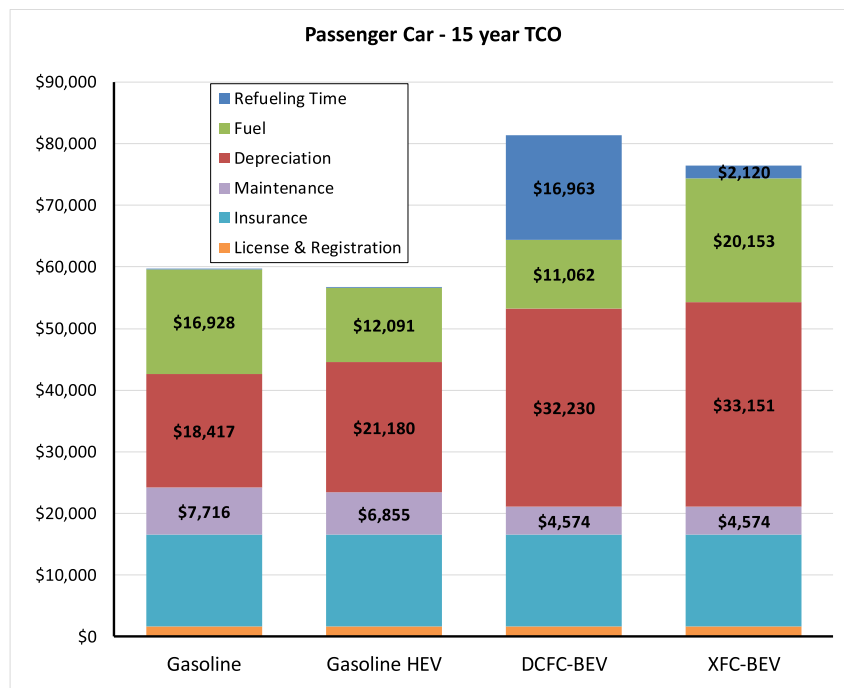


Fig. 4. Passenger vehicle 15 year total cost of ownership based on vehicle propulsion system configuration.

hour. The values will vary for different commercial uses such as taxi, ride-share, and bus. Therefore, analysis of VTTS for these segments is needed to understand XFC potential in commercial applications.

2.5. Social benefits

To the extent that XFC can increase adoption of BEVs, benefits to society can be realized through increased energy security. However, since effects of oil dependence and emissions are not explicitly captured in vehicle or fuel purchases, they are externalities,

therefore consumers tend to consume and emit more than if vehicle and fuel transactions included the costs of externalities [40]. These externalities are market inefficiencies that can limit the benefits that BEVs can potentially provide. Federal, state, and local governments and other public entities may choose to promote BEVs in order to realize some of these benefits [17]. One way to promote BEV adoption would be to support deployment of XFC chargers in order to increase adoption of BEVs by those who cannot conveniently charge vehicles at home or at work. Support can take various forms, such as subsidies, incentives to EVSE network providers, education and outreach, coordination between authorities

Table 2
Summary of sensitivity cases for TCO analysis with costs based on a single XFC port.

Parameter	Units	Inputs-low	Inputs-default	Inputs-high
Charges per Station	#/day	6	12	24
Demand Charge	\$/kW	\$2	\$8	\$20
Gasoline Price	\$/gal	\$2	\$3	\$5
Vehicle Incremental Cost	\$	\$8000	\$16,000	\$24,000
Electricity Base Price	\$/kWh	\$0.02	\$0.10	\$0.20
XFC Hardware Cost	\$	\$35,000	\$245,000	\$300,000
XFC Installation Cost	\$	\$20,000	\$41,000	\$60,000

having jurisdiction over EVSE installation and operation to help reduce regulatory and permitting barriers.

2.6. Economic analysis

2.6.1. TCO analysis

Using the cost data discussed in earlier sections and the AFLEET 2016 Tool, we analyzed the total cost of ownership of an average passenger car with four different powertrain/charging options: (1) gasoline ICEV (2) gasoline HEV (3) BEV solely using DCFC and (4) BEV solely using XFC [46]. The use of a single charging regime (100% use of DCFC or XFC) in this calculation is intended to define a limiting case that highlights the differences in each technology. This may not be a realistic assumption for many BEV drivers, though may represent a case for those who do not have the ability to charge at home or work, such as multi-unit dwellers. Table 1 summarizes key inputs for this analysis.

Results in Fig. 4 from the AFLEET 2016 Tool, show that the incremental price and resulting depreciation of both BEVs account for a significant portion of the TCO. Typically, a BEV will have significantly lower fuel costs due to the low price of electricity. In this scenario, the BEV only uses either DCFC or XFC and the electricity price paid in each scenario includes the cost amortization of the EVSE equipment, installation, maintenance, and demand charges based on the assumed station utilization. The BEV-DCFC has \$6000 lower lifetime fuel costs than the ICEV and \$1000 lower fuel costs than the HEV. The XFC-BEV has higher fuel costs (\$3000) than the ICEV due to the high cost of the XFC EVSE equipment, maintenance, and demand charges. Both the BEVs have lower maintenance and repair costs than the ICEV, as no battery replacement is assumed. When comparing the two BEV scenarios, the value of time travel savings becomes a significant factor in the TCO. The XFC-BEV would

spend about a 900 h less charging than the BEV-DCFC, accounting for about \$15,000 in VTTS. This analysis shows that both XFC vehicle and fuel costs will have to decrease in order for it to show a strong economic benefit versus ICEVs or HEVs.

Another important takeaway of a TCO analysis is to look at how sensitive results are to changes in assumptions. Table 2 has the sensitivity case assumptions. When comparing the XFC-BEV to the ICEV (Fig. 5), the station utilization, electricity demand charge, gasoline price, BEV incremental cost, base electricity price, and EVSE hardware cost all can significantly impact results.

2.6.2. EVSE utilization and demand charges

With the utilization (12 sessions day⁻¹) assumed in the default case, the \$8 kW⁻¹ demand charge accounts for 38% of the estimated total electricity cost. The total electricity cost that the driver would pay (\$0.34 kWh⁻¹ in base case) includes the base electricity price from the utility and the breakeven cost to amortize the EVSE hardware, installation, operation (includes demand charges) and maintenance costs over an assumed 15 year EVSE lifetime and kWh dispensed (profit not included). If the station is used 6 sessions day⁻¹ with the same \$8 kW⁻¹ demand charge, the total electricity cost jumps to \$0.58 kWh⁻¹, with the demand charge accounting for 45% of the cost. As seen in this example, the demand charge can be a significant portion of the price to charge an XFC-BEV. If station utilization is low, fixed costs such as demand charges and hardware equipment cost and maintenance becomes an increasingly important cost factor (Fig. 6). Fig. 6 shows the breakeven charging cost both in \$ kWh⁻¹ and \$ eGallon⁻¹, which takes into account the relative efficiency benefit (3.5 times) of the XFC-BEV versus its gasoline counterpart.

2.6.3. Charging station renewable generation and stationary energy storage

Francfort et al. examined the equipment, installation, and operating costs of a six EVSE XFC complex with and without the use of photovoltaics (PV) and stationary energy storage [29]. Their estimates were based on the PV providing between 30 and 39% of the energy supply and the PV and energy storage reducing maximum grid power demand by 80%. These systems were sized on assumed station utilization patterns (rural locations had longer charge times but were used less frequently than urban locations). The values in Tables 1 and 2 are in close alignment with those generated by Francfort et al. but are scaled to the single XFC port level [29].

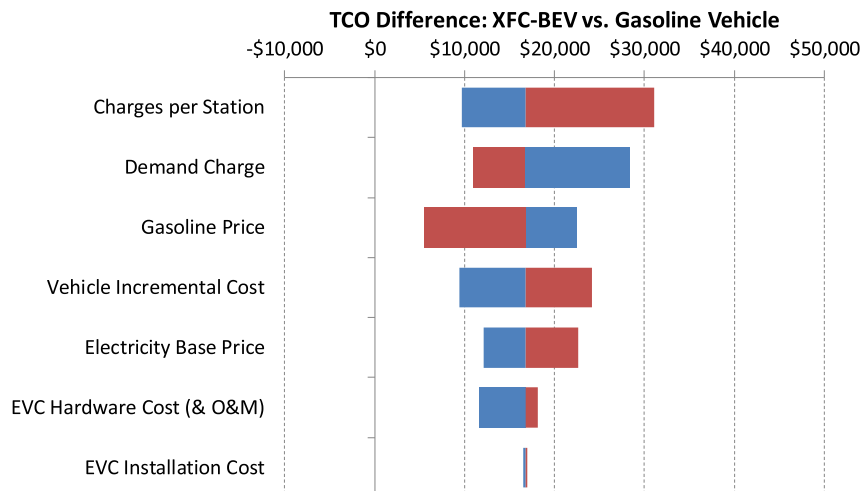


Fig. 5. TCO Difference: XFC-BEV compared with an ICEV.

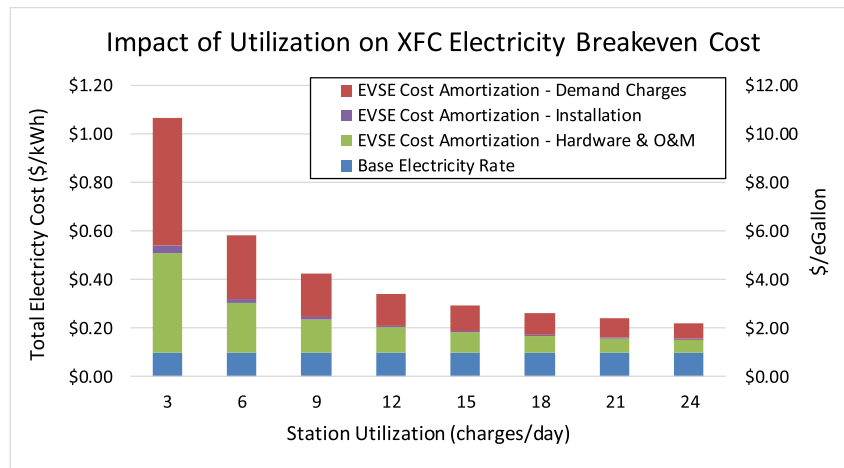


Fig. 6. Passenger vehicle 15 year total cost of ownership based on vehicle propulsion system configuration.

The PV equipment was assumed to cost $\$200 \text{ kW}^{-1}$, with per EVSE cost ranging from $\$2700$ to $\$4000$. The stationary energy storage system (ESS) was assumed to cost $\$400 \text{ kWh}^{-1}$, with the per EVSE cost ranging from $\$21,000$ to $\$84,200$. The total equipment and installation cost of the charging complex with PV and ESS ranged from $\$1.64$ million to $\$2.03$ million. Due to differences in the type of equipment needed with and without PV and ESS the cost of not including ESS and PV changed the price from $-\$302,000$ (more expensive with ESS and PV) to $\$85,000$ (less expensive with ESS and PV). In addition, the annual operating savings due to reduce demand charges for the charging station with PV and ESS ranged from $\$125,500$ to $\$157,500$. While the comparison of the inclusion of ESS and PV needs further analysis, XFC charging complexes are likely to see potential cost savings with the incorporation of energy storage or distributed renewable energy generation integration.

3. R&D, industry, and education considerations

To address uncertainties, challenges, and implications facing the deployment of XFC, a number of questions need to be researched. In addition to R&D questions, resolution of issues facing EVSE network providers, operators, utilities, and users should be addressed, requiring coordination between various actors, standardization of technologies and practices, and education of users and other interested parties.

3.1. Near-term R&D

In the near-term, research is needed to support effective coordination of corridor planning. Understanding where XFC stations need to be sited to serve demand by BEV drivers and where the appropriate grid resources exist to initially serve the greatest number of consumers are two important research areas. Within these issues, there are a number of specific questions and research needs.

To better understand potential adoption levels of XFC and XFC-BEVs, market research is needed for several potential market segments, including both private vehicle owners and commercial and government fleet managers. The market for private vehicles is heterogeneous with individual owners having a different value of travel time, need for range, preferences for other vehicle features, and willingness to pay for XFC. Commercial and government fleets, including drivers of transportation network companies such as Uber or Lyft, are diverse with different requirements for the times

and distance that vehicle are operated, the value of (or lost revenue from) time spent charging, and type of vehicle required. Therefore, many possible use cases need to be considered to assess the utility of XFC to potential user segments. Market research should consider the potential influence of incentives and other policies to promote BEV adoption, since automakers and government agencies may choose to provide funding for XFC stations to increase BEV sales.

Adoption and use patterns will determine charging demand at different locations and times of day. Estimating future demand and potential utilization of XFC stations will be key to assessing the economic viability of these stations and their impacts on the grid. The economics of stations depend not only on installation and operation costs but also on utilization. In the early stages of XFC deployment, even well-sited stations may not be heavily utilized, and revenues from providing charging will very likely be insufficient to defray these costs. Moreover, the costs and revenue for a given station will vary widely depending on site-specific characteristics. Multiple case studies will be needed to assess the range of equipment, installation, and operation costs under different probable utilization patterns. Key to these case studies will be analysis of various approaches to manage the cost of supplying power to the station, particularly the demand charges when station utilization is low. Examples described above represent several of possible approaches to manage high-power, intermittent demand of an XFC station. Further research is needed to better understand the economic tradeoffs and operational benefits of on-site storage, integration with distributed generation, and advanced technologies and management practices for operating distribution networks.

In addition to the above research, more materials research and equipment design engineering are needed. Technological improvements could include advanced materials with better thermal and electrical properties to reduce and manage thermal loads in the EVSE and its cable.

3.2. Long-term R&D

In the long-term, research will be needed to address challenges germane to widespread XFC deployment and possible challenges arising from changes in travel patterns and vehicle ownership. Widespread, heavy use of XFC in combination with automated and connected vehicles, many of which may be shared-used vehicles may result in different demand patterns than those seen in early deployment. Future technology may enable XFC with little or no actions by drivers through automated and even wireless EVSE.

3.3. Industry needs

Beyond R&D, other actions will be needed to implement XFC. Across the country, there are a multitude of different authorities having jurisdiction over permitting, siting, and regulation of charging stations. Coordination and harmonization of permitting, siting and regulatory requirements would simplify XFC planning and deployment. Unifying and harmonizing codes and standards would also be beneficial, including items such as applicability of liquid cooled cables, connector design, and cabling limitations. Industry and AHJ engagement in standardization organizations such as SAE, NFPA, and others will be needed.

3.4. Education needs

Successful deployment of XFC and adoption of XFC-BEVs will require education of both consumers and other stakeholders on the merits of vehicle electrification. The U.S. Department of Energy, through its Clean Cities and Workplace Charging programs has engaged in a range of education and outreach efforts to promote BEV adoption, as are a number of other organizations, such as state agencies, non-governmental organizations, not to mention automakers marketing their BEVs [47]. As XFC challenges are addressed through research and other activities described above, consumers and others need to be educated on XFC and BEVs so they can make informed decisions. Education efforts will need to be tailored to the particular user segment and stakeholder group.

4. Conclusions

Extreme fast charging consisting of DCFC systems capable of power up to 400 kW, would allow BEVs to recharge about 320 km of driving distance in 10 min. This brings BEV recharging much closer to the experience that consumers are accustomed to with ICEVs. While this clearly offers greater utility to BEV drivers than slower charging systems, several important uncertainties need to be addressed before it is clear how these chargers and XFC-capable BEVs might be deployed, including:

- The cost of the charging equipment, installation and operation
- The cost of XFC-capable BEVs
- The future markets for XFC-capable BEVs by different users (commercial and private)
- Planning future XFC installations and networks, including siting and planning for future demand
- Viable business models for XFC stations under low and slowly increasing utilization; in particular, potential revenue streams for XFC network operators other than from selling electricity
- Management of the intermittent, high power demand by XFC stations, particularly when station utilization is low.

Addressing these uncertainties will require research and analysis. Important research needs include.

- Development and analysis of scenarios of possible future deployments of XFC networks to better understand siting, taking into account existing grid resources and potential future XFC utilization. Such scenario analysis should consider how XFC will influence adoption of BEVs and the potential uses and business cases for XFC-BEVs under different market conditions and policies.
- New technology and operations practices to more effectively manage distribution grids with intermittent, high-power loads such as XFC stations with integration of stationary storage and distributed generation.

- Cyber and cyber-physical security of XFC infrastructure.

In addition to research, additional actions will be needed such as.

- Increased coordination between multiple utilities, EVSE network operators, and AHJs over permitting, siting and regulation of charging stations.
- Increased standardization to ensure safety and to increase interoperability and backward compatibility.

Although deployment of XFC faces many issues, with sufficient progress in the above research areas and in battery technology, XFC could offer greater convenience and utility for BEV drivers, in particular private owners without access to charging at home, as well as those traveling along corridors and commercial BEV operators with a high value of time. With increased BEV adoption, there is the potential for decreasing petroleum use and decreasing emissions, with benefits of improved energy independence and reduced impacts to the environment.

Acknowledgements

This work was performed under the auspices of the US Department of Energy, Office of Vehicle Technologies, under Contract Nos. DE-AC02-06CH11357 (Argonne National Laboratory), DE-DE-AC07-05ID14517 (Idaho National Laboratory), and DE-AC36-08GO28308 (National Renewable Energy Laboratory). The U.S. Government retains for itself, and others acting on its behalf, a paid-up nonexclusive, irrevocable worldwide license in said article to reproduce, prepare derivative works, distribute copies to the public, and perform publicly and display publicly, by or on behalf of the Government.

Acronyms

PHEV	Plug-in hybrid electric vehicle
EV	Electric vehicle
BEV	Plug-in battery electric vehicle, includes both EVs and PHEVs
RD&D	Research, development and deployment
EVSE	Electric vehicle supply equipment
ICEV	Internal combustion engine vehicle
DC	Direct current
DCFC	DC Fast Charging
AC	Alternating current
XFC	Extreme fast charging (between 150 and 400 kW)
NFPA	National Fire Protection Association
AHJ	Authorities having jurisdiction
PUC	Public utility commission
DSM	Demand side management
OEM	Original Equipment Manufacturer
TCO	Total Cost of Ownership
AWG	American Wire Gauge
CC-CV	Constant Current, Constant Voltage Charge Regime
DOT	United States Department of Transportation
VTTs	Value-of-travel-time-savings
OSHA	Occupational Safety and Health Administration
ADA	Americans with Disabilities Act
GHG	Greenhouse gas

References

- [1] S. Ahmed, et al, Enabling Fast Charging - A Battery Technology Gap Assessment, J Power Sources tbd.

- [2] M. Keyser, et al, Enabling Fast Charging - A Battery Thermal Management Gap Assessment, *J Power Sources* tbd.
- [3] A. Meintz, et al, Enabling Fast Charging - Vehicle Considerations, *J Power Sources* tbd.
- [4] D. Karner, T. Garetson, J. Francfort, EV Charging Infrastructure Roadmap, INL/EXT-16-39549, Idaho National Laboratory, 2016, <https://avt.inl.gov/sites/default/files/pdf/evse/EVChargingInfrastructureRoadmapPlanning.pdf> (Accessed 17 January 2017).
- [5] Light Duty Electric Drive Vehicles Monthly Sales Updates, Argonne National Laboratory, 2017. <https://www.anl.gov/energy-systems/project/light-duty-electric-drive-vehicles-monthly-sales-updates> (Accessed 3 February 2017).
- [6] O. Egbue, S. Long, Barriers to widespread adoption of electric vehicles: an analysis of consumer attitudes and perceptions, *Energy Policy* 48 (2012) 717–729.
- [7] J. Smart, S. Schey, Battery electric vehicle driving and charging behavior observed early in the EV project, *SAE Int. J. Alt. Power* 1 (2012) 27–33.
- [8] INL/EXT-15-34337, DC Fast Charger Usage in the Pacific Northwest, Idaho National Laboratory, 2015, https://avt.inl.gov/sites/default/files/pdf/evse/INL_WCEH_DCFCUsage.pdf (Accessed 3 February 2017).
- [9] K. Clement-Nyns, E. Haesen, J. Driesen, The impact of charging plug-in hybrid electric vehicles on residential distribution grid, *IEEE Trans. Power Syst.* (2009) 371–380.
- [10] C.H. Dharmakeerthi, N. Mithulanathan, T.K. Saha, Impact of electric vehicle fast charging on power system voltage stability, *Int. J. Electr. Power Energy Syst.* 57 (2014) 241–249.
- [11] A. Lucas, F. Bonavitacola, E. Kotsakis, G. Fulli, Grid harmonic impact of multiple electric vehicle fast charging, *Electr. Pow. Syst. Res.* (2015) 13–21.
- [12] Q. Gong, S. Midlam-Mohler, V. Marano, G. Rizzoni, Study of PEV charging on residential distribution transformer life, *IEEE Trans. Smart Grid* (2011) 404–412.
- [13] Commercial Reference Buildings, 2012. <https://energy.gov/eere/buildings/commercial-reference-buildings> (Accessed 21 February 2017).
- [14] F.D. Martzloff, H.A. Gauper, Surge and high-frequency propagation in industrial power lines, *IEEE Trans. Ind. Appl.* 4 (1986) 634–640.
- [15] Z. Benesova, V. Kotlan, Propagation of surge waves on non-homogeneous transmission lines induced by lightning strike, *Adv. Electr. Electron. Eng.* 5 (2006) 198.
- [16] F.D. Martzloff, The propagation and attenuation of surge voltages and surge currents in low voltage ac circuits, *IEEE Trans. Power App Syst.* 5 (1983) 1163–1170.
- [17] N. Nigro, D. Welch, J. Peace, Strategic Planning to Implement Publicly Available Charging Stations: a Guide for Businesses and Policymakers, Center for Climate and Energy Solutions, 2015. <https://www.c2es.org/docUploads/ev-charging-guide.pdf> (Accessed 17 February 2017).
- [18] G. Strbac, Demand side management: benefits and challenges, *Energy Policy* (2008) 4419–4426.
- [19] P. Finn, C. Fitzpatrick, D. Connolly, Demand side management of electric car charging: benefits for consumer and grid, *Energy* 42 (2012) 358–363.
- [20] D.B. Richardson, Electric vehicles and the electric grid: a review of modeling approaches, Impacts, and renewable energy integration, *Renew. Sustain. Energy Rev.* (2013) 247–254.
- [21] C. Weiller, R. Sioshansi, The role of plug-in electric vehicles with renewable resources in electricity systems, *Rev. d'economie Ind.* 4 (2014) 291–316.
- [22] D. Sbordone, I. Bertini, B. Di Pietra, M.C. Falvo, A. Genovese, L. Martirano, EV fast charging stations and energy storage technologies: a real implementation in the smart micro grid paradigm, *Electr. Pow. Syst. Res.* 120 (2015) 96–108.
- [23] INL/EXT-15-36318, Characterize the Demand and Energy Characteristics of Direct Current Fast Chargers, Idaho National Laboratory, 2015, <https://avt.inl.gov/sites/default/files/pdf/EVProj/CharacterizeDemandAndEnergyDCFC.pdf> (Accessed 3 February 2017).
- [24] California ISO. https://www.aiso.com/Documents/FlexibleResourcesHelpRenewables_FastFacts.pdf, 2013 (Accessed 10 November 2016).
- [25] State of California Department of Motor Vehicles Statistics for Publication January through December 2015, <https://www.dmv.ca.gov/portal/wcm/connect/5aa16cd3-39a5-402f-9453-0d353706cc9a/official.pdf?MOD=AJPERES> (Accessed 10 December 2016).
- [26] T. Franke, I. Neumann, F. Buhler, P. Cocron, J.F. Krems, Experiencing range in an electric vehicle: understanding psychological barriers, *Appl. Psych.* 61 (2012) 368–391.
- [27] INL/EXT-15-36313, What Use Patterns Were Observed for Plug-in Electric Vehicle Drivers at Publicly Accessible Alternating Current Level 2 Electric Vehicle Supply Equipment Sites, Idaho National Laboratory, 2015, <https://avt.inl.gov/sites/default/files/pdf/EVProj/UsePatternsHighlyUtilizedPubliclyAccessibleACLevel2.pdf> (Accessed 3 February 2017).
- [28] Momentum[®] dynamics completes testing of 50kW wireless charging for electric vehicles; to deliver 200kW for buses in 2016, *BusinessWire* 14 (April 2016). <http://www.businesswire.com/news/home/20160414006080/en/Momentum%C2%AE-Dynamics-Completes-Testing-50kW-Wireless-Charging> (Accessed 11 December 2016).
- [29] J. Francfort, S. Salisbury, J. Smart, T. Garetson, D. Karner, Corridor, D.C. Community, Fast Charging Complex System Design: Options & Implications, INL/EXT-17-40829, Idaho National Laboratory, 2017.
- [30] J. Agenbroad, B. Holland, Pulling Back the Veil on EV Charging Station Costs vol 29, Rocky Mountain Institute, April 2014. http://blog.rmi.org/blog_2014_04_29_pulling_back_the_veil_on_ev_charging_station_costs (Accessed 15 March 2017).
- [31] D. Chang, D. Erstad, E. Lin, A. Falken Rice, C. Tzun Goh, A. Tsao, J. Snyder, Financial Viability of Non-residential Electric Vehicle Charging Stations, UCLA, Los Angeles, CA, 2012. <http://luskin.ucla.edu/sites/default/files/Non-Residential%20Charging%20Stations.pdf> (Accessed 15 March 2017).
- [32] N. Nigro, M. Frades, Business Models for Financially Sustainable EV Charging Networks, Center for Climate and Energy Solutions, 2015. <https://www.c2es.org/docUploads/business-models-ev-charging-infrastructure-03-15.pdf> (Accessed 17 February 2017).
- [33] A. Schroeder, T. Traber, The economics of fast charging infrastructure for electric vehicles, *Energy Policy* 43 (2012) 136–144.
- [34] B. Nykvist, M. Nilsson, Rapidly falling costs of battery packs for electric vehicles, *Nat. Clim. Change* 5 (2015) 329–332.
- [35] F. Lambert, Electric Vehicle Battery Cost Dropped 80% in 6 Years Down to \$227/kWh-tesla Claims to Be below \$190/kWh. <https://electrek.co/2017/01/30/electric-vehicle-battery-cost-dropped-80-6-years-227kwh-tesla-190kwh/> (Accessed 6 January 2017).
- [36] J. Voelcker, Tesla boosts Supercharger electric-car charging rate to 145 kW, *Green Car Rep.* 28 (July 2016). http://www.greencarreports.com/news/1105234_tesla-boosts-supercharger-electric-car-charging-rate-to-145-kw (Accessed 27 February 2017).
- [37] Fact #913: February 22, 2016 U.S. Department of Energy, The Most Common Warranty for Plug-in Vehicle Batteries Is 8 Years/100,000 Miles, February 2016, <https://energy.gov/eere/vehicles/fact-913-february-22-2016-most-common-warranty-plug-vehicle-batteries-8-years100000> (Accessed 10 April 2017).
- [38] Y. Zhou, D.J. Santini, T.S. Stephens, J. Ward, “Comparison of value retention of plug-in vehicles and conventional vehicles and potential contributing factors,” in 95th Annual Meeting of the Transportation Research Board, Washington, DC, 2016.
- [39] National Automobile Dealers Association, NADA Used Car Guide: Electric Vehicle Retention Report Card, 2015.
- [40] The Value of Travel Time Savings, Departmental Guidance for Conducting Economic Evaluations Revision 2 (2014 Update), US Department of Transportation, 2014. <https://cms.dot.gov/sites/dot.gov/files/docs/USDOT%20VOT%20Guidance%202014.pdf> (Accessed 10 November 2016).
- [41] Real Median Household Income in the United States, FRED Economic Data: Federal Reserve Bank of St. Louis, Sept. 13, 2016. <https://fred.stlouisfed.org/series/MEHOINUSA672N> (Accessed 2 June 2017).
- [42] Occupational Employment Statistics, United States Department of Labor, Bureau of Labor Statistics, March 31, 2017. https://www.bls.gov/oes/current/oes_nat.htm#00-0000 (Accessed 2 June 2017).
- [43] Employer Costs for Employee Compensation – March 2017, United States Department of Labor, Bureau of Labor Statistics, June 9, 2017. <https://www.bls.gov/news.release/pdf/ecec.pdf> (Accessed 11 February 2017).
- [44] National Transportation Statistics, Table 1-35—U.S. Vehicle Miles, United States Department of Transportation, Bureau of Transportation Statistics, April 2017. http://www.bts.gov/publications/national_transportation_statistics (Accessed 11 June 2017).
- [45] NHTS 2001 Highlights Report, BTS03-05, United States Department of Transportation, Washington DC, 2003.
- [46] A. Burnham, Alternative Fuel Life-Cycle Environmental and Economic Transportation (AFLEET) Tool, Argonne National Laboratory, May 6, 2016. <https://greet.es.anl.gov/afleet> (Accessed 1 December 2016).
- [47] EV Everywhere Grand Challenge Blueprint (January 31, 2013), United States Department of Energy, 2013. https://energy.gov/sites/prod/files/2014/02/f8/ev_everywhere_blueprint.pdf (Accessed 10 November 2016).



U.S. DEPARTMENT OF
ENERGY

Office of
**ENERGY EFFICIENCY &
RENEWABLE ENERGY**

For more information, visit:
energy.gov/eere/vehicles

INL/EXT-17-41638 • October 2017